U.S. DEPARTMENT OF COMMERCE
NATIONAL TECHNICAL INFORMATION SERVICE

N75-32035

FEASIBILITY STUDY OF MODERN AIRSHIPS, PHASE I, VOL. IV-APPENDICES

GOODYEAR AEROSPACE CORP.
AKRON, OH

AUGUST 1975

N O T I C E

THIS DOCUMENT HAS BEEN REPRODUCED FROM THE BEST COPY FURNISHED US BY THE SPONSORING AGENCY. ALTHOUGH IT IS RECOGNIZED THAT CERTAIN PORTIONS ARE ILLEGIBLE, IT IS BEING RELEASED IN THE INTEREST OF MAKING AVAILABLE AS MUCH INFORMATION AS POSSIBLE.

NASA CR-137692 (4)

FEASIBILITY STUDY OF MODERN AIRSHIPS
(PHASE I)

Volume IV - Appendices

Contract NAS2-8643

August 1975

Prepared for

Ames Research Center, Moffett Field, California

by

Goodyear Aerospace Corporation, Akron, Ohio

PRICES SUBJECT TO CHANGE

FOREWORD

This final technical report was prepared for the Ames Research Center, Moffett Field, Calif., by Goodyear Aerospace Corporation, Akron, Ohio, under NASA Contract NAS2-8643, "Feasibility Study of Modern Airships." The technical monitor for the Ames Research Center was Dr. Mark D. Ardema.

This report describes work covered during Phase I (9 December 1974 to 9 April 1975) and consists of four volumes:

Volume I	-	Summary and Mission Analysis (Tasks II and IV)
Volume II	-	Parametric Analysis (Task III)
Volume III	-	Historical Overview (Task I)
Volume IV	-	Appendices

The report was a group effort headed by Mr. Ralph R. Huston and was submitted in May 1975. The contractor's report number is GER-16146.

OVERALL TABLE OF CONTENTS

Section	Title	Page
	VOLUME I - SUMMARY AND MISSION ANALYSIS (TASKS II and IV)	
	SUMMARY	1
	RECOMMENDED PHASE II MAV/MISSION COMBINATIONS	2
	MAV/Mission Combination 1	2
	MAV/Mission Combination 3	3
	MAV/Mission Combination 4	5
	INTRODUCTION	6
	MISSION ANALYSIS OVERVIEW	8
	APPROACH FOR SELECTING POTENTIAL MISSIONS	8
	PRESENT CONVENTIONAL MISSIONS	10
	Passenger and Cargo	10
	Present Conventional Passenger Missions and Competitive Modes	12
	Present Scheduled Airline Missions	16
	Present and Projected Passenger System Capabilities and Limitations	18
	Conventional Passenger MAV Mission Potential	23
	Present Conventional Cargo Missions and Competing Forms	27
	Evaluation of Present Cargo Missions to Determine Potentially Competitive Conventional Missions for MAV's	29
	Intermodal Comparisons	31
	Intermodal Comparisons in Price Competitive Market	39
	Present Scheduled Air Cargo System Capabilities and Limitations	45
	Conventional Cargo MAV Mission Potential	45

Section	Title	Page
	PRESENT UNIQUE TRANSPORTATION AND SERVICE MISSIONS	50
	Present Unscheduled/General Aviation Passenger Missions	50
	General Aircraft Fleet Composition and Use (1971)	52
	Fleet Composition	52
	Present Passenger Equipment Capabilities and Limitations	56
	Unscheduled Passenger Mission Potential	58
	Commercial	59
	Institutional Passenger	59
	Present Unscheduled/General Aviation Cargo Missions	60
	Present Unscheduled Cargo System Capabilities and Limitations	60
	Unscheduled General Cargo MAV Mission Potential	61
	Heavy Lift Large Indivisible Load MAV Mission Potential	61
	Commercial (Heavy Lift)	62
	Institutional (Heavy Lift)	63
	Agricultural Transportation MAV Mission Potential	63
	Platform/Service Mission Potential	65
	Commercial (Platform/Service)	66
	Institutional (Platform/Service)	67
	Resources from Remote Regions - MAV Mission Potential	69
	Military MAV Mission Potential	71
	MAV SYSTEM PERFORMANCE AND OPERATIONAL REQUIREMENTS FOR POTENTIAL MISSIONS	74
	General	74
	Scheduled and Unscheduled Civil Passenger and General Cargo Transportation Missions	86
	Unique Missions	86
	Military Missions	87
	EVALUATION OF MAV's FOR POTENTIAL MISSIONS AND SELECTED MISSION PECULIAR FIGURES OF MERIT	89
	General	89
	Potential Conventional Passenger and Cargo Missions	97
	Potential Unique Missions and Selected Mission Peculiar Figures of Merit	98
	Potential Military Missions and Selected Military Mission Peculiar Figures of Merit	101

Section	Title	Page
	POTENTIAL MISSIONS BY VEHICLE SIZES AND TYPES	103
	General	103
	Civil Missions	103
	Military Missions	107
	EVALUATION AND SELECTION FACTORS	109
	Missions	109
	Parametric Analysis	109
	Selected Combinations	110
	MAV/Mission Combination 1	111
	MAV/Mission Combination 2	115
	MAV/Mission Combination 3	116
	MAV/Mission Combination 4	120
	PHASE II RECOMMENDATIONS	123
	REFERENCES	123

VOLUME II - PARAMETRIC ANALYSIS

(TASK III)

	SUMMARY	1
	INTRODUCTION	2
	BACKGROUND	2
	OBJECTIVES	4
	SCOPE	4
	GENERAL APPROACH	5
	METHODS OF ANALYSIS	6
	PARAMETRIC STUDY OVERVIEW	10
	CONVENTIONAL AIRSHIPS	11
	Design Description (Conventional Rigid)	11
	Pressurized Metalclad	16
	CONVENTIONAL AIRSHIP AERODYNAMICS ANALYSIS	20
	PROPULSION ANALYSIS (PERFORMANCE)	21

Section	Title	Page
	PROPULSION SYSTEM WEIGHTS ANALYSIS	22
	STRUCTURAL WEIGHTS ANALYSIS	22
	CONVENTIONAL AIRSHIP PARAMETRIC ANALYSIS	28
	Introduction	28
	Fineness Ratio Tradeoff Study	31
	Metalclads, l/d Optimization Study	34
	Conventional Airships Heaviness Tradeoff Studies Based on $UL \cdot V_C/EW$	40
	Conventional Airship Heaviness Optimization Study Based on Payload Ton-Mile per Hour as a Function of Range	42
	Conventional Airship Heaviness Tradeoff Study Results	56
	Advanced Ellipsoidal Airship Concepts	66
	PARAMETRIC ANALYSIS OF HYBRID VEHICLES	68
	Overview	68
	Preliminary Configuration Evaluation	69
	Modified Delta Planform Hybrid (Selection Rationale and Configuration Description)	71
	Structural Description	74
	Delta Planform Hybrid Aerodynamics Analysis	78
	GASP Aerodynamics Estimating Procedures	79
	Propulsion	80
	Structural Analysis and Weights Analysis	80
	Hybrid Parametric Analysis	89
	Hybrid Parametric Performance Results	94
	Lifting Body Hybrid/Ellipsoidal Airship Productivity Comparison	102
	HEAVY LIFT HYBRID VEHICLE CONCEPT	107
	Heavy Lift Performance versus Gross Weight: Size Limitations and Scale Effects	111
	Alternate Figure of Merit for Conventional Airships	114
	Fuel Efficiency Considerations	115
	Endurance Capability	118
	Range Capability	119
	Comparison with Historical Results	119
	PARAMETRIC ANALYSIS SUMMARY AND CONCLUSIONS	123
	Conventional Airship/Lifting Body Hybrid	124

Section	Title	Page
	LIMITATIONS OF CURRENT STUDY	125
	REFERENCES	129
	VOLUME III - HISTORICAL OVERVIEW (TASK I)	
	SUMMARY	1
	INTRODUCTION	2
	PARAMETERIZATION OF DESIGN CHARACTERISTICS	8
	Rigid Airships	8
	Non-rigid Airships	22
	Semi-rigid Airships	32
	Analysis of Data (Rigid, Non-rigid, Semi-rigid)	35
	HISTORICAL MARKETS, MISSION COSTS, AND OPERATING PROCEDURES	45
	General	45
	Operations and Economics	46
	Manufacturing	63
	Prior Goodyear Economic Studies (1944 $)	72
	American Military Experiece (1916 to 1961)	72
	Airship Safety	86
	CRITICAL DESIGN AND OPERATIONAL CHARACTERISTICS	94
	General	94
	Maximum Bending Moment Criteria	104
	Operational Aspects of Airships	109
	STATE OF THE ART	116
	Rigid Airships (Materials)	116
	Material Life Characteristics	124
	Non-rigid Airships (Materials)	125
	Rigids (Economically)	126
	Operational Aspects of Conventional MAV's	129
	Recent LTA/HTA Vehicles and Concepts	134
	REFERENCES	143

VOLUME IV - APPENDICES

Appendix	Title	Page
A	(1) General Dimensions and Characteristics of French Dirigibles	A-1
	(2) Characteristics of Italian Semi-rigid Airships	A-1
B	Non-rigid Airships Manufactured by Goodyear	B-1
C	(1) Properties of 7050 Aluminum Alloy	C-1
	(2) Macon Gas Cell Data	C-1
	(3) Additional Chronological History of German Airship Events	C-1
D	Derivation of Conventional Ellipsoidal Airship Structural Weight Estimating Relationships	D-1
E	Aerodynamics Analysis	E-1
F	Propulsion and Take Off Analysis	F-1
G	Sandwich Monocoque Rigid Airship	G-1
H	Design Options	H-1
I	Configuration Screening Exercise	I-1

LIST OF ILLUSTRATIONS (VOLUME IV ONLY)

Figure	Title	Page
E-1	Estimated Variation of Peak Bending Moment Coefficient with Fineness Ratio $C_m = M/qV$	E-5
E-2	Comparison of Hybrid Airfoil Coordinates with Generalized NACA OOXX Section	E-10
E-3	Airfoil Velocity Ratios as a Function of Thickness Ratio	E-12
E-4	$\Delta V_a/V$ Ratios as Functions of Thickness Ratio	E-13
E-5	Baseline Hybrid Pressure Distribution (x/c = .278 and .276)	E-14
E-6	Baseline Hybrid Pressure Distributions (x/c = .266)	E-15
F-1	Propeller Data (Mach 0)	F-5
F-2	Propeller Data (Mach 0.1)	F-6
F-3	Propeller Data (Mach 0.2)	F-7
F-4	Bare Engine Weight Characteristics	F-11
F-5	Typical Transition Analysis Results (GW = 40,000 Lb, B = 0.65, No Wind)	F-15
F-6	Typical Transition Analysis Results (GW = 40,000 Lb, B = 0.20, V_W = 15 Knots)	F-15
G-1	Transverse Frame Configuration	G-17
H-1	Weight Density of Various Propulsion of Engine Cycles	H-7
H-2	Specific Fuel Consumption of Various Propulsion Engine Cycles	H-8
H-3	Relation of Superheat, Volume Rates, and Aerostatic Lift Ratio	H-15
H-4	Envelope Temperature	H-17
H-5	Heat Rate Required to Maintain Superheat and Heat Rate Available from Propulsion Engine Cycles	H-18

LIST OF ILLUSTRATIONS (VOLUME IV ONLY) (CONTINUED)

Figure	Title	Page
H-6	Comparison of BLC Airship with Conventional for Equal Volume	H-21
H-7	Horsepower Requirements versus Flight Velocity for BLC and Conventional Airships ($\forall = 10^6$)	H-21
H-8	Percentage of Baseline Useful Lift versus Lift per 1000 Cu Ft of Volume	H-27
H-9	Useful Lift Ratio versus Lift per 1000 Cu Ft of Volume .	H-29
I-1	Semi-rigid Vehicle Concepts	I-5
I-2	Winged Airship Configuration Schematics for Evaluation/Screening Exercise	I-7
I-3	Winged Airship Aerodynamic Estimates	I-13
I-4	Winged Airship Aerodynamic Estimates	I-14
I-5	Winged Airship Aerodynamic Estimates	I-15
I-6	Winged Airship Aerodynamic Estimates	I-16
I-7	Ultimate Shear and Bending Moment Diagrams (Configuration 9 A/B)	I-28
I-8	Ultimate Shear and Bending Moment Diagrams (Configuration 11 A/B/C)	I-29
I-9	Ultimate Shear and Bending Moment Diagrams (Configuration 12 A/B)	I-30

LIST OF TABLES (VOLUME IV ONLY)

Table	Title	Page
H-I	Comparison of Baseline (Turboprop) with Alternate Propulsion System	H-5
H-II	Sample GASP Output for Baseline Sensitivity Study Vehicle	H-25
H-III	Sensitivity Study Results	H-31
I-I	Qualitative Evaluation Matrix Results	I-9
I-II	General Comments on Winged Airship Configurations	I-10
I-III	Summary of Parameters Used in Wing Weight Estimation - Rectangular Wings	I-25
I-IV	Summary of Parameters Used in Wing Weight Estimation - Delta Wings	I-26
I-V	Winged Airship Configuration Characteristics and Evaluation Results	I-32

APPENDIX A

1) GENERAL DIMENSIONS AND CHARACTERISTICS OF FRENCH DIRIGIBLES

2) CHARACTERISTICS OF ITALIAN SEMI-RIGID AIR-SHIPS

CONVERSION FACTORS FOR APPENDIX A

1 foot	=	0.3048
1 ft^2	=	0.0929 m^2
1 ft^3	=	0.02832 m^3
1 lb	=	0.4536 Kg
1 mph	=	0.447 m/sec

GENERAL DIMENSIONS AND CHARACTERISTICS OF FRENCH DIRIGIBLES

		Mont-golfier	Fleu-reus	D'Arlan des Cham-pagne	Lor-raine & Tuni-sie	Capt. Causs'm	Cruiser La Flanders	Cruiser Zodiac	T.3/16
1	Length	237	256	302	306	267	328	331	230
2	Max Width Ft.	55.7	47.5	55	49.7	47.5	62.3	50.8	46
3	Dia. Ft.	40.	47.7	52.4	V-52.0 H-45.8	46.2	57.5	V-50.1 H-47.5	37.7
4	Fineness Ratio	5.9	5.4	5.8	5.9	5.8	5.7	6.6	
	Height Ft.	70.5	74.3	87.7	77.7	75.5	852	85.2	59.3
6	Volume Cu. Ft.	233000	229000	503000	370000	321000	582000	459000	194000
7	Meridian Sec.Sq.Ft.	7430	8890	13400	12810	10440	18580	18000	7280
8	Vert.Fin Sq.Ft.	335	411		688	1160	1127	360	790
	% Meridian	450	4.62		5.36	11.1	6.06	2.00	10.87
9	Vert.Rudder Sq.Ft.	88.7	156		237	307	269	207	258
10	% Meridian	1.19	1.75		1.85	2.94	1.45	1.15	3.55
11	Hor.Fin& Rudder Sq.Ft.	194	161		549	517	1632	570	591
12	% Meridian	2.61	1.81		4.29	4.95	8.8	3.17	8.12
13	Car Length Ft.	57.3	42.1	51.1	52.5	42.1	68.8	54.2	35.1
14	Car Sec. W.xH.	7.45x7.3	8.2x9.85	7.5x8.2				5.7x7.5	
15	Useful Load Lbs.	4990	5800	13320	9910	10130	18810	13900	3750
16	Crew	4	4	5	5	6	5	5	5
17	Vel. MPH	32.3	34.9	43.5	43.5	46.6to55.9	49.6	43.5to 46.5	46.6 to 52.7
18	Propellers	2-2 blade	D=15.4 2-2	2-2	D=16.15 2-2	D=11.14 2-2	4-2	2-2	D=10.3 2-2
19	Power Plant	C-B	C-B	2-Zodiac	C-B	Salmson	Renault	Zodiac	Salmson
20	Motors No. &Type	4-4	4-4	6	2-6	2-9	4-2	2-6	2-9
21	Total H.P.	280?-140	280?-140	450	440	480	960	450	320

ORIGINAL PAGE IS
OF POOR QUALITY

CHARACTERISTICS OF ITALIAN SEMI-RIGID AIRSHIPS

Type	Date	Total Lgth.	Max. Dia.	Asp. Rat.	VOLUME Design	VOLUME Actual	Total Lift	Dead Lift	Usfl. Lift	Pct. Usfl. Lift	Speed	H.P.
P	1912	203.4	41.3	4.9	167700	173000	11140	8360	2780	25.0	40.6	140
M	1914	271.2	55.4	4.9	427500	441200	28410	18040	10370	36.5	43.7	390
V-2	1916	285.7	67.9	4.2	542200	554200	35490	25080	10610	30.0	48.7	540
E	1916	158.7	33.1	4.8	88600	91800	5910	3960	1950	33.0	42.5	100
M	1916	271.2	55.4	4.9	427500	441200	28410	15840	12570	44.5	46.2	440
O	1918	177.8	35.4	5.0	123500	127000	8180	5830	2350	29.0	56.9	240
PV	1918	203.4	42.3	4.8	176500	183600	11820	8800	3020	25.5	56.2	380
A	1918	321.4	60.7	5.3	617700	635400	40920	22000	18920	46.0	50.0	950
M	1918	271.2	55.4	4.9	427500	441200	28410	18700	9710	34.0	52.7	640
T-34	1919	410.0	74.4	5.5	1203700	1239000	79790	47080	32710	41.0	68.6	2100
FV 1	Prop	328.0	62.3	5.2	617000	635400	40920	25570	15350	37.5	62.5	700
F-5	1916	295.2	65.6	4.5	628300	646000	41600	22000	19600	47.0	46.6	480
F-6	1918	295.2	65.6	4.5	628300	646000	41600	24200	17400	42.0	54.3	760
U-5	1917	180.4	34.8	5.2	137000	141200	9090	6600	2490	27.5	44.8	240
T-42	Prop	525.0	74.5	7.0	1486000	1532000	98660	53680	44980	45.5	72.0	2100
N	Prop	348.0	66.2	5.3	607500	637500	41050	24250	16800	41.0	63.0	750
SCA 1	1921	128.0	27.9	4.6	53000	54600	3520	2440	1080	31.0	46.9	80
RS 1	Gdyr	282.0	70.5	4.0	710000	735000	47330	26630	20700	44.0	70.0	1200

Data on size, weight, HP and speed supplied by Nobile. The "actual" volume is about 103% of the "Design" volume. The lift is calculated for 64.4 lbs. per thousand on a basis of Actual volume. All linear dimensions are feet. Lift and weight are pounds. V = Volume in cubic feet. S = Speed in miles per hr.

APPENDIX B

NON-RIGID AIRSHIPS MANUFACTURED BY GOODYEAR

CONVERSION FACTORS FOR APPENDIX B

$1\ ft^3 = 0.02832\ m^3$

AIRSHIPS MANUFACTURED AND DELIVERED BY GOODYEAR TO U.S. NAVY (1917 - 1960)

Type	No. delivered	Envelope volume (cu ft)	Delivery
AB or B	9	89,000	1917 - 1918
C	6	172,000	1918 - 1921
D	4	180,000	1920 - 1921
E	1	95,000	1918
F	1	95,000	1918
G	8	183,000	1935 - 1944
H	1	43,000	1921
J	1	175,000	1923
K	134	320,000 456,000	1938 - 1943
L	18	123,000	1943 - 1944
M	4	725,000	1944
ZSG-4	15	527,000	1954 - 1955
ZS2-2, G-1	18	650,000	1955 - 1958
ZPG-1	1	875,000	1952
ZPG-2	12	975,000	1953 - 1956
ZPG-2, W Type	5	975,000	1955 - 1957
ZPG-3W	4	1,465,000	1959 - 1960

AIRSHIPS MANUFACTURED AND DELIVERED TO U.S. ARMY BY GOODYEAR (1919 - 1933)

AIRSHIP	U.S. ARMY TYPE	VOLUME	DELIVERED
E-113	D-4	180,000 cu ft	3-21-21
	A-4	95,000	4-2-19
	OA	35,500	10-19-20
	OA	35,500	11-22-20
	OA	35,500	10-26-21
	OA	35,500	9-6-21
	AC Military	185,000	6-3-22
121	H	43,000	7-25-22
E-4	TC-1	200,000	4-9-23
E-5	TC-2	200,000	5-21-23
E-6	TC-3	200,000	8-13-23
E-9	TA-1	130,000	10-30-23
E-10	TA-2	130,000	11-23-23
E-14	TA-3	120,600	5-16-25
E-15	TA-4	130,600	6-3-25
E-22	TA-5	130,600	12-16-25
E-19	TC-7	200,000	4-16-25
E-20	TC-8	200,000	12-16-25
E-21	TC-9	200,000	9-19-25
	TE	80,200	6-29-29
	TE	80,200	8-15-29
	TC-13	350,000	3- -33

GOODYEAR COMMERCIAL AIRSHIPS

ENVELOPE	CAPACITY	NAME	BUILT
D-44	95,000	Wingfoot Express	June 1919
D-45	35,300	Pony Blimp	Dec 1919
D-57	35,300	Pony Blimp	April 1920
D-58	35,300	Sport Ship	June 1920
D-94	47,700	Pilgrim I	April 1925
D-113	86,000	Puritan I	June 1928
D-120	86,000	Volunteer I	May 1929
D-121	86,000	Mayflower I	May 1929
D-122	55,000	Pilgrim II	April 1929
D-123	86,000	Vigilant I	June 1929
D-124	178,000	Defender I	August 1929
D-125	96,000	Puritan II	Nov 1929
D-126	96,000	Puritan III	July 1930
D-127	86,000	Neponset I	May 1930
D-130	96,000	Volunteer II	Jan 1931
D-131	112,000	Columbia I	June 1931
D-132	112,000	Mayflower II	May 1931
D-134	112,000	Puritan IV	Sept 1931
D-135	112,000	Reliance I	Dec. 1931
D-136	112,000	Resolute I	Feb. 1932
D-137	112,000	Volunteer III	May 1932
D-139	112,000	Reliance II	May 1933
D-140	112,000	Volunteer IV	June 1933
D-142	112,000	Resolute II	May 1934
D-144	123,000	Enterprise I	Aug 1934
D-145	183,000	Defender II	Sept. 1935
D-147	123,000	Puritan V	Oct. 1935
D-149	112,000	Volunteer V	Feb. 1937
D-150	123,000	Reliance III	June 1937
D-151	123,000	Resolute III	Oct. 1938
D-155	123,000	Enterprise II	Feb. 1939
D-156	123,000	Rainbow I	March 1939
D-157	123,000	Reliance IV	1939
D-158	123,000	Ranger I	1939
D-160	123,000	Reliance V	Oct. 1940
D-166	123,000	Ranger II	Jan 1942
D-327	123,000	Ranger II, III	May 15, 1946
D-268	123,000	Enterprise II,III	Sept 11,1946
D-324	123,000	Volunteer II, VI	Sept 26,1946
D-237	425,000	Puritan II, VI	Mar. 1, 1947
D-247	123,000	Mayflower II,III	May 2, 1947
D-194	123,000	Ranger IV	Oct. 13, 1947

GOODYEAR COMMERCIAL AIRSHIPS (Continued)

ENVELOPE	CAPACITY	NAME	BUILT
D-250	123,000	Volunteer VII	Mar 16, 1948
D-219	123,000	Mayflower IV	May 24, 1948
D-468	123,000	Enterprise IV	Apr 25, 1948
D-472	123,000	Ranger V	Jan 20, 1949
D-474	123,000	Ranger VI	Nov. 20, 1952
D-594	123,000	Enterprise V	Mar 26, 1954
D-600	123,000	Ranger VII	August 1955
D-627	132,500	Mayflower III, V	Sept 2, 1958
D-635	147,300	Columbia II	1963
D-636	147,300	Mayflower VI	1963
	147,300	Mayflower VII	Sept 4, 1968
	202,700	America	Apr 6, 1969
	202,700	Columbia	Aug 18, 1969
	202,700	Europa	Mar 8, 1972

APPENDIX C

1) PROPERTIES OF 7050 ALUMINUM ALLOY

2) MACON GAS GELL DATA

3) ADDITIONAL CHRONOLOGICAL HISTORY OF GERMAN AIRSHIP EVENTS

CONVERSION FACTORS FOR APPENDIX C

1 ft^3	=	0.02832 m^3
1 yd^2	=	0.8361 m^2
1 oz/yd^2	=	0.03385 Kg/m^2
1 lb	=	0.4536 Kg

AIA

AEROSPACE INDUSTRIES ASSOCIATION OF AMERICA, INC.

1725 DE SALES STREET, N.W., WASHINGTON D.C. 20036 TEL 347-2315

ATCouncil
MSC 74-27
May 2, 1974

To: MATERIALS AND STRUCTURES COMMITTEE

Subject: Substitution of 7050 Aluminum Alloys

Attachment: NAVAIR letter with (3) enclosures

The attached NAVAIR letter with enclosures is provided for your company's review and comment.

NAVAIR proposes to substitute 7050 alloy for all new weapon systems airframe components and spare parts that are currently being manufactured from 7075, 7079, 7178 and 2014 aluminum alloys. Substitution of the 7050 alloy is expected to result in improved reliability and lower life cycle costs.

Comments from AIA concerning procedures for accelerating the application of 7050 are requested.

Please provide your comments via the attached reply sheet to the following who will act as sponsor in summarizing industry comments:

Dr. M. A. Steinberg
Deputy Chief Scientist
01-10, 61, A-1
Lockheed Aircraft Corporation
Post Office Box 551
Burbank, California 91503

THE REPLY SHEET WITH YOUR COMPANY'S COMMENTS SHOULD BE SUBMITTED TO THE SPONSOR TO ARRIVE ON OR BEFORE:

May 30, 1974

The sponsor's summary should be forwarded to this office not later than June 14, 1974.

J. P. Reese
Executive Secretary

/sfe

FIRST CIRCULATION

MECHANICAL PROPERTIES OF 7050-T76 SHEET

(NASC Contract No. N00019-72-C-0512)

(Tentative)

Sample Thickness, in.	Sample Number	Specimen Direction†	Tensile Strength, ksi	Tensile Yield Strength,* ksi	Elong in 2 in., or 4D, %	Compressive Yield Strength,* ksi	Shear Strength, ksi	Bearing Strength,§ ksi e/D=1.5	Bearing Strength,§ ksi e/D=2.0	Bearing Yield Strength,§ ksi e/D=1.5	Bearing Yield Strength,§ ksi e/D=2.0
0.040		L									
		LT									
0.040		L									
		LT									
0.063	411378	L	83.0	77.7	10.5	77.1	50.4‡	126.0	165.9	102.9	120.8
		LT	84.3	78.2	10.0	82.2		126.9	167.9	103.2	119.5
0.063		L									
		LT									
0.090	411182	L	84.5	78.9	11.0	78.9	51.2‡	133.3	173.4	112.1	127.6
		LT	83.9	77.0	11.0	83.6		133.3	172.9	113.6	133.7
0.090	411183	L	83.8	78.3	11.0	78.9	50.0‡	131.3	168.8	111.2	125.0
		LT	82.4	75.5	11.0	81.0		129.4	171.0	110.5	129.5
0.125	411212	L	83.6	79.6	11.0	79.3	49.7‡	131.5	169.1	110.7	121.5
		LT	83.7	77.9	11.5	83.4		130.7	170.0	111.2	127.0
0.125	411213	L	83.1	78.7	11.0	77.8	50.2‡	130.3	169.0	109.4	122.8
		LT	83.0	77.2	11.5	82.8		131.1	168.7	112.5	125.2
0.187	413150	L	81.1	75.0	11.0	76.8	47.6‡	131.6	162.7	112.7	121.3
		LT	83.3	74.5	11.5	80.4		131.1	166.8	111.4	131.8
0.249	416020	L	83.4	78.6	11.0	81.3	54.0	134.0	170.6	117.3	125.9
		LT	84.6	78.3	11.0	84.1	53.2	129.1	171.0	111.9	130.9
0.249	411309	L	83.2	80.2	12.5	80.3	49.7	132.9	169.4	111.3	124.1
		LT	83.5	78.4	13.0	84.0	51.9	132.0	169.1	111.6	127.2
					Tentative Minimum Properties						
0.040-0.249		L	78	71	8	—	—	—	—	—	—
		LT	78	69	8	—	—	—	—	—	—

* Offset equals 0.2 per cent.
† L - Longitudinal; LT - Long-Transverse
‡ Punch-type sheet shear specimens
§ Specimens cleaned ultrasonically; yield strength offset equals 2 per cent of pin diameter.

MECHANICAL PROPERTIES OF 7050-T7651X EXTRUDED SHAPES
(NASC Contract No. N00019-72-C-0512)

(Tentative)

Sample Thickness, in.	Sample Number	Die No.	Specimen Location†	Specimen Direction‡	Tensile Strength, ksi	Tensile Yield Strength,* ksi	Elong in 2 in., in 4D, %	Compressive Yield Strength,* ksi	Shear Strength, ksi	Bearing Strength,§ ksi e/D=1.5	Bearing Strength,§ ksi e/D=2.0	Bearing Yield Strength,§ ksi e/D=1.5	Bearing Yield Strength,§ ksi e/D=2.0
0.187	411288	86366	W/4	L	85.1	75.9	10.0	81.9	47.4	122.1	159.0	101.9	121.5
			W/2	LT	85.4	76.9	10.0	78.9	45.9	123.2	160.2	102.7	121.9
0.402	411289	191282	W/4	L	83.8	75.6	14.0	78.2	49.4	128.8	164.2	109.7	124.3
			W/2	LT	83.4	73.0	10.0	81.3	49.6	131.2	167.6	112.8	135.7
0.665	411290	213592	T/2,W/4	L	85.4	78.2	14.3	78.8	48.9	126.7	162.4	108.7	123.9
			T/2,W/2	LT	84.1	76.9	12.9	80.0	46.8	127.7	163.2	108.7	130.7
0.841**	411552	53717	T/2,W/2	L	82.8	75.2	11.0	79.1	47.1	121.9	160.2	104.4	122.2
				LT	81.6	74.1	11.0	76.0	45.1	124.7	159.1	105.1	122.2
1.161	411287	231372	T/2,W/4	L	83.6	76.4	12.0	76.9	49.6	127.9	163.7	109.0	124.3
			T/2,W/2	LT	82.5	74.4	11.0	79.2	48.7	126.3	163.2	107.5	132.4
1.5x7.5	411284	††	T/2,W/4	L	85.0	78.4	13.0	80.5	48.5	126.9	163.6	105.9	120.0
			T/2,W/2	LT	82.0	75.3	12.0	79.9	48.3	126.5	164.3	105.4	124.6
			T/2,W/2	ST	82.3	69.8	8.0	82.2	--	--	--	--	--
2.0x8.0**	411279	††	T/4,W/4	L	81.6	75.6	13.0	76.5	45.8	120.9	156.9	101.3	115.5
			T/2,W/2	LT	76.9	71.0	10.0	75.3	44.4	119.2	154.2	101.9	115.1
			T/2,W/2	ST	76.0	66.7	6.0	75.7	40.8	--	--	--	--
3.5x7.5	411285	††	T/4,W/4	L	86.6	80.5	11.0	82.1	48.2	124.9	158.8	104.0	119.1
			T/2,W/2	LT	80.3	74.1	7.0	79.0	47.0	121.5	156.9	103.2	121.4
			T/2,W/2	ST	79.9	70.9	2.9	76.9	43.6	--	--	--	--
4.0x8.0**	411280	††	T/4,W/4	L	84.6	79.7	11.0	81.0	46.8	123.6	156.1	104.9	120.4
			T/2,W/2	LT	76.1	71.8	4.0	77.3	45.7	116.3	153.4	103.2	117.9
			T/2,W/2	ST	75.1	68.9	2.9	75.3	39.3	--	--	--	--
5x6.25	411286	††	T/4,W/4	L	87.6	82.3	11.0	84.8	48.3	118.9	156.3	105.7	122.9
			T/2,W/2	LT	77.2	72.0	3.0	77.8	46.7	106.8	143.1	101.1	119.7
			T/2,W/2	ST	76.5	70.3	3.0	76.0	42.4	--	--	--	--
Tentative Minimum Properties													
Up to 0.249 (Area ≥ 20 in.^{2})				L	78	70	7	--	--	--	--	---	--
0.250-0.499 (Area ≥ 20 in.^{2})				L	81	73	7	--	--	--	--	--	--
0.500-1.499 (Area ≥ 20 in.^{2})				L	81	72	7	--	--	--	--	--	--
1.500-2.999 (Area ≥ 20 in.^{2})				L	81	72	7	--	--	--	--	--	--

* Offset equals 0.2 per cent.
† T-Thickness, W-Width
‡ L-Longitudinal, LT-Long Transverse, ST-Short Transverse
§ Specimens cleaned ultrasonically; yield strength = offset equals 2 per cent of pin diameter.
** Producer B, others from Producer A.
†† Rectangle

C.6

U. S. S. MACON GAS CELL DATA

Cell No.	Volume, 100% Ft^3	Location of C.B.	Distance From 102.5	% Lift on Fr. Fwd	Aft	Area Yd^2	Oz/yd^2	Weight lbs	No. of Valves	Valve Setting H_2O
0	120000	-7.9	-110.4	66.4	33.6	1719	5.91	635	1	1.54
I	270000	-10.1	-92.4	57.5	42.5	2665	5.93	988	1	1.53
II	425000	.27.0	075.5	54.4	45.6	3896	6.46	1573	2 *	1.78
III	740000	46.9	-55.6	52.9	47.1	5583	6.47	2258	3 *	1.85
IV	880000	69.0	-33.5	51.3	48.7	6275	6.64	2605	3 *	1.91
V	948000	91.3	-11.2	50.3	49.7	6527	6.46	2634	3 *	1.94
VI	970000	113.6	+11.1	49.3	50.7	6693	6.51	2722	3 *	1.83
VII	855000	136.0	+33.5	49.1	50.9	5843	6.91	2523	3 *	1.54
VIII	849000	158.3	+55.8	48.0	52.0	6181	6.5	2512	3 *	1.78
IX	496000	178.0	+75.5	45.7	54.3	4458	6.45	1798	2 *	1.81
X	210000	192.4	+89.9	43.8	56.2	2544	6.45	1025	2	1.71
XI	83000	201.9	+99.4	26.3	73.7	1464	6.20	567	0 **	

* Indicates that one of the valves is a combined automatic and maneuvering

** Cell XI valves through Cell X

ADDITIONAL CHRONOLOGICAL HISTORY OF GERMAN AIRSHIP EVENTS

1910

As early as 1910 the "Deutsche Luftschiffahrts-Aktien-Gesellschaft", "DELAG", a subsidiary of the Luftschiffbau Zeppelin Company, operated sightseeing and inter-city trips. The airship LZ-6 maintained service between August 25, 1909, and September 14, 1910, while the airship LZ-7 "Deutschland" was operated from June 19, 1910, to June 28, 1910.

1911-14

The airship LZ-8 "Ersatz Deutschland" operated in similar passenger sightseeing flights from March 30, 1911, to May 16, 1911. The airship LZ-10 "Schwaben" was placed into service on June 26, 1911, and was operated until July 28, 1912. In 143 flying days she made 234 trips totaling 400 hours and covering 27,321 kilometers with 4,354 passengers. The LZ-11 "Victoria Luise" was placed into service on February 14, 1912, the LZ-13 "Hanse" on July 30, 1912, and the LZ-17 "Sachsen" on May 3, 1913. Those three airships were operated until the outbreak of the World War, i.e. till July 31, 1914. The "Victoria Luise" made 409 trips lasting 981 hours, carrying 9738 passengers over 54,312 km.

1914-18

During the World War the Luftschiffbau Zeppelin Company, Friedrichshafen, designed and built 88 airships at four plants, which added to the 25 pre-war airships, totaling 113 built to

the end of the World War. Between 1919 and 1924, 4 more were built, the last, the LZ-126, or ZR-III, or "Los Angeles" coming to the United States on reparations account.

1917

The World War developed no great need for airships of great range, since common in airship service, but there might be mentioned the first 100-hour airship flight, that of the LZ-120, later the "Bodensee". In the summer of 1917 it cruised for this length of time over the Baltic in an observation mission and demonstrated the practicability of airships as a means of transport to distant lands.

From November 21 to November 25, 1917, the airship L-59 made its remarkable long-distance flight in relief of a beleaguered garrison in German East Africa. From Jamboli, Bulgaria, it flew over Asia Minor, the Aegian Sea, Smyrna, across the Mediterranean, the Sahara to the vicinity of Khartum, more than half the distance to its proposed destination, when it received a radio message to return, the situation of the garrison having been reported hopeless. The airship, thereupon, turned about for its base. When the ship reached its base, it had flown a crew of 22 and 14 tons of freight, including ammunition and medical supplies, a total of 95 hours a non-stop distance of 4,225 miles, yet there remained aboard, in addition to the payload, enough fuel for a further two day's flight at reduced speed. During the World War German Army and Navy airships flew about 26,000 hours, a distance of almost two million kilometers, and made approximately 5,000 flights.

1919

The airship LZ-120 "Bodensee", which made its first flight on August 20, 1919, followed its predecessors in passenger service, after the war interval. Operated by "DELAG", the converted war airship was 98 days in service, making 103 trips with 2,380 passengers and covering 32,292 miles from August 20 to December 1, 1919.

The LZ-120 "Bodensee" was then lengthened to meet the dimensions of the LZ-121 "Nordstern", with which two ships, carrying 30 paying passengers each, it was intended to open an airship line in the spring of 1920 between Switzerland and Stockholm, Sweden, via Berlin and to Italy and Spain. The Estente objected, however, and both ships had to be turned over to the Allies. The LZ-121 "Nordstern", which made its first flight on June 8, 1921, was delivered to France on June 13, 1921, and was named "Mediteranne" by the French Navy. The LZ-120 "Bodensee" was delivered to Italy on July 3, 1921, and named "Esperia" by the Italian Army, having been flown from Friedrichshafen to Rome, via Zurich, Berlin, Geneva, Cannes, Nice, Monaco, Corsica and Elba, a distance of 825 miles, in 12 hours 49 minuts.

1924

The airship LZ-126, or ZR-III, or "Los Angeles", which made its first flight on August 27, 1924, was flown from Friedrichshafen to Lakehurst, N. J., a distance of 5,066 statute miles, in 81 hours and 17 minutes, with a crew of 27 and 4 others, i.e., a total of 31, on October 12 to 15, 1924.

1928

The LZ-127 "Graf Zeppelin" was launched on September 18, 1928, and withdrawn from service on June 18, 1937. The airship LZ-129 "Hindenburg" was operated from March 4, 1936, to May 6, 1937, when the ship was destroyed by fire while landing at Lakehurst, N. J. The LZ-130 "Graf Zeppelin" made the first flight on September 14, 1938, and was scheduled to be placed into transoceanic service of the Deutsche Zeppelin-Reederei [German Zeppelin Transport Company]. 119 airships were constructed in all, but 11 serial numbers did not pass beyond the plans on the drawing boards. The serial numbers LZ-70, 115, 116, 117, 118, 119, 122, 123, 124, 125, and 128 were not built.

On October 11 to October 15, 1928, a Friedrichshafen - Lakehurst non-stop trip was made by LZ-127 "Graf Zeppelin", covering a 6,168 miles in 111 hours, 44 minutes, over Dasle, Lyon, Barcelona, Valencia, Gibralter, Agadir, Madeira, Azores, Washington and New York, with a crew of 40 and 20 passengers. Heavy weather was successfully overcome en route, though a proposed routing over Havana was omitted. This was the second trans-Atlantic airship crossing.

On October 29 to November 1, 1928, a Lakehurst-Friedrichshafen non-stop trip was made by LZ-127 "Graf Zeppelin", covering 4,535 miles in 71 hours, 51 minutes, with 25 passengers, 66 persons in all, via Newfoundland, Brest, Nantes, Tours and Basle.

In all, the LZ-127 "Graf Zeppelin" made 11 trips in 1928, carrying 565 passengers a distance of 15, 585 miles in a flying time of 269 hours and 5 minutes.

1929

IN 1929 the LZ-127 "Graf Zeppelin" made the following trips:

March 26 to March 28, 1929, with a crew of 41 and 27 passengers, non-stop Friedrichshafen-Palestine and return, 4,970 miles in 81 hours and 28 minutes.

April 23 to April 25, 1929, with crew of 41 and 22 passengers, non-stop Friedrichshafen - Spain - Algeria and return, 3,355 miles in 56 hours and 53 minutes.

August 1 to August 5, 1929, with crew of 40 and 18 passengers, non-stop Friedrichshafen - Lakehurst, via Cadiz and Azores, 5,188 miles in 95 hours and 22 minutes.

August 7 to August 10, 1929, with crew of 40 and 22 passengers, non-stop Lakehurst - Friedrichshafen, via New York and Paris, 4,391 miles in 55 hours and 22 minutes.

1930

In 1930 the LZ-127 "Graf Zeppelin" made the following trips:

April 15 to April 17, 1930, from Friedrichshafen to Seville [Spain] and return after a stop at Seville, carrying 34 and 36 passengers respectively, for 3,240 miles in 51 hours and 45 minutes round trip.

April 26 to 27, 1930, Friedrichshafen - Cardington [England] and return. A total of 65 passengers were carried the 1,496 miles in 24 hours and 6 minutes.

May 18 to May 25, 1930, First South American trip, Friedrichshafen - Seville - Pernambuco - Rio de Janeiro, with stops at each, 7,117 miles in flying time of 118 hours and 50 minutes. Passenger total was 105.

May 25 to June 6, 1930, return voyage from Rio de Janeiro via Pernambuco, Lakehurst and Seville to Friedrichshafen, with stops at each, 11,298 miles in 181 hours and 8 minutes, the total of 138 passengers being carried one stage or another.

July 9 to 11, 1930, Friedrichshafen - North Cape and return, non-stop, 4,854 miles in 70 hours and 41 minutes with 35 passengers for the round trip.

July 16 to July 18, 1930, flew 37 passengers 4,667 miles to Iceland and return, non-stop from Friedrichshafen, in 60 hours and 41 minutes.

September 9 to September 11, 1930, Friedrichshafen - Moscow and return, with 38 and 40 passengers respectively, the 2,833 miles being covered in a total of 47 hours.

The total operations of LZ-127 "Graf Zeppelin" in 1930 added up to 109 flights 1,155 hours and 23 minutes in the air for 71,934 miles. Passengers carried were 2,656, while the toal number persons on board, including the crew, amounted to 7,070.

1931

Trips by LZ-127 "Graf Zeppelin" in 1931:

April 9 to April 13, 1931, Friedrichshafen - Cairo and return, with an ascent at Cairo of 10 hours and 46 minutes. The voyage

both ways covered 5,089 miles in 84 hours and 40 minutes, with passengers in both directions.

June 30 to July 3, 1931, Friedrichshafen - Iceland and return, non-stop, 4,297 miles in 72 hours and 43 minutes.

July 24 to July 31, 1931, Friedrichshafen - Arctic exploration flight with stops at Berlin, Leningrad, Franz Joseph Land, Berlin, 8,316 miles for the five stages, a trip of 136 hours and 26 minutes.

August 18 to August 20, 1931, paid another visit to England, flying from Friedrichshafen to London, a distance of 1,298 miles round trip in 23 hours and 1 minute. While there the ship made a circuit over England covering 1,214 more miles in another 23 hours and 10 minutes.

Between August 29, 1931, and October 28, 1931, 3 round trips between Germany and Brazil, covering 30,154 miles in 475 hours and 49 minutes.

Scores of other voyages about its Friedrichshafen base or to other cities, non-stop or in stages, were made during the year. In all, the LZ-127 "Graf Zeppelin" made 73 trips, covering 73,566 miles in a flying time of 1,186 hours and 59 minutes, carrying in all 2,056 passengers, and 4,959 persons, including the crew.

1932

On March 20, 1932, the first regularly scheduled transoceanic air service was inaugurated, when the LZ-127 "Graf Zeppelin" left from Friedrichshafen on her first scheduled voyage to

South America, carrying passengers, mail and freight. The bulk of all long distance voyage made in 1932 were those between Friedrichshafen and Bernambuco or Rio de Janeiro, 9 round trips being made across the South Atlantic, covering 98,765 miles in 1,560 hours and 57 minutes flying time. The service was maintained with the regularity and dependability of a steamship service, and passengers enjoyed many of the advantages and comforst found on ocean liners. On most voyages the airship was booked to capacity, and for season sailing very often the demand became so heavy that a system of waiting lists had to be introduced. Many other trips were made, of course, pleasure cruises over Germany and Switzerland in particular enjoying the preference of passengers from all parts of the world.

In 1932, flights totaled 59, mileage 112,521 and duration 1,770 hours and 11 minutes. 1,309 passengers were carried, and 3,781 persons, including crew, were on board.

1933

Eight round trips between Europe and South America were made by the LZ-127 "Graf Zeppelin" in 1933, the terminals being Friedrichshafen and Rio de Janeiro and intermediate landings being made at Bermanbuco and Seville. Between October 14 and November 2, 1933, a triangular flight was made from Friedrichshafen via Bernambuco, Rio de Janeiro, Bernambuco, Miami, Akron, Chicago, Akron, Seville and Friedrichshafen.

In 1933, the total number of flights was 64, covering 131,936 miles, carrying 1,314 passengers, and 4,070 persons, including the crew, in a flying time total of 2,064 hours and 48 minutes.

1934

Flights were made from May 26 to December 19, 1934. Again this year the operations over the South Atlantic between Friedrichshafen and Rio de Janeiro made up practically the entire total of the LZ-127 "Graf Zeppelin". The ship made 12 round trips to South America. One side excursion was made to Buenos Aires.

The total operations were 68 flights,159,958 miles, 2,495 hours and 22 minutes, 1,600 passengers, and 4,420 persons carried including crew, aside from mail and express.

1935

This year the LZ-127 "Graf Zeppelin" made 16 round trips between Germany and Brazil, flying 352,478 kilometers in 3,512 hours and 56 minutes, carrying 553 passengers over the entire route - Friedrichshafen - Rio de Janeiro.

The whole year's operations totaled 82 flights, 3,535 hours and 56 minutes, 355,257 kilometers, and 1,429 passengers, aside from large quantities of mail and freight.

1936

On March 4, 1936, the airship LZ-129 "Hindenburg" made its first trial flight, and on March 31, 1936, the ship left Friedrichshafen for its first flight to Rio de Janeiro non-stop. On May 6, 1936, the ship sailed from Friedrichshafen on its first flight to Lakehurst, N. J., non-stop. In 1936, the LZ-129 "Hindenburg" made 7 round trips between Germany and Brazil, and 10 round trips between Germany and the United States. In the

South American service the LZ-129 "Hindenburg" covered 148,335 kilometers in 1,365 hours and 53 minutes, and in the North Atlantic service 136,949 kilometers in 1,163 hours and 42 minutes. 1,006 passengers were carried by both the LZ-127 "Graf Zeppelin" and the LZ-129 "Hindenburg" in the South American service in 1936, while the LZ-129 "Hindenburg" carried 1,002 passengers in the North Atlantic service.

Between April 13 and December 1, 1936, the LZ-127 "Graf Zepplin" made 13 round trips between Germany and Brazil, covering 280,349 kilometers in 2,793 hours and 50 minutes.

In all, both airships covered in 1936 the tremendous figure of 598,490 kilometers in 5,697 hours and 5 minutes and carried, including a number of shorter flights, a total of 3,080 passengers, of whom 2,008 were carried in transoceanic service.

1937

The LZ-129 "Hindenburg" made one round trip to South America, and the LZ-127 "Graf Zeppelin" made 3 round trips to South America. Service was discontinued, when the LZ-129 "Hindenburg" was destroyed by fire at Lakehurst, N.J., on May 6, 1937. The LZ-127 "Graf Zeppelin" was retired after 9 years of service and thrown open for inspection by the general public at the Rhine-Main airship port near Frankfort-on-Main. Since July 8, 1937, until the end of 1938, more than 700,000 visitors from all parts of the world inspected the interior of the veteran airliner.

From September 18, 1928, to June 18, 1937, the LZ-127 "Graf Zeppelin" made 590 trips, 144 ocean crossings, covered

1,695,272 kilometers in 17,178 hours, carried 13,110 passengers, 39,219 kilograms of mail, and 30,446 kilograms of freight. The ship crossed the South Atlantic 136 times, the North Atlantic 7 times, and the Pacific Ocean once. From November 22 to November 27, 1936, the ship established a long endurance record in the air, remaining in the air 118 hours and 40 minutes, being prevented from landing by communist uprisings in Brazil. The shortest flight time from Friedrichshafen to Bernambuco was 61 hours and 24 minutes on September 15, 1934, and the shortest time from Bernambuco to Friedrichshafen 67 hours and 27 minutes on September 18, 1932.

The performance data of the LZ-129 "Hindenburg" from March 4, 1936, to May 6, 1937, were: 332,626 kilometers, 3,059 passengers carried, 37 ocean crossing [South Atlantic 16 times, North Atlantic 21 times].

The shortest flight times of the LZ-129 "Hindenburg" were:

Frankfort-on-Main - Lakehurst, N. J.:
52 hours and 49 minutes on June 30, 1936

Lakehurst, N. J. - Frankfort-on-Main:
42 hours and 52 minutes on August 10, 1936

Frankfort - Rio de Janeiro:
83 hours and 13 minutes on May 28, 1936

Rio de Janeior - Frankfort:
93 hours and 17 minutes on May 30, 1936

1938

The airship LZ-130 "Graf Zeppelin" made its first trial flight on September 14, 1938. Until the end of 1938, the ship made 8 trial flights over Germany, only members of the crew and of the technical staff being on board.

APPENDIX D

DERIVATION OF CONVENTIONAL ELLIPSOIDAL AIRSHIP STRUCTURAL WEIGHT ESTIMATING RELATIONSHIPS

CONVERSION FACTORS FOR APPENDIX D

1 ft^3 = 0.02832 m^3

1 knot = 0.51389 m/sec

Presented in this Appendix is the derivation of the Structural Weight Estimating Relationships, WER's, for conventional ellipsoidal airships used in the Goodyear Airship Synthesis program during the Phase I study. Key structural design assumptions and the WER derivation are presented for the following types of airship construction: Rigid, three types of pressurized metal-clad airships, and pressurized fabric non-rigids, as described in Reference D-1.

RIGID AIRSHIP STRUCTURAL WEIGHT ESTIMATING EQUATIONS

These weight estimating equations establish the weight of the hull shell structural fabric components for rigid airships parametrically as a function of volume, speed, fineness ratio, and aerodynamic lift or heaviness. The structural components are listed below. Due to the proprietary nature of the structural weight equations, only their functional formulation is presented.

1. Main frames
2. Intermediate frames
3. Axial girder
4. Longitudinals
5. Stern and bow
6. Diagonal shear wiring
7. Gas cells
8. Gas valves
9. Gas bag wiring
10. Outer cover
11. Outer cover wiring
12. Empennage
13. Cruciform
14. Control car

15. Corridors
16. Crew quarters
17. Cooring and handling equipment

GENERAL

The method used in developing the weight estimating relationships is similar to that used by Normand as outlined on Page 20 of Reference D-2.

The parameters that affect component weight would be one or a combination of airship velocity, volume, length, diameter, frame spacing, material strength, gust velocity, aerodynamic moment, fin area, and altitude.

To minimize the number of variables the following assumptions were made:

1. The hull structure will be designed by the gust loads. Maneuvers will be limited so that their stresses will not exceed the gust loads.
2. The frame spacing is constant and equal to 20 ft.
3. The spacing of the longitudinals is a constant and the same as on the Akron and Macon.
4. The number of main frames is constant and equal to 10.
5. The length/depth ratio of the longitudinals is constant.
6. The equation for the contour of the airship is assumed to be that used on non-rigid airships:

$$Y = R\left(1.02062 - 0.21263 \times \frac{2X}{L}\right)\left[1 - \left(\frac{2X}{L} - 0.2\right)^2\right]^{1/2}$$

where

X is measured from maximum diameter
R is maximum radius, and
L is hull length

Employing the contour expressed by the above equation, one obtains for the volume:

$$V = 0.64381 \ \pi R^2 L$$

$$V = 0.16095 \ \pi D^2 L$$

$$V = 0.16095 \ \pi (D/L)^2 L^3$$

or

$$V = 0.16095 \ \pi (L/D) D^3 \sim (L/D) D^3$$

which for L gives

$$L = 1.25522 \ V^{1/3} \ (L/D)^{2/3} \sim V^{1/3} \ (L/D)^{2/3}$$

For D

$$D = 1.25522 \ V^{1/3} \ (D/L)^{1/3} \sim V^{1/3} \ (D/L)^{1/3}$$

The surface area, S, derived from the contour equation is

$$S = 3.80243 \ V^{2/3} \ (L/D)^{1/3} \sim V^{2/3} \ (L/D)^{1/3}$$

Normand breaks the total weight of the airship into various components. The weight of each component can be expressed as a product of some constant times the parameters that affect the weight of the component raised to some appropriate factor. As an example

$$W_Z = KL^x D^y \alpha^z \beta^w$$

where L and D are the airship length and diameter and α and β

could be such parameters as airship velocity and altitude.

The factor, K, can be best arrived at from actual weight data of airships. The factor, K, was derived from the following sources:

1. Akron and Macon actual weights
2. Goodyear design studies of a 10,250,000 cu ft airship
3. Goodyear design studies of a 3,500,000 cu ft airship
4. Tests on 75 ST aluminum airship girders made by Goodyear Aerospace on a company-funded R&D program
5. Studies of allowable strengths of materials available today.

The loads developed in the various structural components depend upon one or more of the following parameters: aerodynamic moment [M_A], aerodynamic shear, static moment [M_S], static shear, gas shear, gas pressure, aerodynamic pressure, and acceleration.

It can be shown that the above loads are a function of airship volume, length, diameter, velocity, altitude, and gust velocity:

$$M_A \sim \rho \mu v V$$

$$\text{Aerodynamic shear} \sim \frac{M_A}{L} \sim M_A \; V^{-1/3} \; (L/D)^{-2/3}$$

$$M_S \sim V \times L \sim V \times V^{1/3} \; (L/D)^{2/3} \sim V^{4/3} \; (L/D)^{2/3}$$

$$\text{Static shear} \sim V$$

$$\text{Gas pressure} \sim D \sim V^{1/3} \; (L/D)^{-1/3}$$

$$\text{Aerodynamic pressure} \quad q \sim \rho v^2$$

$$g \text{ acceleration } \frac{\text{(aerodynamic pressure area) (area)}}{\text{mass}}$$

$$g \sim \frac{(\rho\mu v)\ (LD)}{V} \sim \frac{\rho\mu v\ LD}{LD^2}$$

$$g \sim \frac{\rho\mu v}{D}$$

Using the relationships established above, equations can now be developed for the various structural components.

MAIN FRAMES AND AXIAL GIRDER

The main frames are designed principally by the deflated cell condition. Burgess ha- shown [Page 26 of Reference D-2] that if this is the case the weight of main frames is

$$ND^4 \sim NV^{4/3}\ (L/D)^{-4/3}$$

where N is the number of main frames.

INTERMEDIATE FRAMES

The intermediate frames are subjected to aerodynamic shear loads, static shear loads, and gas pressure loads. The load in the frame due to shear is equal to KQ/a, where Q is the shear on the airship, a is the number of longitudinals, and K is dependent upon the type of shear bracing. The weight would then be proportional to the product of load and circumference:

$$\text{Circumference} = \pi D = a \times s$$

where s is spacing or longitudinal.

$$\text{Weight} \sim \frac{KQ}{a} \times \text{as} \sim KQs$$

where s is assumed constant in this study; therefore, weight is proportional to Q.

$$\text{The aerodynamic shear} \sim \frac{M_A}{L} \sim \frac{M_A}{V^{1/3}\ (L/D)^{2/3}}$$

Therefore,

$$\text{Aerodynamic weight} \sim \frac{M_A}{V^{1/3}\ (L/D)^{2/3}}$$

The static shear $\sim$ lift $\sim$ V

Therefore, static weight is approximately equal to V.

The gas pressure will produce bending moments in the longitudinals, which in turn will produce axial loads in the booms of the frame. This equivalent axial load is

$$F = Kw\ (s/h)$$

where:

w	=	the running load of the girder,
s	=	the spacing of the longitudinals,
h	=	the depth of frame, and
K	=	a constant.

$w \sim d \cdot \ell$

s is constant in this study

h will be assumed $\sim$ D

Then

$$F \sim \frac{D\ell S}{D}$$

Since ℓ is also a constant in this study, F is a constant.

Therefore:

$$\text{Gas pressure weight} \sim F \times D \sim D \sim V^{1/3} \ (D/L)^{1/3}$$

The weight of the longitudinals is also proportional to their number.

$$\text{Total number of frames} = \frac{\text{Length}}{20} - 1 = \frac{L}{20} - 1$$

Number of intermediate frames = $n = \frac{L}{20} - 1 - N$, where N is number of main frames (10).

$$L = 1.2552 \ V^{1/3} \ (L/D)^{2/3}$$

$$n = \frac{1.2552 \ V^{1/3} \ (L/D)^{2/3}}{20} - 11$$

$$n = 0.062762 \ V^{1/3} \ (L/D)^{2/3} - 11$$

If V is expressed in millions of cubic feet

$$n = 6.2762 \ V^{1/3} \ (L/D)^{2/3} - 11$$

From the above, the weight of the intermediate frames is obtained:

$$w = [cM_A \ (L/D)^{-1/3} \ V^{2/3} + dv + e \ V^{1/3} \ (L/D)^{-1/3}]$$

$$[6.2762 \ V^{1/3} \ (L/D)^{2/3} - 11]$$

Outer Cover

The basic formula developed for the envelope for the non-rigid airship is applicable to the outer cover of the metalclad provided the necessary modifications are made to substitute aluminum for fabric. An ultimate safety factor of three will be maintained. Substituting aluminum for fabric, the weight equation takes the form:

$$W = V\ [K_5 V^{-1}\ (L/D)\ M_A + K_6 V^{1/3}\ (L/D)^{1/3} + K_7 \rho v^2 + K\ ]$$

Ballonets

Individual ballonets will be required for each compartment. They will be cylindrical in cross-ection rather than lenticular as in the non-rigid airship. Because of this difference, the weight required will be greater than that of the non-rigid airship. As in the non-rigid airship, their weight will be proportional to the volume:

$$W = K_3 V$$

Effect of flight heaviness on the weight of the following components will have to be included: outer cover, car structure, landing gear, main frames, and miscellaneous hull.

The same formulas developed for the non-rigid airship will be applicable to the car structure and landing gear. The same formulas developed for the rigid airship will be applicable to the main frames and miscellaneous hull weight. The formula for the outer cover will be of the same form but with a different constant:

$$W = K_4 H V^{1/3}\ (L/D)^{5/3}$$

The formulas for the effect of flight heaviness can be summarized in a single expression:

$$W_H = H\ [K_4 V^{1/3}\ (L/D)^{5/3} + K_5]$$

Summary

The formulas for the weights of the various Metalclad 1 components are summarized below:

Main frames	$W = (a + b\rho v)\ V^{4/3}\ (L/D)^{-4/3}$
Intermediate frames	$W = [cM_{40}\ (L/D)^{-2/3}\ V^{1/3} + dV]$
	$[6.2762\ V^{1/3}\ (L/D)^{2/3} - 11]$
Longitudinals	$W = K_1 M_{40}\ (L/D)$
Outer cover	$W = V\ [K_5 V^{-1}\ (L/D)\ M_A$
	$+ K_6 V^{1/3}\ (L/D)^{-1/3} +$
	$K_7 \rho v^2 + K_8]$
Gas Diaphragm	$W = K_2 V^{2/3}\ (L/D)^{-2/3}$
Gas valves	$W = K_{10} V$
Stern and bow	$W = K_{11} v$
Misc gas cells valves	$W = K_{12} V$
Misc hull weight	$W = K_{13} V$
Empennage and cruciform	$W = K_{14} uv\rho V^{1/3}\ (L/D)^{-1/3} A$

DIAGONAL SHEAR WIRES

The loads in the shear wires are due principally to aerodynamic and static shear loads. The weight due to the aerodynamic shear would be proportional to the product of the aerodynamic shear and L:

$$W_A \sim \text{aero shear} \times L \sim \frac{M_A}{L} \times L \sim M_A$$

The weight due to static shear would be proportional to the product of the static shear and L

$$W_S \sim \text{static shear} \times L \sim V \times L \sim V$$

$$\times V^{1/3} (L/D)^{2/3} \sim V^{4/3} (L/D)^{2/3}$$

Therefore

$$W = K_1 M_A + K_2 V^{4/3} (L/D)^{2/3}$$

LONGITUDINALS

The stresses in the longitudinals are due principally to the aerodynamic load and the gas pressure load.

Weight Due to Aerodynamic Moment - The axial load in a longitudinal due to the aerodynamic moment is

$$P = \frac{4M}{\text{No.} \times D}$$

Where:

M = moment,

No. = number of longitudinals, and

D = diameter.

$$\text{Area long} \sim P \sim \frac{4M}{\text{No.} \times D}$$

Total area of longitudinal at a cross-section is proportional to No. × P

$$A_T \sim \frac{4M}{\text{No.} \times D} \times \text{No.} \sim \frac{M}{D}$$

$$\text{Weight} \sim A_T \times L \sim \frac{M}{D} \times L \sim M(L/D)$$

<u>Weight Due to Gas Pressure Load</u> - The gas pressure on a longitudinal produces bending in the longitudinal:

Running load on long × ∿ pressure × longitudinal spacing

$$\sim D \times \frac{D}{\text{No.}} \sim \frac{D^2}{\text{No.}}$$

Moment in longitudinal ∿ runnning load × length^2

$$\sim \frac{D^2}{\text{No.}} \times \ell^2$$

$$\text{Load in boom} \sim \frac{M}{h} \sim \frac{D^2 \ \ell^2}{\text{No.} \quad h}$$

where h is longitudinal depth

$$\text{Weight longitudinal} \sim \text{load in boom} \times \ell \ \frac{D^2 \ \ell^3}{\text{No.} \times h}$$

Weight long/bay $\sim$ load in boom $\times$ No. $\sim \frac{D^2 \ \ell^3}{\text{No.} \times h}$ No. $\sim \frac{D^2 \ \ell^3}{h}$

Total weight $\sim$ weight long/bay

$$\times \text{ No. bays} \sim \frac{D^2 \ \ell^3}{h} \times \frac{L}{\ell} \ \frac{D^2 \ \ell^2 \ L}{h}$$

$\frac{\ell}{h}$ will be assumed constant in this study

Therefore:

$$\text{Total weight} \sim D^2L^2 \sim V \times V^{1/3} \ (L/D)^{2/3} \sim V^{4/3} \ (L/D)^{2/3}$$

The weight of longitudinals can then be expressed in the form

$$W = K_3 M_A \ (L/D) + K_4 V^{4/3} \ (L/D)^{2/3}$$

OUTER COVER

The weight of the outer cover is proportional to the surface area $S \sim V^{2/3}(L/D)^{1/3}$ and to some power of the velocity. The assumption will be made that

$$W \sim K_5 V^{2/3} \ (L/D)^{1/3} \rho^{1/2} v$$

OUTER COVER WIRES

The weight of wires will be assumed to be proportional to the product of the surface area and the dynamic pressure

$$W \sim K_6 V^{2/3} \ (L/D)^{1/3} \ \rho v^2$$

GAS BAG WIRING AND NETTING

The tension in a wire subjected to a uniformly distributed load with no initial tension is

$$T^3 = \frac{EaP^2}{24}$$

$$T^2 = E\ (a/T)\ \frac{P^2}{24}$$

$$T^2 = \frac{E}{F_T}\ \frac{P^2}{24}$$

where

T = wire tension,
P = total transverse load on wire,
E = Young's modulus,
a = wire area, and
F_t = tensile stress

If spacing of longitudinals is kept constant,

$$P \sim D$$

$$T^2 \sim \frac{E}{F_t} \times \frac{D^2}{24}$$

$$T \sim D\ (E/F_T)^{1/2}$$

$$a = \frac{T}{F_t} \sim \frac{D\ (E/F_t)^{1/2}}{F_t} \sim \frac{D}{F_t^{3/2}}$$

Total weight $\sim$ a (surface area) $\sim$ aLD $\sim D^2L \sim V$

Therefore:

$$W = K_7 V$$

GAS CELLS

The weight of gas cell fabric per square yard will be assumed constant. The total area of fabric would then be proportional to the sum of the surface area and twice the sum of the areas of the main frames.

Surface area $\sim V^{2/3} (L/D)^{1/3}$

Bulkhead areas $\sim D^2N \sim V^{2/3} (L/D)^{-2/3} N$

Since N is taken as a constant equal to 10 in this study:

Bulkhead areas $\sim V^{2/3} (L/D)^{-2/3}$

The weight of the gas cells can then be expressed by the formula

$$W = V^{2/3} [K_8 (L/D)^{1/3} + K_9 (L/D)^{-2/3}]$$

GAS VALVES; STERN AND BOW; MISCELLANEOUS GAS CELLS, VALVES, AND SUPPORTS; MISCELLANEOUS HULL WEIGHT

All of these components will be assumed to be a constant percentage of the volume.

EMPENNAGE AND CRUCIFORM

The expression developed for the non-rigid airship will be used

except that the weight will be increased to account for the cruciform weight

$$W = K_{14} uv\rho V^{1/3} \ (L/D)^{-1/3} \ A$$

CORRIDORS, CONTROL CAR, AND CREW QUARTERS

The weight of the corridors, control car, and crew quarters is assumed to $\sim L \sim V^{1/3} \ (L/D)^{2/3}$. Therefore:

$$W = K_{15} V^{1/3} \ (L/D)^{2/3}$$

MOORING AND HANDLING EQUIPMENT

This weight is assumed to vary directly with the volume:

$$W = K_{16} V$$

EFFECT OF FLIGHT HEAVINESS ON WEIGHT

When the airship is flying heavy, the shear and moment on the airship will be increased. Therefore, those components affected by shear and moment loads will increase in loads and consequently weight. The affected components are main frames, intermediate frames, diagonal shear wires, longitudinals, and miscellaneous hull weight.

The following assumptions can be made:

Shear due to heaviness $\sim$ heaviness

Moment due to heaviness $\sim$ heaviness $\times$ L $\sim HV^{1/3} \ (L/D)^{2/3}$

Substituting these values of shear and moment for the previously used aerodynamic and static shears and moments in the equations previously developed, one obtains for the weight due to heaviness.

Main frames $W = K_{17}H$

Intermediate frames $W = K_{18}HV^{1/3}(L/D)^{-1/3}[6.2762V^{1/3}(L/D)^{2/3} - 11]$

Diagonal shear wires $W = K_{19}HV^{1/3}\ (L/D)^{2/3}$

Longitudinal $W = K_{20}HV^{1/3}\ (L/D)^{5/3}$

Misc. Hull weight $W = K_{21}H$

WEIGHT SUMMARY [RIGIDS]

The weight equations for the various rigid airship components are summarized below.

Main frames $W_1 = (a + b\rho v)V^{4/3}\ (L/D)^{-4/3}$

Intermediate frames $W_2 = [cM_A\ (L/D)^{-2/3}V^{-1/3} + dV + \rho V^{1/3}\ (L/D)^{-1/3}]]6.2762\ V^{1/3}\ (L/D)^{2/3} - 11]$

Diagonal wires $W_3 = K_1M_A + K_2V^{4/3}\ (L/D)^{2/3}$

Longitudinals $W_4 = K_3M_A\ (L/D) + K_4V^{4/3}\ (L/D)^{2/3}$

Outer Cover $W_5 = K_5V^{2/3}\ (L/D)^{1/3}\ \rho^{1/2}v$

Outer cover wires $W_6 = K_6 V^{2/3} (L/D)^{1/3} \rho v^2$

Gas bag wires and netting $W_7 = K_7 V$

Gas cells $W_8 = V^{2/3} [K_8 (L/D)^{1/3} + K_9 (L/D)^{-2/3}]$

Gas valves $W_9 = K_{10} V$

Stern and blow $W_{10} = K_{11} V$

Misc gas cells, valves $W_{11} = K_{12} V$

Misc hull weight $W_{12} = K_{13} V$

Empennage and cruciform $W_{13} = K_{14} uv\rho V^{1/3} (L/D)^{-1/3} A$

Corridors, control car, crew quarters $W_{14} = K_{15} V^{1/3} (L/D)^{2/3}$

Mooring and handling $W_{15} = K_{16} V$

Effect of flight heaviness

Main frames $W_{16} = K_{17} H$

Intermediate frames $W_{17} = K_{18} HV^{1/3} (L/D)^{-1/3}$

$[6.2762 V^{1/3} (L/D)^{2/3} - 11]$

Diagonal shear wires $W_{18} = K_{19} HV^{1/3} (L/D)^{2/3}$

Longitudinal $W_{19} = K_{20} H V^{1/3} (L/D)^{5/3}$

Misc. hull weight $W_{20} = K_{21} H$

where:

V = volume

L/D = length/maximum diameter

M_A = aerodynamic moment

ρ = mass air density

v = airship velocity

u = gust velocity

H = airship heaviness

a,b,c = constants

$K_1 \rightarrow K_{21}$ = Goodyear propriatary constants

NON-RIGID AIRSHIPS

GENERAL

The same basic approach can be used to develop the structural WER's for the non-rigid airships that was used for the rigid airships. The only basic difference is that, because of the many non-rigid airships built and the many studies made by Goodyear, much more accurate data was available for establishing the necessary constants.

Developing weight equations involved a review of weights of 11 non-rigid airships ranging in size from 200,000 cu ft to

2,800,000 cu ft. The stress analysis of each also was reviewed. The airships investigated covered 1945 to 1975. Because most of the airships studied were designed for different missions and therefore to different requirements each had to be analyzed separately, with consideration given to the mission requirements peculiar to each.

ENVELOPE

The envelope pressure is selected so that it will not wrinkle when subjected to the limit design flight conditions. The pressure required at the equator is readily obtained form the formula.

$$P_e = \frac{2M}{\pi R^3}$$

where M is the moment and R is the radius. In this study, M will be taken as the maximum moment and R the maximum radius even though the maximum moment and the maximum radius do not necessarily occur at the same point. The error is not significant. M is the total moment acting on the section and is the sum of the aerodynamic moment, load lift moment, gas gradient moment, and rigging moment. A review of past airships shows that the total moment (M) can be expressed as a constant times the aerodynamic moment

$$M = K_1 M_A$$

The maximum tension in the fabric occurs in the circumferential direction and is obtained from

$$\sigma = P_T R$$

where P_T is the total pressure.

The total pressure at the top of the envelope would be the sum of

1. The required pressure (P_e) at the equator
2. The difference in pressure between the equator and the top due to the gas gradient, $P_g = 0.06\ R$
3. The negative dynamic pressure acting on the envelope, which can be expressed as $P_D = K_2 q = K_3 pv^2$
4. Any overpressure that might occur as the airship rises above pressure height in an emergency condition. This pressure is dependent upon the vertical ascent rate and the design of the helium valve, both of which are considered constant in this study [$P_D = K_4$].

$$P_T = P_e + 0.06R + K_3\ pv^2 + K_4$$

If the fabric stress is known, the weight of the fabric can readily be found by multiplying the fabric stress by an appropriate factor, which includes a factor of safety, effect of stress concentrations, and the effect of fabric strength deterioration due to creep rupture effects.

The unit fabric weight as a function of strength was obtained empirically from a study of existing fabrics and can be expressed as

$$W = G_{break} + K5$$

The surface area of the envelope is

$$S = 0.43094\ V^{2/3}\ (L/D)^{-1/3}$$

where

$$V = \text{volume} \times 10^{-6}\ \text{cu ft}$$

and the radius is

$$R = 62.76\ V^{1/3}\ (L/D)^{-1/3}$$

If the unit weight of the fabric and the surface area as known, the envelope weight can radily be obtained from

$$W = wSK_6$$

where K_6 is a constant that allows for the added weight for seams.

Substituting in this formula, we obtain

$$W = K_7V^{2/3}\ (L/D)^{1/3}\{K_8V^{1/3}\ (L/D)^{-1/3}[K_9V^{-1}\ (L/D)\ M_A + K_{10}V^{1/3}\ (L/D)^{-1/3} + K_{11}\ \rho v^2 + K_{12}] + K_{13}\}$$

<u>Suspension System</u> - A review of past airship designs shows that the suspension system weight varies directly with the suspended load. The total suspended load is made up of the static and the aerodynamic g load:

$$\text{Static load} \sim \rho V$$

$$\text{Aero g load} \sim V \times \frac{V}{D} \rho \sim \frac{vV\rho \ (L/D)^{1/3}}{V^{1/3}} \sim \rho v V^{2/3}$$

The weight can then be expressed as

$$W = K_{14}\rho V + K_{15}\rho v V^{2/3} \ (L/D)^{1/3}$$

Bow Stiffening - Statistically, the bow stiffening varies directly as volume

$$W = K_{16}V$$

Ballonets and Airlines - Ballonets of a particular configuration [two, three, or four ballonet system] will vary in volume and in weight directly with envelope volume. For this analysis, only a four-ballonet system will be considered:

$$W = K_{19}V$$

MISCELLANEOUS ENVELOPE WEIGHT

The miscellaneous envelope weight will be assumed to vary directly with volume:

$$W = K_{18}V$$

EMPENNAGE

Empennage weight varies with area [A] and loading. Area will be computed separately based on stability and control requirements

and therefore will be considered as a variable in the weight equations. The weight equation for empennage is generated through the following relationships:

Moment in fin frames $\sim$ A $\times$ unit loading $\times$ moment arm

Area of frame flanges $\sim$ M/h where h = depth of frame at base

Volume of material $\sim$ area of flanges $\times$ length of frame

Unit loading $\sim$ ρuv; moment arm $\sim$ D

Weight $\sim$ volume of material

$$\sim \frac{A\rho uv \times D \times \text{length of frame}}{h}$$

Assume length of frame/h = constant, then

$$\text{Weight} \sim Auv\rho V^{1/3} \ (L/D)^{-1/3}$$

$$W = K_{19} Auv\rho V^{1/3} \ (L/D)^{-1/3}$$

PRESSURE SYSTEM

The pressure system is made up of the valves, blowers, associated control systems, and provisions for mounting. Statistically, the pressure system weight varies with volume

$$W = K_{20} V$$

CAR STRUCTURE AND OUTRIGGER

For this non-rigid parametric weight study, it is assumed that all ships will have a tricycle landing gear, with the main gear located in outriggers attached to the car. For this reason, the outrigger weight is included with the car structure. The form of the weight equation will be the same as that developed for the suspension system.

$$W = K_{21}\rho V + K_{22}\ \rho v V^{2/3}\ (L/D)^{1/3}$$

LANDING GEAR

The assumption is made that only tricycle gears will be considered. Landing gear weight varies with envelope volume and sinking speed. It is further assumed that airship sinking speeds will be equivalent to the ZPG-3W. If these assumptions are used, the landing gear weight is $W = KV$.

EFFECT OF HEAVY FLIGHT ON STRUCTURE WEIGHT

Source of Additional Weight - Heaviness is defined as the difference between the static lift and the gross weight. It is assumed that heaviness results from additional weight [as opposed to a reduction in lift] and that all of this weight will be added in the car. This added weight will have the following effect:

1. Increase in envelope weight resulting from the added heaviness moment.

2. Increase in car structure, suspension system, and landing gear weight resulting from the gross weight increase in the amount of the heaviness.

Heaviness Moment Effect on Fabric Weight - The increase in total moment is given by:

$$M_H = K_{23} H V^{1/3} (L/D)^{2/3}$$

This increase in moment will require an increase in pressure at the equator of

$$\Delta P_e = \frac{2M_H}{\pi R^3}$$

Substituting the value of M_H and R previously developed into this equation, one obtains

$$\Delta P_e \sim K_{24} H V^{2/3} (L/D)^{5/3}$$

The increase in fabric weight would be

$W \sim \Delta P_e \times R$ [slope of unit fabric weight curve] [surface area]

Making the appropriate substitutions

$$W = K_{25} V^{1/3} (L/D)^{5/3} H$$

Car Structure - By definition, heaviness will increase car gross weight. The increase in weight would be proportional to the heaviness:

$$W = K_{26}H$$

Suspension System - The suspension system weight also would increase proportionally to the heaviness:

$$W = K_{27}H$$

LANDING GEAR

Landing gear weight varies with volume and airship sinking speed. In considering heaviness only, the volume remains constant; however, it will be assumed that a significant increase in heaviness will result in an increase in sinking speed with associated increase in gear weight.

By comparing the weights of the ZPG-1 and the ZPG-3W landing gears, the formula for the weight increase can be developed:

$$W = K_{28}H$$

SUMMARY OF EFFECT OF HEAVINESS ON WEIGHT OF NON-RIGID AIRSHIPS

The equations developed above can be summarized into a single equation that takes the form

$$W = K_{29}H\ [K_{30}V^{1/3}\ (L/D)^{5/3} + 1]$$

WEIGHT SUMMARY [NON-RIGID]

The weight equations for the various non-rigid structural components are summarized on the following page.

Envelope	$W_1 = K_7 V^{2/3} (L/D)^{1/3} \{K_8 V^{1/3} (L/D)^{-1/3} [K_9 V^{-1} (L/D) M_A + K_{10} V^{1/3} (L/D)^{-1/3} + K_{11} \rho v^2 + K_{12}] + K_{13}\}$
Suspension system	$W_2 = K_{14} \rho V + K_{15} \rho v V^{2/3} (L/D)^{1/3}$
Bow stiffening	$W_3 = K_{16} V$
Ballonets and air lines	$W_4 = K_{17} V$
Miscellaneous	$W_5 = K_{18} V$
Empennage	$W_6 = K_{19} A u v \rho V^{1/3} (L/D)^{-1/3}$
Pressure system	$W_7 = K_{20} V$
Car structure and outriggers	$W_8 = K_{21} \rho V + K_{22} \rho v V^{2/3} (L/D)^{1/3}$
Landing gear	$W_9 = KV$
Effect of heavy Flight	$W_H = K_{29} H [K_{30} V^{1/3} (L/D)^{5/3} + 1]$

where:

V = volume

L/D = airship length/maximum diameter

ρ = mass density of air

v = airship velocity

K_i = Goodyear proprietary constants

METALCLAD AIRSHIPS

The same basic approach was used to develop the structural WER's the metalclad airships that was used in the rigid and non-rigid analysis. Since only one metal clad airship has been built, there is not the wealth of information that was available for establishing the necessary constants for the rigid and non-rigid airship. Three different approaches were investigated for the pressurized metalclad airships.

METALCLAD 1

General

The metalclad airship will be similar in concept to the rigid airship except that it will be pressurized. It will employ compartmentalization. As in the rigid airship concept, it will employ 10 main frames and intermediate frames spaced at 20-ft intervals. Main frames will be wire braced. Compartmentalization will be obtained by placing a fabric membrane across each wire braced frame. Ballonets will be separate fabric containers placed between main frames as required. Sufficient strength will be provided in the structure to fly at approximately 40 knots in the one-cell out condition. The skin will be made from 7050 alclad.

Because of the similarity between Metalclad 1 and the rigid airship, the formulas developed for the rigid airship for the following components can be used without change:

1. Main frames
2. Gas valves

3. Stern and bow
4. Miscellaneous gas cells and valves
5. Miscellaneous hull weight
6. Empennage and cruciform
7. Mooring and handling
8. Control car, corridors, crew quarters

The weight of the pressure system will be the same as that developed for the non-rigid airship. In addition to the above, formulas for the following components will have to be developed: intermediate frames, longitudinals, gas diaphragm, outer cover, and ballonets. These formulas in most cases will be a modification of formulas previously developed for the rigid and non-rigid airships.

Intermediate Frames

The weight of the intermediate frames for the rigid airship results from aerodynamic, static, and gas pressure loads. The one-cell deflated condition will probably be the critical condition, in which case the loads on the frames would be similar to those on the rigid airship except that the gas pressure loads would be eliminated.

It will be assumed that with one cell deflated the airship speed will be reduced to 40 knots. Therefore M_{40} will be substituted for M_A in the rigid airship formula, and the term which accounts for the gas pressure loads will be eliminated. The resulting formula is:

$$W = [cM_{40}(L/D)^{-2/3} + dV]\ [6.2762\ V^{1/3}\ (L/D)^{2/3} - 11]$$

Longitudinals

The weight of the longitudinals for the rigid airship results from the aerodynamic moment and the gas pressure loads. In the metalclad, the longitudinals will furnish bending strength in the deflated cell condition for a speed of 40 knots. They will not be subjected to the gas pressure loads. The formula developed for rigid airships will be employed except that the effect of gas pressure will be eliminated, M_{40} will be substituted for M_A, and the weight will be increased by a suitable factor to account for increased secondary stresses and an increase in static moment due to the deflated cell condition. The formula then takes the form:

$$W = K_1 M_{40} \ (L/D)$$

Gas Diaphragm

The gas cell for the rigid airship was a function of the surface area of the airship and the cross-sectional area of the main frames. In the metalclad airship, the gas cell fabric need cover only the area of the main rings. Therefore, only that portion of the rigid airship formula will be used.

Since only one layer of fabric per frame is needed in the metalclad compared with two in the rigid, the weight will be reduced by a factor of 2.0. It is anticipated that more chaffing strips will be required. To account for this, the weight will be increased a factor of 1.5. The resulting equation takes the form

$$W = K_2 V^{2/3} \ (L/D)^{-2/3}$$

Control car corridors	$W = K_{15} V^{1/3} (L/D)^{2/3}$
Mooring and handling	$W = K_{16} V$
Pressure system	$W = K_{20} V$
Ballonets and air lines	$W = K_{17} V$
Effect of flight heaviness	$W_H = H [K_4 V^{1/3} (L/D)^{5/3} + K_5]$

where:

H	=	heaviness
V	=	volume
L/D	=	length/maximum diameter
M_{40}	=	aerodynamic moment at 40 knots
ρ	=	mass density of air
u	=	gust velocity
v	=	airship velocity
A	=	total fin area
a, b, c, d, K_i	=	Goodyear proprietary constants

METALCLAD 2

General

The weights of the Metalclad 2 airship will be the same as those for the Metalclad 1 airship except for the main frames, intermediate frames, gas diaphragm, and miscellaneous gas cells, valves, and supports.

Main Frames

Since the main frames are not subjected to the one-cell out condition, their weight can be considerably reduced; it will be assumed that their weight can be cut in half. The form of the weight equation would remain the same; only the constant would change:

$$W = \frac{1}{2} (a + b\rho v) V^{4/3} (L/D)^{-4/3}$$

Intermediate Frames

Proposals by the Detroit Aircraft Corporation show that for the MC-74 the intermediate frames are approximately one-third the weight of the main frames. Burgess felt that this was not sufficient. In this study, one-half the main frame weight will be used for a 7.5 million cubic foot airship. The weight formula then takes the form:

$$W = \frac{1}{4} (a + b\rho v) V^{4/3} (L/D)^{-4/3} [6.2762 V^{1/3} (L/D)^{2/3} - 11]$$

Gas Diaphragm

The gas diaphragm will be eliminated since the airship is not compartmented.

Miscellaneous Gas Cells, Valves, and Supports

Since there will be no gas cells, this weight will be reduced 50 percent.

$$W = \frac{1}{2} K_{12} V$$

Summary

The weight equations for the various Metalclad 2 components are summarized below:

Main frames	$W = \frac{1}{2} (a + b\rho v) V^{4/3} (L/D)^{-4/3}$
Intermediate frames	$W = \frac{1}{4} (a + b\rho v) V^{4/3} (L/D)^{-4/3}$ $[6.2762 V^{1/3} (L/D)^{2/3} - 11]$
Longitudinal	$W = K_1 M_{40} (L/D)$
Outer cover	$W = V [K_5 V^{-1} (L/D) M_A + K_6 V^{1/3} (L/D)^{-1/3} + K_7 \rho v^2 + K_8]$
Gas valves	$W = K_{10} V$
Stern and bow	$W = K_{11} V$
Misc gas cells, valves	$W = K_{12} V$
Misc hull height	$W = K_{13} V$
Empennage and cruciform	$W = K_{14} uv\rho V^{1/3} (L/D)^{-1/3} A$
Control car, corridors	$W = K_{15} V^{1/3} (L/D)^{2/3}$

Mooring and handling	$W = K_{16}V$
Ballonets, air lines	$W = K_{19}V$
Pressure system	$W = K_{20}V$
Effect of flight	$W_H = H\ [K_4 V^{1/3}\ (L/D)^{5/3} + K_5]$

where:

H	=	heaviness
V	=	volume
L/D	=	length/maximum diameter ratio
M_{40}	=	aerodynamic moment at 40 knots
ρ	=	mass density of air
u	=	gust velocity
v	=	airship velocity
A	=	total fin area
a,b,c,d,K_i	=	Goodyear proprietary constants

METALCLAD 3

General

The Metalclad 3 weights will be identical to those of Metalclad 2 except that the ballonets will be eliminated; gas cells will be added [their weight will be the same as that used for the rigid airship]; and the miscellaneous gas cells, valves, and supports will be increased to that used for the rigid airship.

Summary

The weight equations for the various Metalclad 3 components are summarized below:

Main frames	$W = \frac{1}{2}\ (a + b\rho v)\ V^{4/3}\ (L/D)^{-4/3}$
Intermediate frames	$W = \frac{1}{4}\ (a + b\rho v)\ V^{4/3}\ (L/D)^{-4/3}$
	$[6.2962\ V^{1/3}\ (L/D)^{2/3} - 11]$
Longitudinals	$W = K_1 M_{40}\ (L/D)$
Outer cover	$W = V\ [K_5 V^{-1}\ (L/D)\ M_A +$
	$K_6 V^{1/3}\ (L/D)^{-1/3} +$
	$K_7 \rho v^2 + K_8]$
Gas cells	$W = V^{2/3}\ [K_8 (L/D)^{1/3} + K_9\ (L/D)^{-2/3}]$
Gas valves	$W = K_{10} V$
Stern and bow	$W = K_{11} V$
Misc gas cells, valves	$W = K_{12} V$
Misc hull weight	$W = K_{13} V$

Empennage and cruciform	$W = K_{14} uv\rho V^{1/3} (L/D)^{-1/3} A$
Control car	$W = K_{15} V^{1/3} (L/D)^{2/3}$
Mooring and handling	$W = K_{16} V$
Pressure system	$W = K_{20} V$
Effect of flight	$W_H = H [K_4 V^{1/3} (L/D)^{5/3} + K_5]$

where:

H = heaviness
V = volume
L/D = length/maximum diameter
M_{40} = aerodynamic moment at 40 knots
ρ = mass density of air
u = gust velocity
v = airship velocity
A = total fin area
a, b, K_i = Goodyear proprietary constants

REFERENCES

D-1 Goodyear Aerospace Corporation, "Feasibility Study of Modern Airships" - Vol. II - Parametric Analysis, NASA-CR-137692, July 1975.

D-2 Burgess, C. P. - "Airship Design" Ronald Press Co., 1927.

APPENDIX E

AERODYNAMICS ANALYSIS

CONVERSION FACTORS FOR APPENDIX E

1 ft^2 = 0.0929 m^2

1 ft/sec = 0.3048 m/sec

Presented in this appendix are the basic methods of analysis, assumptions and pertinent results related to the aerodynamics of both the ellipsoidal airships and lifting body hybrid vehicle.

CONVENTIONAL AIRSHIP AERODYNAMICS ANALYSIS

Aerodynamic drag characteristics for conventional airships utilized in the GASP are based on Goodyear's data base of airship drag data, both model scale and full scale. The basic drag area expression for a complete airship is

$$(C_{D_O}S)_{Total} = C_{D_O}S)_{Hull} + C_{D_O}S)_{Fins} + C_{D_O}S)_{Engines\ \&\ Outrigger}$$

$$+ (C_{D_O}S)_{Car} + (C_{D_O}S)_{Misc}$$

where

$$(C_{D_O}S)_{Hull} = C_f\ [1 + 1.5\ (d/l)^{2/3} + 7\ (d/l)^3]\ S_W$$

after Reference E-1.

where

d/l = the inverse of the vehicle fineness ratio, length/diameter,

and

S_W = total hull wetted area

The component drag area contributions generally are expressed as percentage contributions of $C_{D_o}S)_{Hull}$ with the K factors based on experimental and full-scale data of past airship. C_f is the Schoenherr frictional resistance coefficient. Vehicle volume to the 2/3 power is utilized for the aerodynamic reference area.

Representative Drag K values are presented in Table E-1, below.

TABLE E-I

Component	DRAG VALUE Rigid	Metalclad	Non-Rigid
Fins	.167 (1)	.25	.33
Engines & Outriggers	.10	.14	.14
Car	20 (2)	.115 (3)	.115
Miscellaneous	.05	.05	.05

(1) Unless noted, values shown are ratio of component Drag to Hull Drag

(2) 20 Square Feet

(3) Limited to 10 square feet minimum value

Aerodynamic lift estimates are based on the data of Reference E-2. Tabulated values of angle of attack, alpha versus lift coefficient, C_L are used due to the highly nonlinear characteristics of airship lift.

Drag due to lift also is based on the data of Reference E-2, which is approximated with sufficient accuracy as

$$C_{D_i} = 0.9\ C_L^2$$

Fin area requirements are calculated as a function of fineness ratio to satisfy a stability index criteria utilized in a broad spectrum of successful rigid and non-rigid airships, including the Los Angeles, Akron, Macon and the Non-Rigid M and N airships.

The Lift and Drag equations above form the basis of the aerodynamics calculations required by the Goodyear Airship Synthesis Program, GASP to evaluate the cruise performance of conventional ellipsoidal airships.

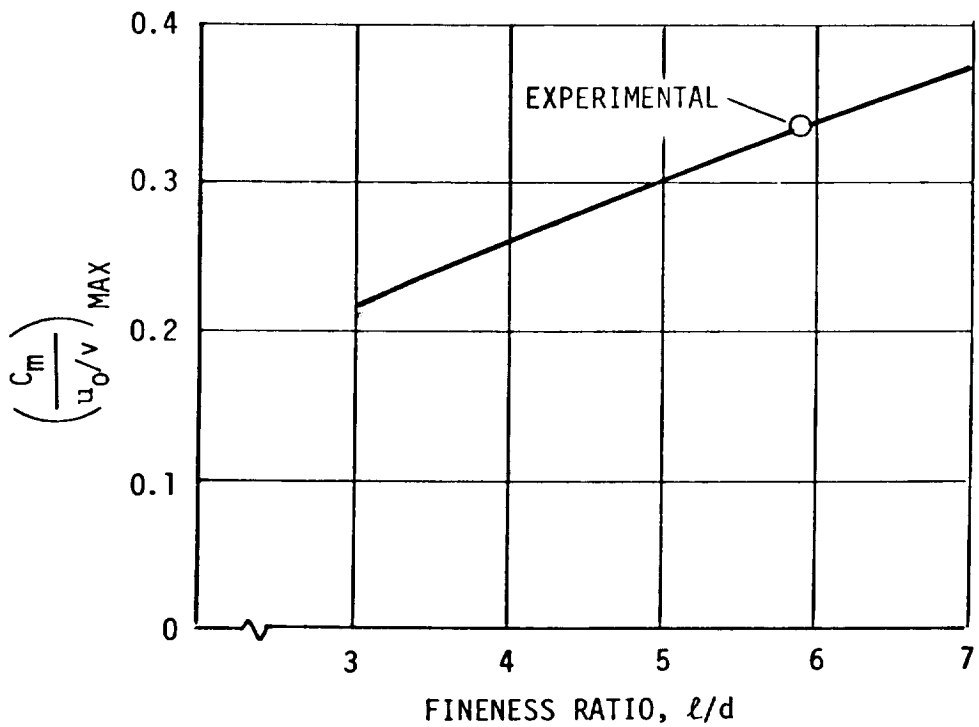

Figure E-1 - Estimated Variation of Peak Bending Moment Coefficient with Fineness Ratio $C_m = M/q\ V$

GASP also calculates the aerodynamic bending moment, M_A, based on the input gust velocity [35 ft/sec unless otherwise defined] and the bending moment coefficient formulation discussed in the Reference E-3. Specifically,

$$M_A = C_M \frac{u}{V_D} q\forall$$

where

C_M = the bending moment coefficient presented in the Reference E-3 and reproduced in Figure E-1,

u = the design gust velocity of 35 ft/sec,

V = the vehicle design velocity,

V_D = $[V_C + V_W]$ 1.08,

V_C = cruise velocity,

V_W = wind velocity,

q = dynamic pressure at V_D, and

$\forall$ = vehicle volume

M_A is used in the structural weight estimating equations presented in Appendix D.

DELTA PLANFORM HYBRID AERODYNAMICS ANALYSIS

Detailed aerodynamic pressure distributions were developed by the Neilsen Engineering and Research [NEAR] for use in the airloads calculations required for the point design structural and weight analysis of Reference E-4. The initial NEAR analysis was based on the methods of Reference E-5. Subsequently, the initial results were confirmed by the results of a modified

vortex lattice computer analysis.

The baseline lifting body hybrid airship concept consists of a parabolic planform and an elliptic distribution of cross-sectional area. The general equation for the semithickness distribution is:

$$z = \frac{3}{(AR)\ F^2}\ x^{\frac{1}{2}}\ (1 - x)\ \sqrt{1 - \frac{9y^2}{AR^2\ x}}$$

where AR is the aspect ratio and F is the fineness ratio [based on the equivalent diameter of the maximum cross section, which occurs at 50 percent of the root chord]. If we define new variables:

$$\alpha = \frac{3}{(AR)\ F^2}\ ;\quad \beta = \frac{3}{AR};\quad \bar{y} = \beta y;\quad \bar{x} = \frac{x - y^2}{1 - \bar{y}^2}$$

then

$$z = (1 - \bar{y}^2)^{3/2}\ (1 - \bar{x})\ \sqrt{\bar{x}}$$

Note that $\bar{y}$ runs from 0 at the root chord to 1 at the wing tip, and $\bar{x}$ runs from 0 at the leading edge of the wing to 1 at the trailing edge.

Differentiating z with respect to $\bar{x}$ and setting it equal to zero gives the point of maximum thickness as $\bar{x} = \frac{1}{3}$ for all airfoil sections. The maximum semithickness is:

$$z_{max} = \frac{2\alpha}{\sqrt{27}}\ (1 - \bar{y}^2)^{3/2}$$

If we define $\bar{z}$ as z/z_{max}, then the non-dimensionalized airfoil shape is:

$$\bar{z} = \frac{\sqrt{27}}{2} (1 - \bar{x}) \sqrt{\bar{x}}$$

The chord at any spanwise station is:

$$c = 1 - y^2$$

and the thickness ratio of the airfoil at that section is:

$$\left(\frac{t}{c}\right)_{max} = \frac{4\alpha}{27} \sqrt{1 - \bar{y}^2}$$

The non-dimensionalized coordinates of the Goodyear airfoil are compared with the generalized NACA 00XX section in Figure E-2. For preliminary analysis, it is deemed sufficient to assume that the pressure distribution for NACA 00XX will suffice for analysis of the Modified Delta Planform lifting body hybrid.

To obtain the pressure coefficients on the upper and lower surfaces, the spanwise lift distribution was assumed elliptical and the method described in Reference E-5 used to obtain the chordwise pressure coefficients. The equations are:

$$P_U = 1 - \left(\frac{v}{V} + c_\ell \frac{\Delta v_a}{V} \right)^2$$

$$P_L = 1 - \left(\frac{v}{V} - c_\ell \frac{\Delta v_a}{V} \right)^2$$

where P_U and P_L are the pressure coefficients on the upper and lower surfaces, $P = (p - p_o)/q_o$, the velocity ratios are obtained from Reference E-5, and c_ℓ is the section lift coefficient.

Assuming an elliptic lift distribution, we have:

$$cc_\ell = c_o c_{\ell_b} \sqrt{1 - \frac{4y^2}{b^2}}$$

This can be integrated to obtain:

$$C_L S_W = \frac{\pi}{4} \; b \; c_o c_{\ell_b}$$

and

$$c_{\ell_o} = \frac{4}{\pi} \frac{C_L S_W}{b \; c_o} = \frac{8}{3\pi} \; C_L$$

This section lift coefficient is then given by:

$$c_\ell = \frac{c_o \; c_{\ell_o}}{c} \sqrt{1 - \frac{4y^2}{b^2}} = \frac{8C_L}{3\pi} \; (1 - \bar{y}^2)^{-1/2}$$

For this study, it was assumed that $C_L = 0.5$, $R = 1.5$, and $F = 2.5$. For these values, the section lift coefficients and maximum ratios are:

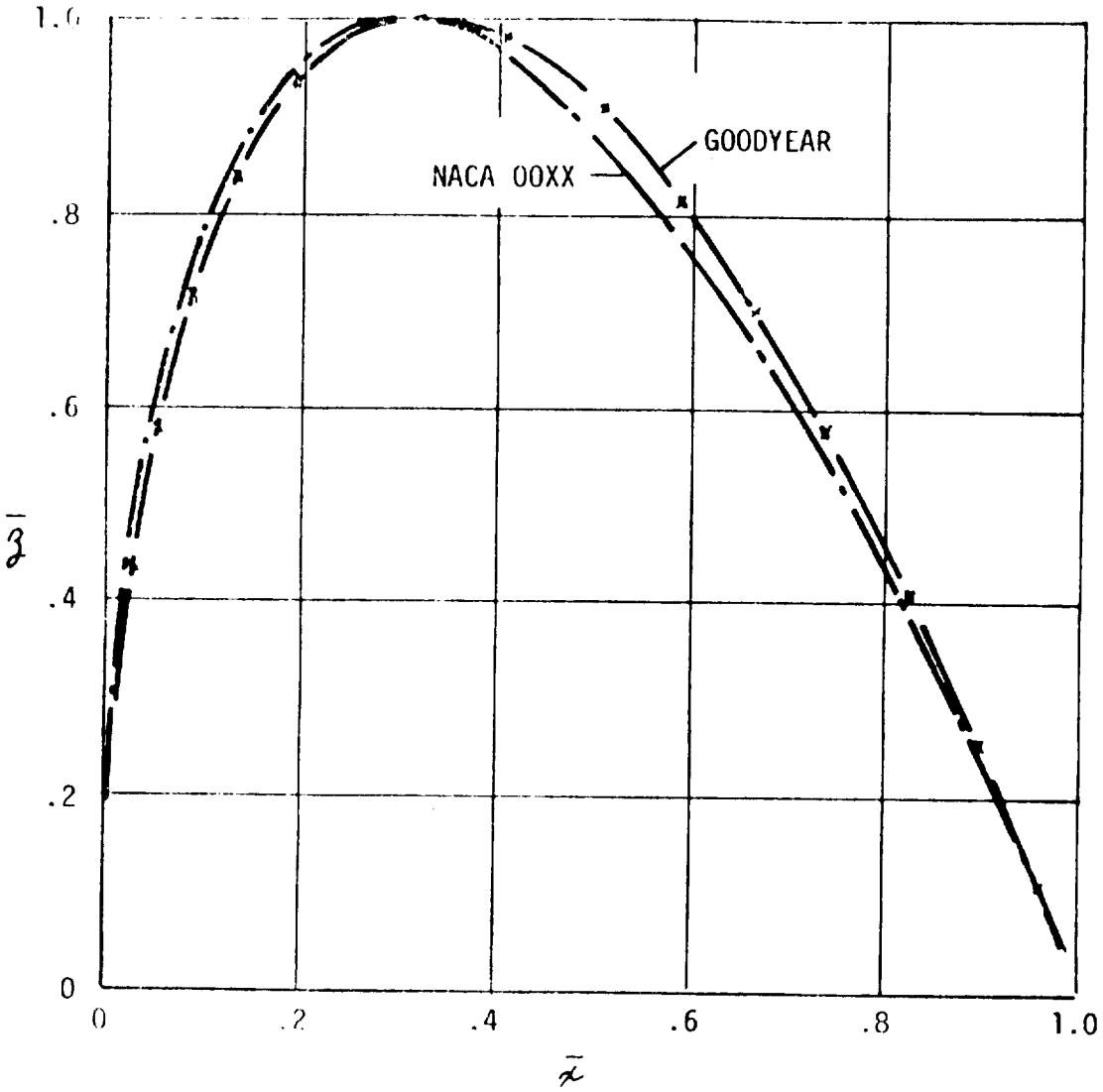

Figure E-2 - Comparison of Hybrid Airfoil Coordinates with Generalized NACA 00XX Section

Y	$\bar{Y}$	c_ℓ	$(t/c)_{max}$
0	0	.424	.246
.125	.25	.438	.238
.25	.50	.490	.213
.375	.75	.642	.613
.50	1.0	∞	0

The infinite lift coefficient at the tip is not a problem as the load will be transferred to neighboring sections with little overall effect.

To obtain the velocity ratios for NACA 00XX airfoils at intermediate thickness ratios, the velocity ratios given in Reference E-5 for the 0006, 0009, 0012, 0015, 0018, 0021, and 0024 airfoils were plotted as a function of maximum thickness ratio. Figure E-3 gives v/V as a function of thickness ratio, and Figure E-4 gives $\Delta v_a/V$ as a function of thickness ratio. Using these velocity ratios and the section lift coefficient shown above, pressure distributions were obtained at the desired spanwise locations. The computations and results are shown in Figures E-5 and E-6.

The center of pressure of the lift also is of importance to airship design. If the aerodynamic center of all the airfoil sections were at the same location in percent of chord, the integrating the moments about the trailing edge would give the following result:

$$C_{M_{TE}} S_W = \frac{3\pi}{16} \; b \; c_o \; c_{\ell_o} \; (1 - \bar{c}) \; c_o$$

where $\bar{c}$ is the aerodynamic center location in percent of the chord. This gives:

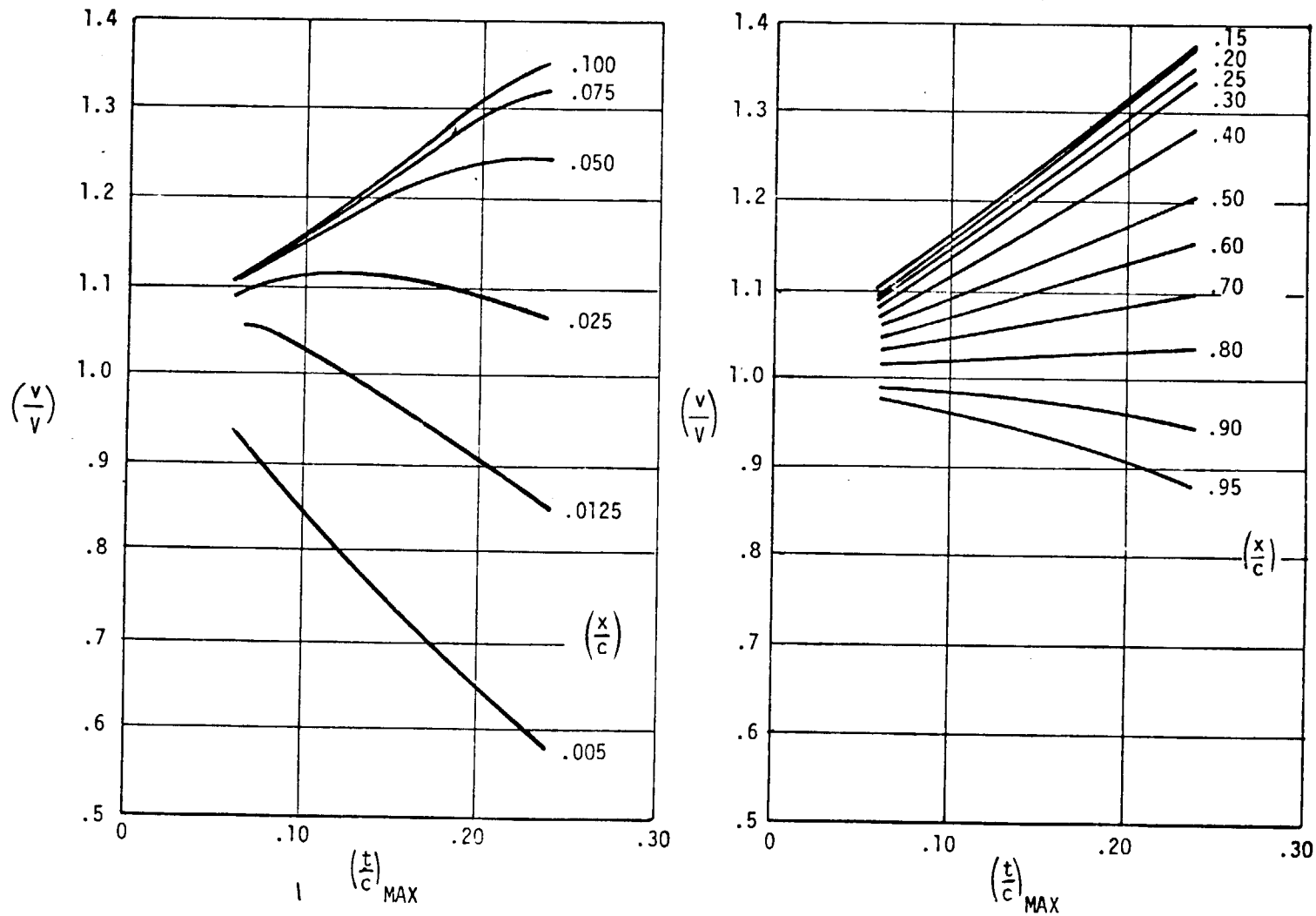

Figure E-3 - Airfoil Velocity Ratios as a Function of Thickness Ratio

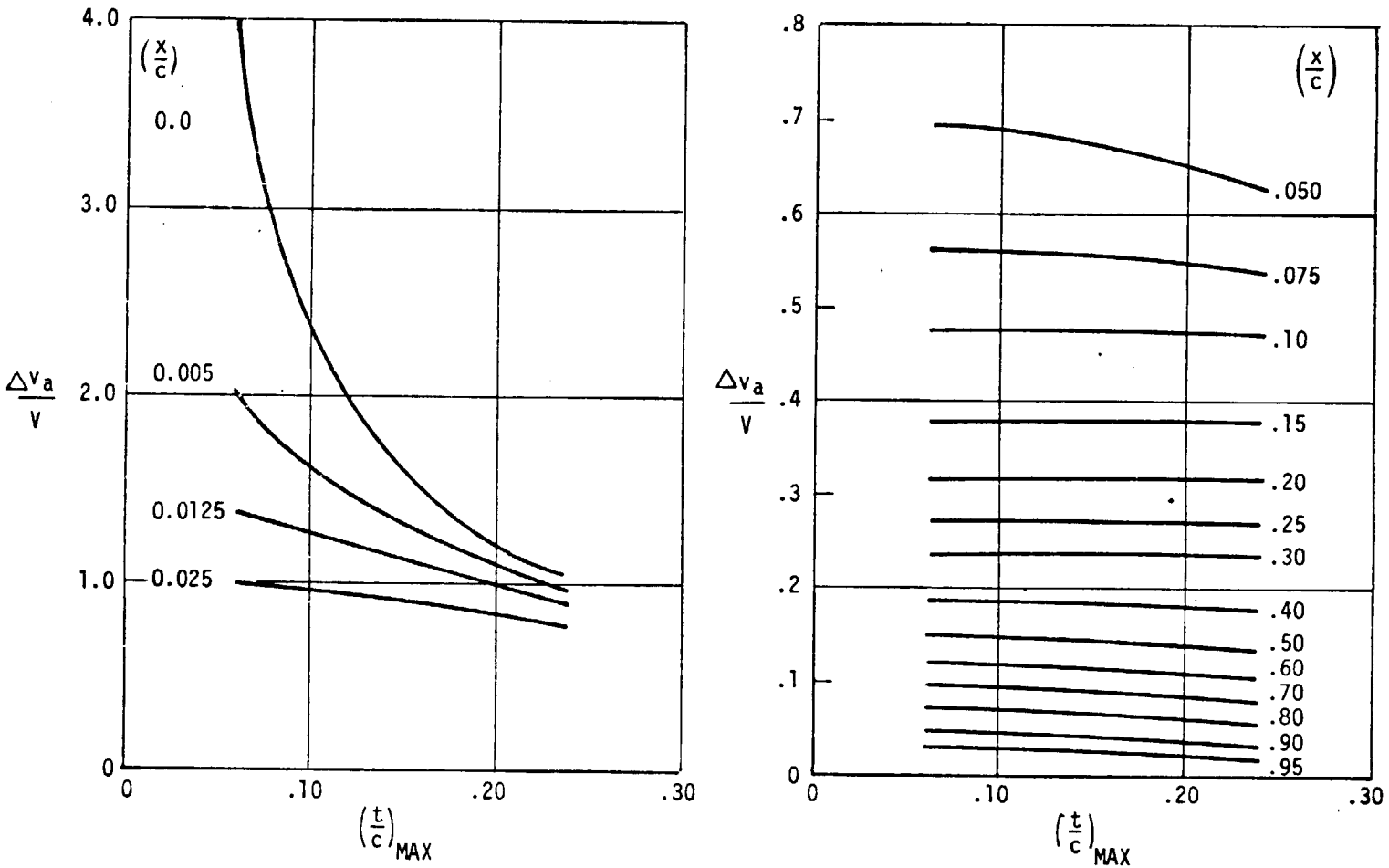

Figure E-4 - $\Delta v_a/V$ Ratios as Function Thickness Ratio

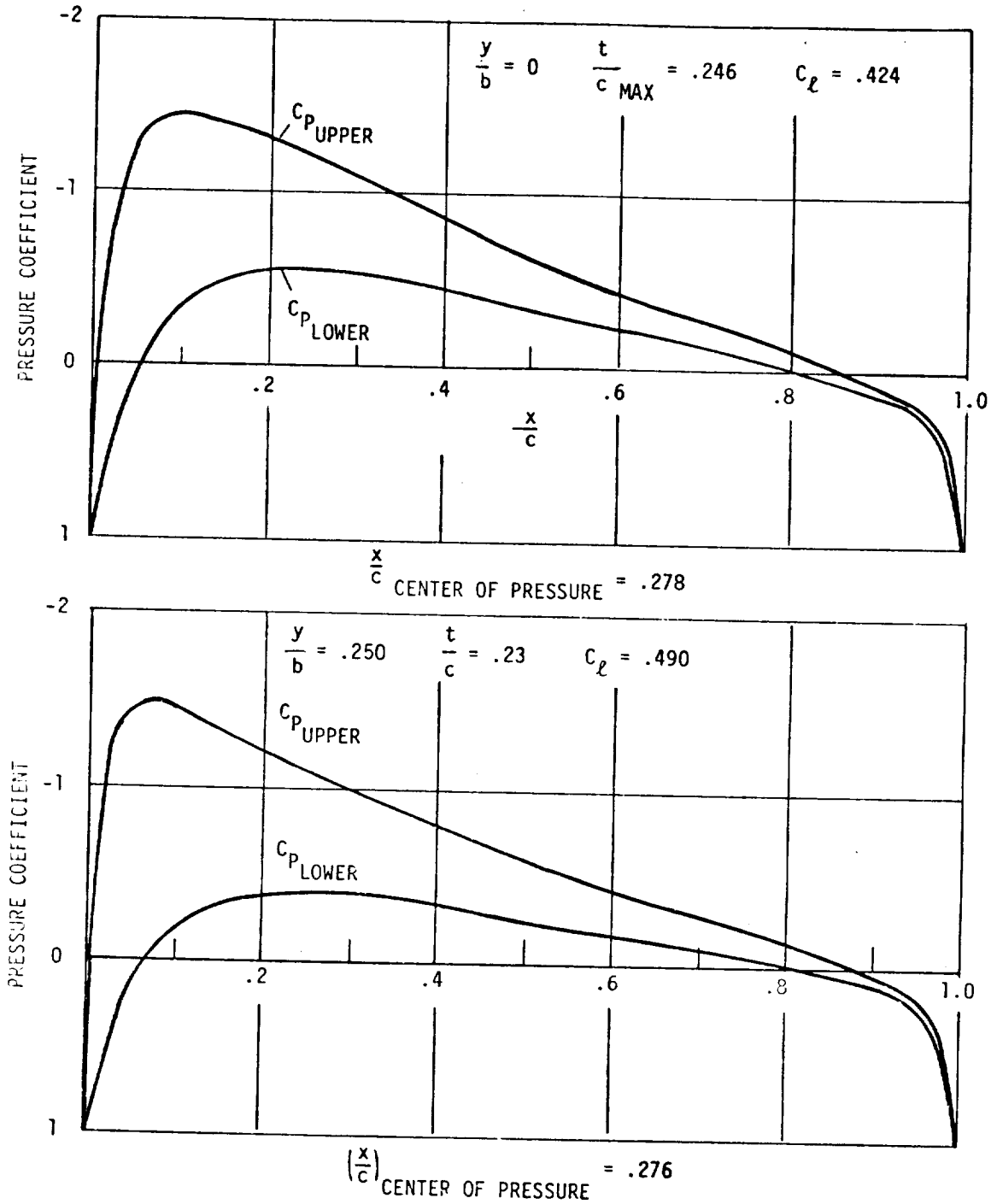

Figure E-5 - Baseline Hybrid Pressure Distribution (x/c = .278 and .276)

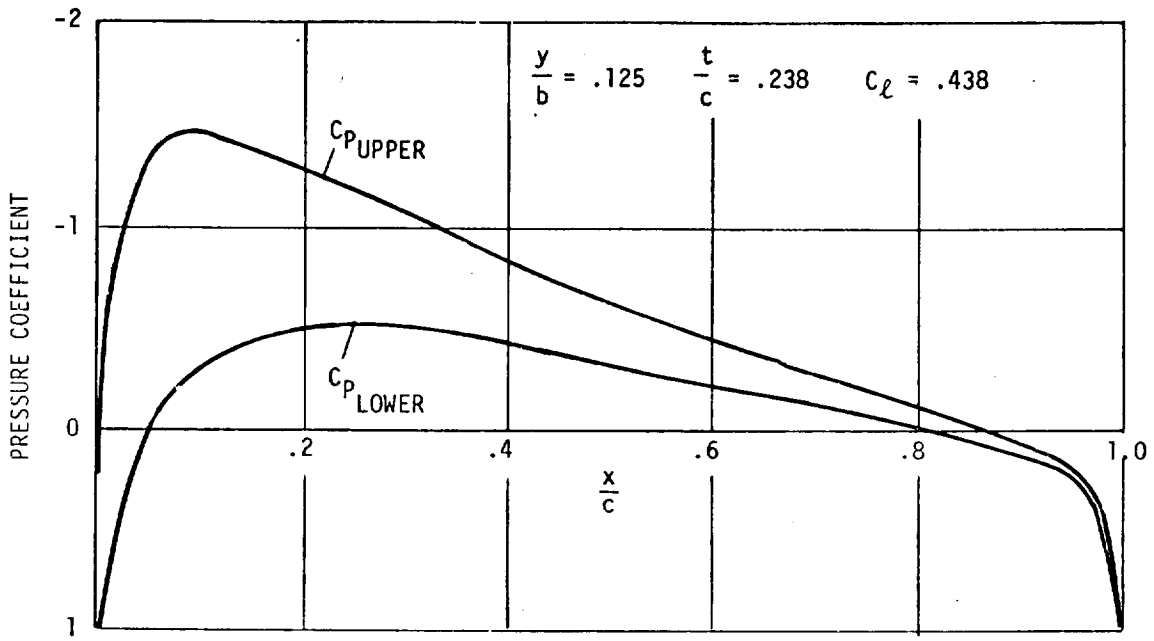

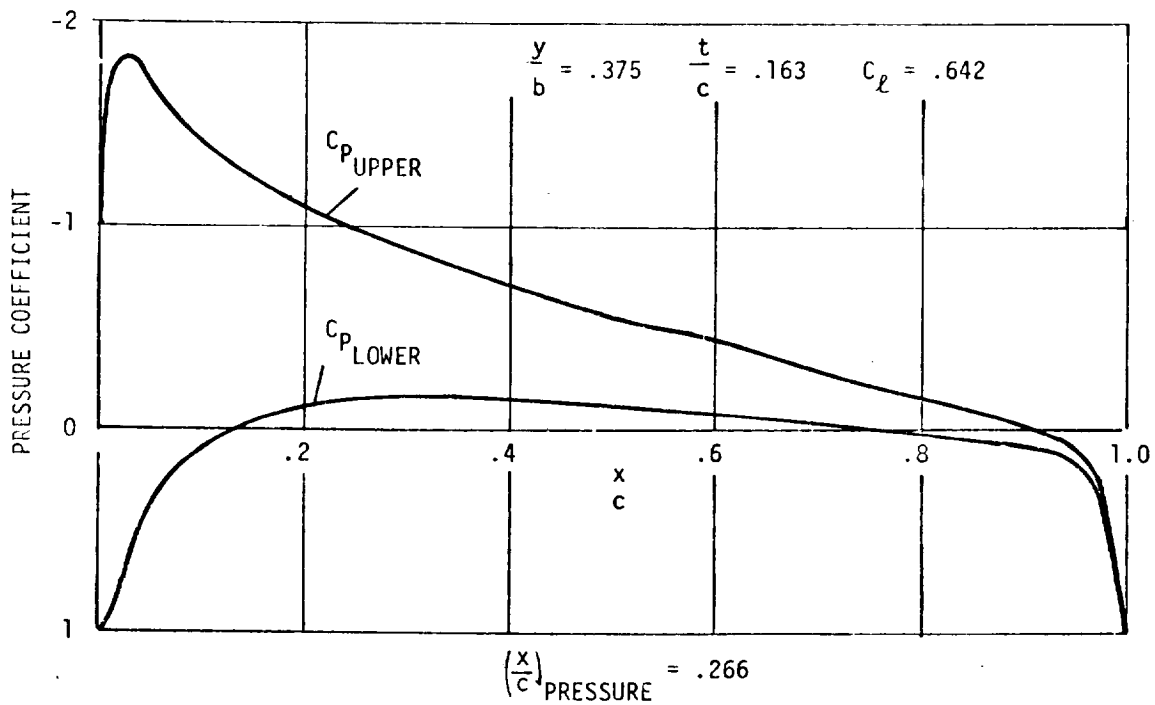

Figure E-6 - Baseline Hybrid Pressure Distributions (x/c = .266)

$$\frac{C_{M_{TE}} S_W}{C_L S_W} = \frac{3}{4} \; c_o \; (1 - \bar{c})$$

and measured from the nose of the vehicle:

$$\frac{x_{ac}}{c_o} = \frac{1}{4} + \frac{3}{4} \bar{c}$$

For the NACA OOXX airfoil series, $\bar{c}$ is 25 percent for zero thickness and increases to about 28 percent for a 25-percent thick airfoil section. Values obtained by using a planimeter on the pressure distributions given in Figures E-5 and E-6 are:

Y	$\bar{Y}$	$(t/c)_{max}$	$\bar{c}$
0	0	.246	.278
.125	.25	.238	--
.25	.50	.213	.276
.385	.75	.163	.266
.50	1.0	0	.250

If we use 27 percent as an average aerodynamic center location, the aerodynamic center for the entire shape will be located about 45-percent of the root chord from the nose.

Subsequent to the initial analysis, the lifting body hybrid was run on the NEAR vortex-lattice computer program. Pressure coefficients were computed at 100 locations for a zero thickness parabolic wing at 10-degree angle of attack.

The spanwise lift distribution for the vortex-lattice method was compared with the elliptic lift distribution used in the simplified method above. The vortex-lattice results are extremely

close to the elliptic lift distribution, but there is a slight inboard shift in the lift distribution which was expected. The curves for the vortex-lattice results are virtually independent of spanwise location, but there is a slight trend to a more rearward center of pressure for outboard airfoil sections. The vortex-lattice results also indicated a more rearward C_p than the two-dimensional NACA airfoil data; they were corrected for thickness in order to make a comparison with the simplified method.

A further comparison of upper and lower surface pressures between the vortex-lattice method with thickness and the previous simplified method based on an elliptic lift distribution and two-dimensional airfoil characteristics showed that the simplified method gives a very good estimate of the pressure coefficients.

The major difference between the two methods is the more rearward C_p predicted by the vortex-lattice method. For a zero thickness wing, two-dimensional theory gives a center of pressure at 25 percent of the chord. Integrating this over the parabolic planform would give a center of pressure at 7/16 of the root chord, or 43.75 percent. The vortex-lattice method gives a C_p at 44.8 percent. Increased thickness tends to move the C_p rearward, and a C_p of 45 percent was estimated using the simplified method. The vortex-lattice results would indicate a further rearward shift of 1 or 2 percent.

GASP AERODYNAMICS ESTIMATING PROCEDURES

The aerodynamic estimating procedures used in GASP were developed during the precontract efforts. Since it was not known what type of configurations(s) would be selected for further study, the methodology was required to be generally applicable to a broad

range of delta and modified delta configurations. The methodology of Reference E-6 was selected. It was developed for the subsonic aerodynamics and landing flare analysis of low aspect ratio lifting body configurations and has been shown to predict with reasonable accuracy the aerodynamic characteristics of a broad range of delta and modified delta configurations.

Aerodynamic characteristics are calculated in the body fixed axis system based on empirically derived correlations of experimental data. The method reasonably predicts the non-linearities resulting from the vortex flow, which becomes significant at large angles of attack. The basic normal force expression near $\alpha = 0$ is

$$C_{N_\alpha} = \left[\frac{\pi}{2} (AR) + 2\left(\frac{S_F}{S} \right) \right] \left(\frac{4}{4 + AR} \right) K_1$$

where:

AR = aspect ratio,

S_F = the maximum cross-sectional [frontal] area,

S = the reference [planform] area, and

K_1 = the empirically derived correction factor based on leading edge radius/geometry

The normal force coefficient at 20-degree angle of attack is calculated and a cubic relationship derived to define the normal force coefficient as a function of α over the range from 0 to 20 degrees.

$$C_{N_{\alpha=20}} = 2.195 \left(\frac{AR + 0.61}{AR + 4} \right) K_2$$

where: K_2 is an empirical correction factor based on leading edge geometry

$$C_N = C_{N_\alpha}(\alpha) + 8.21\ (C_{N_{20}} - 0.349\ C_{N_\alpha}) \times [K_3 + 2.86\ (1 - K_3)\alpha](\alpha)^2$$

where: K_3 is an empirical correction factor based on leading edge geometry.

Vehicle center of pressure is based on the theoretical delta planform center of pressure corrected for thickness and hose blunting. The resulting C_P prediction was in surprisingly good agreement with the NEAR analysis, predicting the total body alone C_P of 45.2 percent.

Zero normal force axial force is based on the method of Reference E-7. In the reference, an expression is developed that adequately predicts the minimum profile drag characteristics of thick cambered [Clark Y model airfoil section] delta planform lifting bodies up to thicknesses of 0.3c. The basic expression as used in GASP is

$$C_{A_{\alpha=0}} = C_f \left[\frac{A_W}{S_W} + 2G\left(\frac{t}{c}\right) + 120\left(\frac{t}{c}\right)^4 \right]$$

where:

G = $0.8\ [1 + 5\ X_t^2]$ with X_t the chordwise position of the maximum thickness,

$\frac{t}{c}$ = maximum airfoil thickness ratio,

A_W = wetted area,

S_W = planform [reference area], and

C_f = Schroenherr frictional resistance coefficient.

This expression is used as the zero normal force axial force coefficient which for the symmetrical hybrid lifting body vehicle is the axial force at zero angle of attack.

The ratio of the wetted area to planform area was estimated on the basis of a correlation of the data of Reference E-7 as a function of thickness ratio.

Vertical tail sizes for the hybrid vehicle are based on empirical correlation of re-entry body data, corrected for buoyancy by a β factor but limited to values no less than those of a conventional airship of the same volume and fineness ratio.

A very preliminary investigation of the longitudinal stability characteristics of the baseline hybrid vehicle was conducted. The entire area of both directional and longitudinal stability of semibuoyant hybrid vehicles is hampered both by the lack of a specific stability criteria that would provide acceptable flying qualities and the uncertainty in the values of the stability derivatives required for evaluation of the vehicle stability. The preliminary effort included a preliminary layout of actual and apparent mass and inertia characteristics as well as a best estimate of the required coefficients. The results, although of the most preliminary nature, indicated that the baseline vehicle would be dynamically stable despite the small static instability margin for β greater than or equal to approximately 0.5. For these β's, horizontal tail surfaces would be required primarily for control. Between $\beta = 0.5$ and 0, the vehicle might become dynamically unstable. Thus, it was decided to use a smooth fairing between a tail size of 2 percent of the planform area at $\beta > 0.5$ and the tail size required for static stability at intermediate β's < 0.5. Even at the lowest β's however, the horizontal tail area required was small due to the small $C_P - C_B$

separation. Further investigations into the specifics of the configuration geometry showed that the C_B could be shifted forward of the C_P by leaving a small percentage of the trailing edge portion of the vehicle empty of lifting gas. This was the final configuration assumed for the parametric analysis; hence, the horizontal tail area was taken as 2 percent of the planform for control.

Total vehicle characteristics [C_A, C_N, C_M] are obtained by summing the component characteristics and transforming them into a wind axis coordinates system for use in the synthesis program. The result is total vehicle C_L, C_D, and C_P as a function of α.

REFERENCES

E-1 Hoerner, S. F.; Fluid Dynamic Drag, published by the author, 1961

E-2 Freeman, H. B.; Force Measurements on a 1/40 Scale Model of the U.S. Airship "AKRON", NACA - TR-432, 1932

E-3 Goodyear Aerospace Corporation, "Feasibility Study of Modern Airships" Volume III, - Historical Overview, NASA - CR-137692, July 1975

E-4 Goodyear Aerospace Corporation; "Feasibility Study of Modern Airships" Volume II - Parametric Analysis, NASA CR-137692, July 1975

E-5 Abbott, E. H.; Summary of Airfoil Data, NACA Report No. 824, 1945

E-6 U.S. Air Force Stability and Control DATCOM, Oct. 1960, Revised 1974

E-7 Subsonic Characteristics of Low Aspect Ratios, AFFDL-TDR-64-103, July 1964.

APPENDIX F

PROPULSION AND TAKE OFF ANALYSIS

CONVERSION FACTORS FOR APPENDIX F

1 ft	=	0.3048 m
1 ft/sec	=	0.3048 m/sec
1 ft^2	=	0.0929 m^2
1 lb	=	0.4536 Kg
1 ft-lb	=	0.1381 Kg-m
1 slug/ft^3	=	514.8 Kg/m^3
1 lb/ft^2	=	4.882 Kg/m^2

This appendix describes the methods of analysis and assumptions used in the Goodyear Airship Synthesis Program in the areas of propulsion system performance and weights analysis and take off analysis.

PROPULSION ANALYSIS [PERFORMANCE]

The propulsion analysis used in the GASP for both the conventional airships and hybrid vehicles is based on momentum theory and is modified by the use of propeller efficiency. The propeller efficiencies are based on data supplied by Hamilton Standard.

Horsepower required for the desired cruise velocity, at altitude, is first calculated. Sea level installed horsepower is determined assuming normal cruise power being 80 percent of the take-off power.

If VTOL is required, the propulsion requirements are calculated from the lift thrust requirement. A vertical thrust 20 percent in excess of the gross weight minus static lift is used for VTOL engine sizing. A minimum of four engines is allowed for VTOL vehicles.

The maximum sea level installed horsepower requirement [cruise or VTOL] dictates the engine power requirements. Turboprop engines are used throughout the bulk of the parametrics. Engine specific fuel consumption was based on data for the General Electric T64 turboprop. Propulsion performance estimates were coordinated with the Hamilton Standard Division of United Aircraft Corporation.

The propulsion analysis used in the synthesis program is derived

below. The propeller efficiences are based on the performance of a free four-bladed propeller [120 activity factor]. This data was supplied by Hamilton Standard and is given in Figures F-1, F-2 and F-3 for Mach numbers of 0, 0.1 and 0.2. The disk and power loading factors in these curves differ from the corresponding factor in this analysis by a factor of $\pi/4$. The thrust and power loadings are normalized by the true disk area, $\pi D^2/4$. The disk loading for the propeller for a required cruise [T_c] is then

$$(T/A)_c = T_c/(N\pi D^2/4)$$

The slip stream velocity for the cruise velocity (V_c) is

$$\omega = \sqrt{2\ (T/A)_c/(\sigma_c\ \sigma_o) + V_c^2}$$

The thrust-to-horsepower ratio is then given by

$$(T/HP)_c = 1100\ \eta/(\omega + V_c)$$

where η is the propeller efficiency.

The calculations are made at the cruise altitude. The total thrust is divided equally amont the N engines, and the sea level horsepower per engine corresponding to the cruise condition is

$$HP_{CSL} = (T_c/N)/\ [\sqrt{\sigma}\ (T/HP_c)]$$

The installed horsepower of the engine then is calculated from the assumed normal cruise power being 80 percent of the take-off power. Based on this take-off power, the take-off thrust will be given by

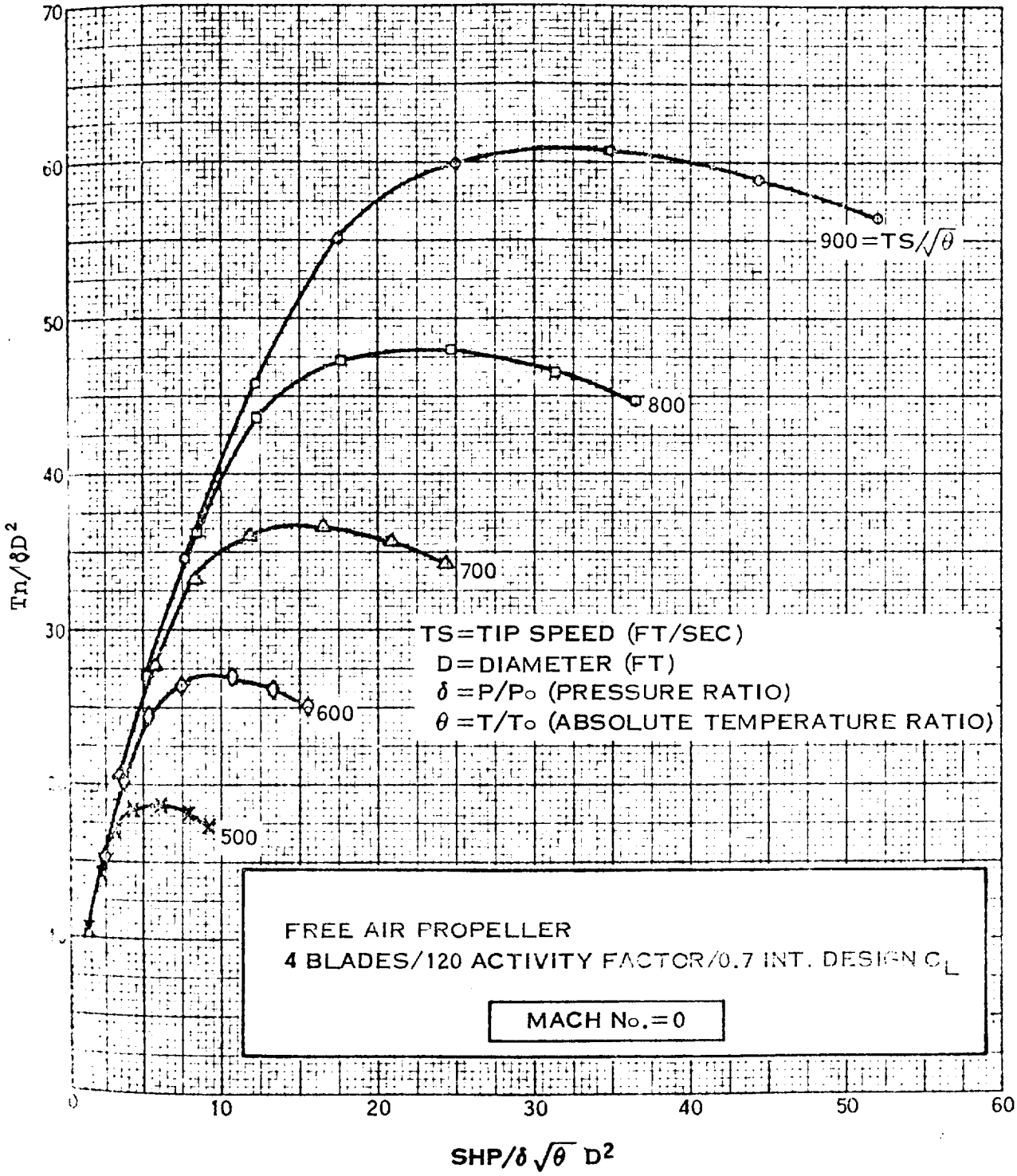

Figure F-1 Propeller Data (Mach 0)

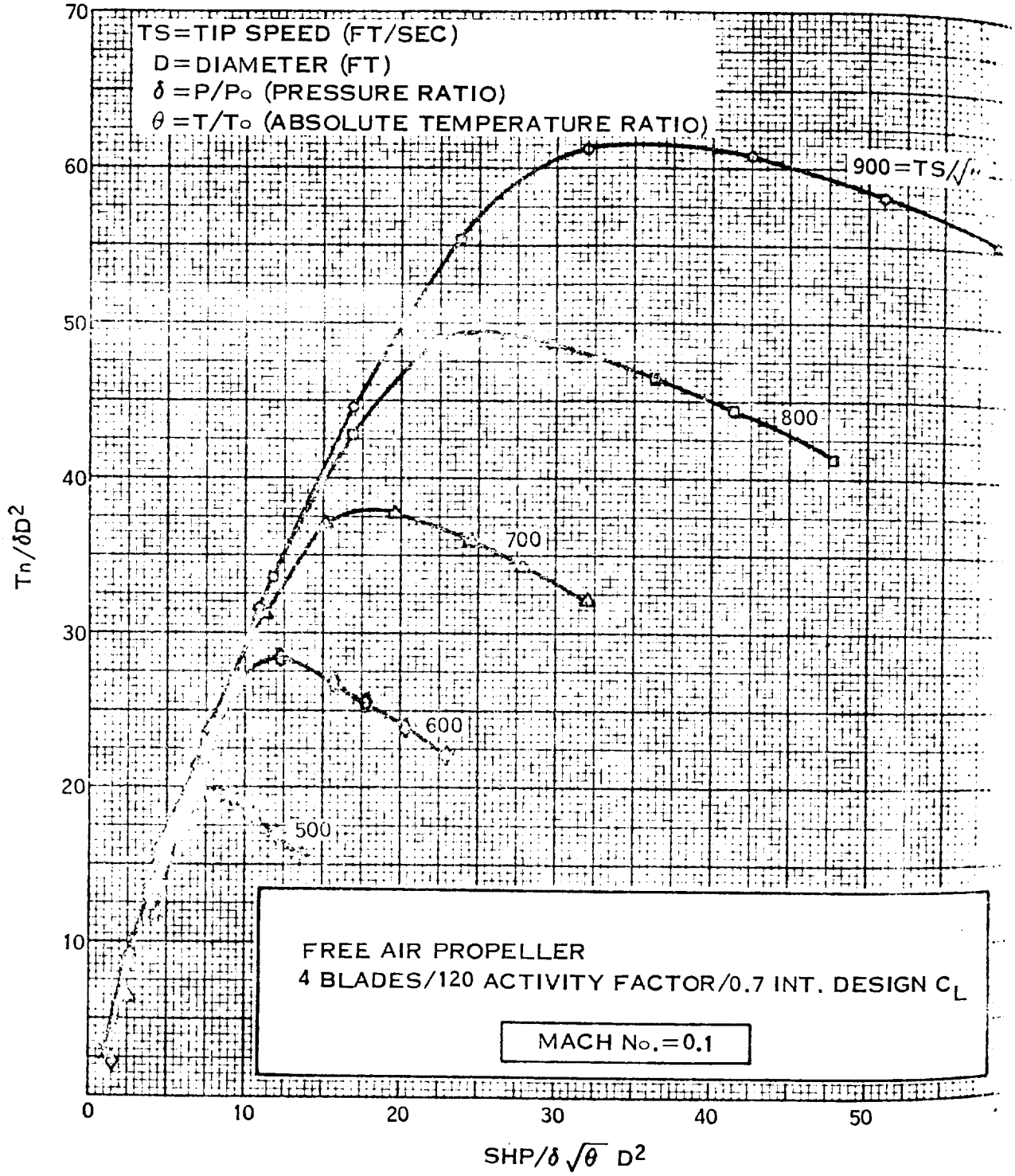

Figure F-2 - Propeller Data (Mach 0.1)

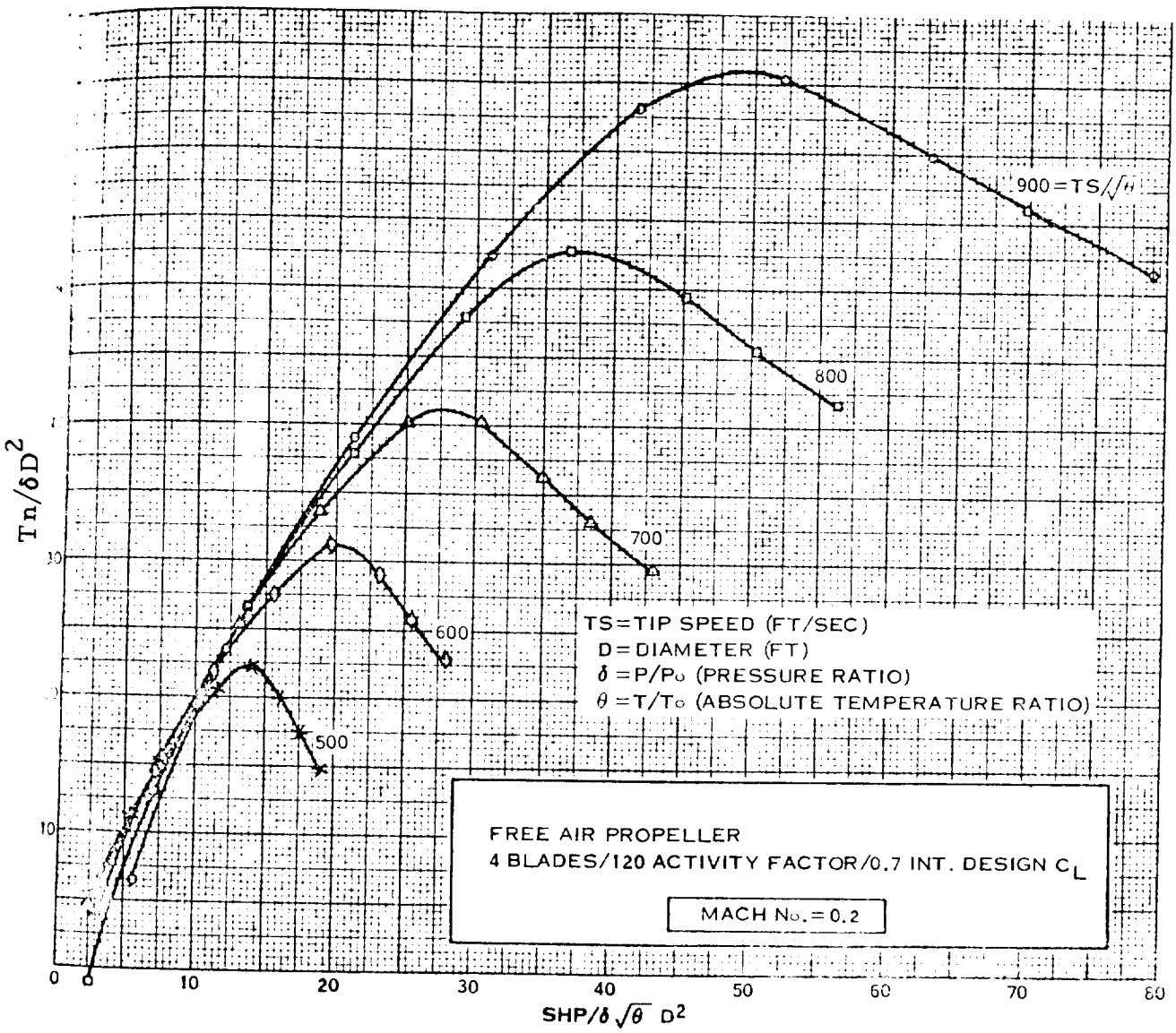

Figure F-3 - Propeller Data (Mach 0.2)

$$T_{TO} = (\eta \, HP_{TO} \, 550 \sqrt{\rho_o} \, A)^{2/3}$$

The shaft torque at takeoff is

$$TQ_{TO} = 550 \, HP_{TO} \cdot D/(2 \, V_{TIP})$$

The propulsion requirements for the VTOL vehicles are computed from the lift thrust requirements. The vertical thrust was set 20 percent above the gross weight minus static lift figure. The disk loading again is

$$(T/A)_{VTO} = T_{VTO}/(N \, \pi \, D^2/4)$$

The air velocity at the disk is

$$V_D = \sqrt{(T/A)_{VTO}/(2 \, \rho_o)}$$

The thrust-to-horsepower ratio is

$$(T/HP)_{VTO} = \eta \frac{550}{V_P}$$

where η is the propeller efficiency. However, in this part of the program because of the rapid variation of efficiency with disk loading and tip speed the Hamilton Standard propeller data for Mach 0 was replotted as thrust to horsepower ratio versus disk loading. These curves were then programmed as empirical equations. Using these relations, the thrust-to-horsepower ratio is calculated.

$$(T/HP)_{VTO} = f \, [(T/A)_{VTO}]$$

The required engine horsepower is then

$$HP_{VTO} = (T_{VTO}/N) \ / \ [(T/HP)_{VTO}]$$

For cruise, the disk loading will be

$$(T/A)_c = T_c/(A \cdot N)$$

The slip stream velocity will be

$$\omega = \sqrt{2 \ (T/A) \ / \ (\sigma \ \rho_o) + V_c^{\ 2}}$$

For these conditions, the thrust-to-horsepower ratio is given by

$$(T/HP)_c = \eta\left(\frac{1100}{\omega + V_c}\right)$$

and the horsepower is

$$HP_c = T_c/(T/HP)_c$$

Now, if this horsepower is over 80 percent of the takeoff horsepower the propulsion system must be resized. In the synthesis program, if this is true, the data is transferred to the cruise option and the engines and propellers are size for cruise.

During vertical takeoff and conventional takeoff calculations, the thrust decay with velocity was based on the use of a constant speed propeller.

The propulsion system noise is based on the installed horsepower,

the propeller tip speed, and the number of propellers. During Phase I, the vehicles were not constrained by a noise limit. However, the propeller efficiencies over a wide range of tip speeds are available within the program, and a noise constraint can be used for engine and propeller sizing. The noise data was taken from the general aviation propeller study [Reference F-1] performed by Hamilton Standard.

A list of symbols for this section of the appendix is given below:

T	=	thrust in pounds
V	=	velocity in feet per second
D	=	propeller diameter in feet
A	=	propeller disk area in square feet
HP	=	engine power in horsepower
TQ	=	torque in foot-pounds
N	=	number of engines
ω	=	slip stream velocity in feet per second
ρ	=	air density in slugs per cubic foot
η	=	propeller efficiency
σ	=	air density ratio
π	=	3.14159

PROPULSION SYSTEM WEIGHT DATA

The bare engine weight characteristics used in GASP are shown in Figure G-4. A 25 percent accessory and installation factor is applied to the bare engine weight.

Propeller and gear box weights are based on data supplied by Hamilton Standard for an integral gear box type propeller.

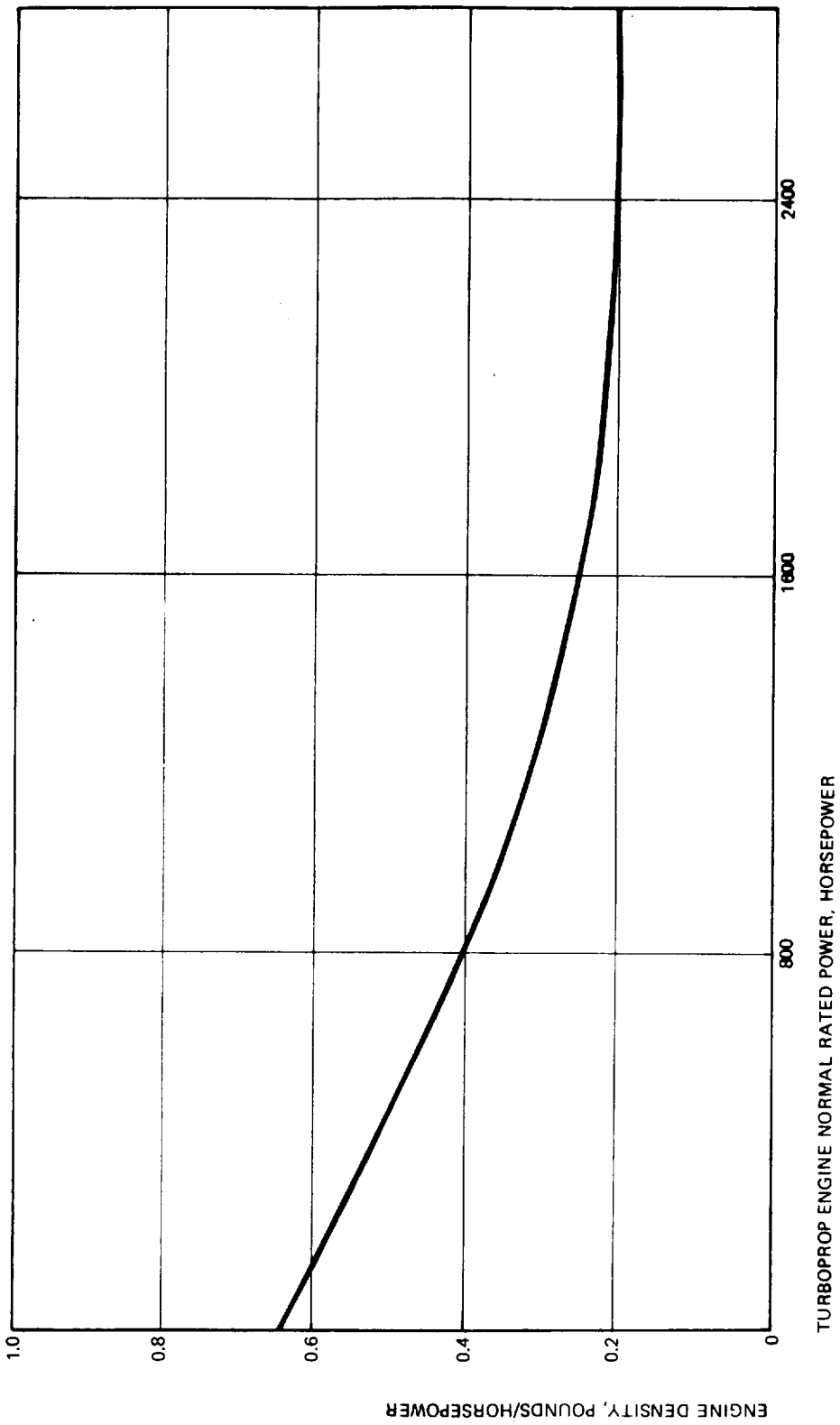

Figure F-4 - Bare Engine Weight Characteristics

Propeller weight:

$$W_p = 285 \left[\left(\frac{D}{10} \right)^2 \left(\frac{\text{Activity Factor}}{100} \right)^{0.75} \left(\frac{\text{Tip Speed}}{1047} \right)^{0.5} \left(\frac{SHP/D}{10} \right)^{0.12} \right]$$

Gear box weight:

$$W_g = 0.095 \left[\frac{SHP \times D}{\text{Tip Speed}} \times 275 \right]^{0.84}$$

An outrigger weight value of 1.5 times the engine weight was assumed for vertical takeoff propulsion.

CTOL AND STOL CALCULATIONS

The takeoff, flare, and climbout calculations used in the program are based on an adaptation of the method of Reference F-2 corrected for added mass effects.

VERTICAL TAKEOFF CALCULATIONS

An auxiliary program to the vehicle synthesis program was written to check on the vertical takeoff characteristics of the various configurations. A simple transition logic was incorporated that reduced the percentage of excess vertical thrust δ from Δ at takeoff to zero at a constant climbout with $C_L = 0.8\ C_L$ maximum at a velocity V_{CL}.

$$\delta = \Delta\ (V_{CL} - V)/V_{CL}$$

The thrust vector for a vehicle of gross weight W and static lift to gross weight ratio of β is given by

$$\alpha = \arcsin [(1 - \beta) W (1 + \delta) + (C_D \sin - C_L \cos\gamma) qS)/T]$$

The vertical acceleration is

$$\ddot{Z} = [T \sin\alpha - (1 - \beta) W - (C_D \sin\gamma + C_L \cos\gamma) qS] g/W$$

The horizontal acceleration is

$$\ddot{X} = [T \cos\alpha - (C_D \cos\gamma + C_L \sin\gamma) qS] g/W$$

$$\gamma = \arctan (\dot{Z}/\dot{X})$$

Integrating these equations gives the trajectory of the take-off. A horizontal wind may be introduced as an initial conditions XD_i = XDW by transforming the vehicle horizontal velocity to be $V_H = \dot{X} - V_W$ and $\gamma = \arctan (\dot{Z}/V_H)$.

Typical results from this transition analysis program are presented in Figures F-5 and F-6.

A list of symbols for this section of the appendix is given below:

δ	=	excess thrust fraction
Δ	=	initial excess thrust fraction
α	=	thrust vector angle with horizontal
γ	=	flight path angle
β	=	static lift-to-gross weight ratio

W = vehicle gross weight in pounds

C_D = vehicle drag coefficient

C_L = vehicle lift coefficient

q = dynamic pressure in pounds per square foot

T = total thrust in pounds

g = gravitational acceleration in feet per second per second

S = vehicle reference area in square feet

X = horizontal distance

$\dot{X}$ = horizontal velocity

$\ddot{X}$ = horizontal acceleration

Z = vertical distance

$\dot{Z}$ = vertical velocity

$\ddot{Z}$ = vertical acceleration

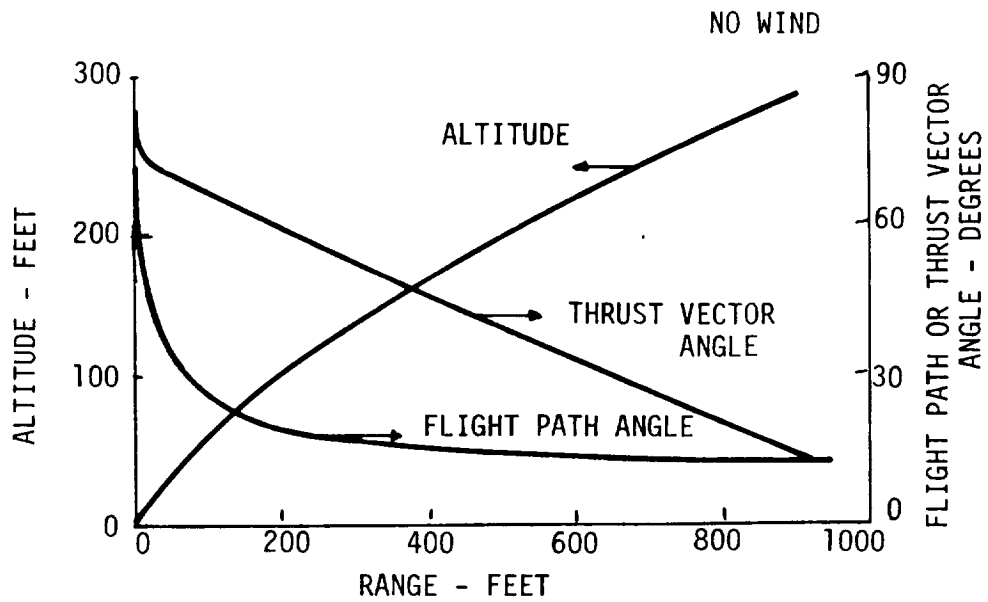

Figure F-5 -TYPICAL TRANSITION ANALYSIS RESULTS
GW = 40,000 LB, β = 0.65 NO WIND

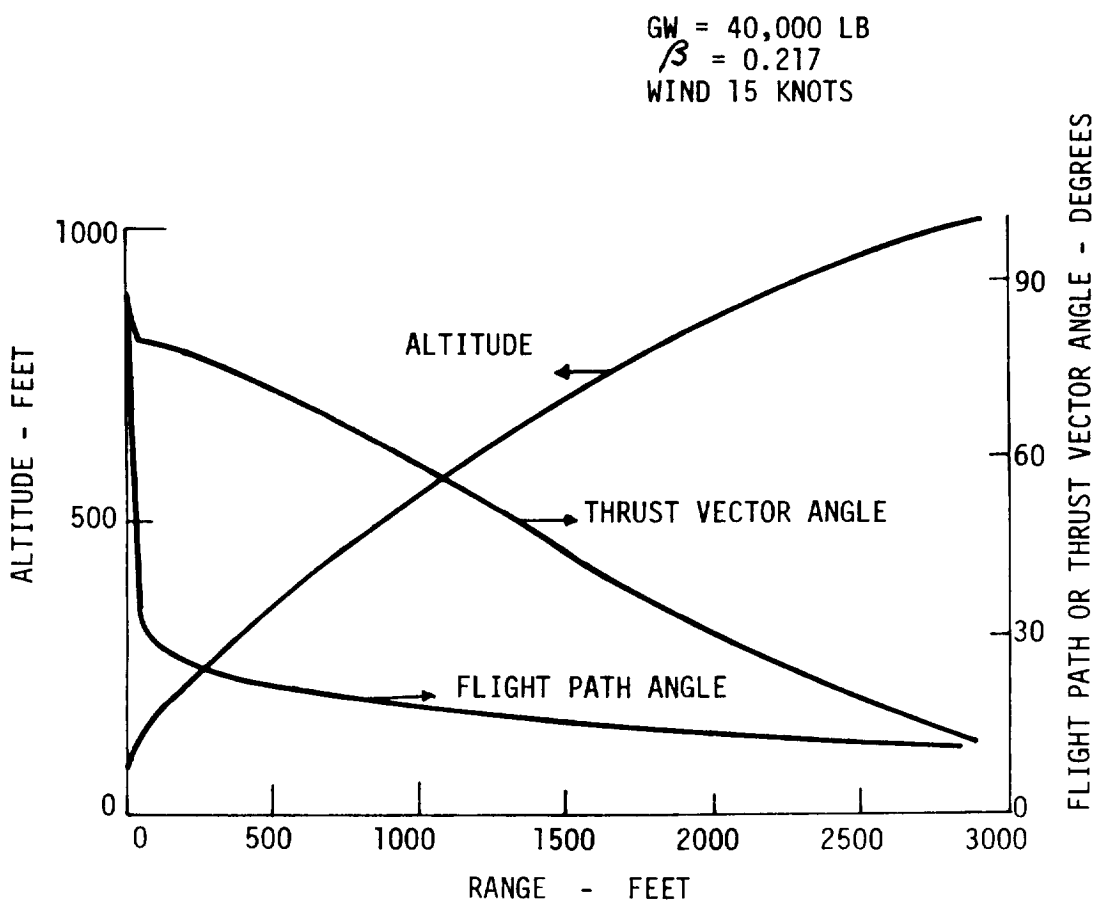

Figure F-6 - TYPICAL TRANSITION ANALYSIS
RESULTS, GW = 40,000 LB, β = 0.20, V_W = 15 KNOTS

REFERENCES

F-1 Worobel, Rose and Mayo, M.G.; Advanced General Aviation Propeller Study, NASA CR-114289, April, 1971

F-2 Logie, R. H., et al; Evaluation of a Combination Thrust Reverser - Jet Deflector Concept, AIAA Paper No. 64-287, July, 1964.

APPENDIX G

SANDWICH MONOCOQUE RIGID AIRSHIP

CONVERSION FACTORS FOR APPENDIX G

1 ft	=	03048 m
1 ft^2	=	0.0929 m^2
1 ft^3	=	0.02832 m^3
1 lb/ft^2	=	4.882 Kg/m^2
1 ft/sec	=	0.3048 m/sec
1 inch	=	0.0254 m
1 ft-lb	=	0.1381 Kg-m
1 lb	=	0.4536 Kg
1 ton mi/hr	≅	1460 Kg-Km/hr
1 ton	=	970.2 Kg
1 mile	=	1.609 Km
1 mph	=	0.447 m/sec
1 yd^2	=	0.8361 m^2

INTRODUCTION

For a long time there has been an interest in eliminating the fabric covering of airships in favor of a metal surface [Reference G-1]. This interest led to the successful metalclad, pressure stabilized, ZMC-2 and subsequent activities along the same lines. More recently, several investigators [Reference G-2] have suggested that the honeycomb sandwich may be a viable approach for future airships.

It is the purpose of this investigation to establish the range of parameters in terms of airship size, design speed, and fineness ratio which lead to an acceptable hull weight fraction for the sandwich monocoque design.

HULL BENDING MOMENTS

In historical airship design it has been the practice to arrange the distribution of components and load carrying provisions such that the weight distribution closely matches the buoyant [static] lift distribution so that the static bending moment is very low [negligible].

The design bending moment for the hull is then determined by the aerodynamic forces associated with flight maneuvers and gust conditions. These forces are reacted by a mass distribution which matches the longitudinal distribution of the displacement.

It is obvious that the above approach will not be valid for an airship with arbitrary weight distribution and may grossly underestimate the strength required for an airship with heavy concentrations of weight [payload for example].

For purposes of this study, however, it is assumed that the weight is distributed in the historical pattern, and design bending moments are essentially independent of the specific weight distribution.

Calculations are presented for two different formulations of the critical bending moment. The historical value:

$$M = 0.018\ q\ \forall^{2/3}\ L \qquad (1)$$

and a new formulation introduced in Reference G-3

$$M = CBM\ \frac{U}{V}\ q\ \forall \qquad (2)$$

where:

$\forall$ = airship gross volume in ft^3

q = aerodynamic pressure at the design speed and altitude - lb/ft^2

L = airship length - ft

U = design gust velocity - ft/sec

CBM = Bending Moment Coefficient which varies with fineness ratio and can be characterized with sufficient accuracy as:

$$CBM = 0.11 + \frac{3F}{80}$$

where: F is the airship fineness ratio.

Both of the formulations are for "limit" loads and are increased by a factor of safety of 1.5 in subsequent calculations.

BUCKLING CHARACTERISTICS OF SANDWICH CYLINDERS

For axial compression, the critical buckling conditions are based on the formulae in Reference G-4 which reduct to:

$$F_{cr} = 0.4\ E\ \frac{h}{r}$$

with sufficient accuracy for proportions of interest in this study, where

F_{cr} = critical face sheet compressive stress

h = sandwich depth, C to C of face sheets

r = mean radius of curvature

E = Young's Modulus for face sheets

A cricular sandwich cylinder in bending will probably exhibit a higher critical compression stress than for the case of pure compression. An increase of 30 percent is a reasonable expectation and is used here. Neglected here is the minor difference between the core thickness t_c and the effective thickness h of the sandwich.

Taking $$F_{cr} = 0.4\ E\ \frac{t_c}{R} \times 1.3 = 0.52\ E\ \frac{t_c}{R}$$

The critical load in pounds per inch is:

$$N_{cr} = 2\ t_f \left(\frac{0.52\ E\ t_c}{R} \right) = \frac{1.04\ t_c\ t_f}{R}$$

and the critical hull bending moment becomes

$$M_{cr} = 0.52\ E\ t_c\ t_f\ D$$

where:

t_c = core thickness - inches

R = cylinder radius - inches

t_f = face thickness - inches

M = hull bending moment - ft lbs

D = hull diameter - ft

[The small difference between the hull outside diameter and the diameter to the center of the sandwich is neglected here.]

Expressing the sandwich weight in terms of the face thickness, the core thickness and the two densities and solving for minimum weight proportions results in:

$$\text{Core Weight} = \text{Face Weight}$$

for a minimum weight proportions:

Gerard [Reference G-5] shows that the lightest weight sandwich structures result from using the lightest available core. Selecting aluminum honeycomb core material it can be shown that the lightest honeycomb [2 lb/cu. ft] has adequate strength and stiffness for the application treated here.

Confining the discussion to aluminum face sheets and 2 lb aluminum honeycomb cores yields minimum weight when

$$t_c = 172\ t_f$$

Making the substitution in the M_{cr} equation yields

$$t_f = \frac{10^{-3}}{53.0} \left(\frac{M}{D} \right)^{1/2}$$

$$t_c = 3.24 \times 10^{-3} \left(\frac{M}{D} \right)^{1/2}$$

and

$$W = 1.08 \times 10^{-3} \left(\frac{M}{D} \right)^{1/2}$$

where W is the weight of the optimum sandwich [less glue] in lbs/ft^2 and t_c and t_f are the core and face thicknesses.

SANDWICH SHELL WEIGHT

It is clear from the above that if the sandwich proportions remain constant over the entire airship hull, the bending strength envelope will match the shape of the airship profile. This provides the kind of strength distribution which is desirable for an airship with a good weight distribution. The total shell weight is therefore defined simply as the product of the weight per square foot of the sandwich from above and the hull surface area.

Perusal of Table 3 of Reference G-6 indicates that

$$S = 2.75 \text{ DL}$$

is a representative value for the surface area of traditional "ellipsoidal" airship shapes.

The total sandwich shell weight now becomes

$$\begin{aligned} W_S &= 1.08 \times 10^{-3} \left(\frac{M}{D} \right)^{1/2} \times 2.75 \text{ DL} \\ &= 2.86 \, M^{1/2} \, D^{1/2} \, L \times 10^{-3} \qquad + \text{ glue} \end{aligned}$$

where it is implicitly assumed that the design bending moment occurs at the point of maximum diameter.

Taking the ellipsoid as representative of the airship shape, we express the shell weight as a function of the design bending moment, the airship volume and fineness ratio as follows

$$\forall = \frac{\pi}{6} D^2 L = \frac{\pi}{6} D^3 F, \qquad \frac{L}{D} = F$$

$$D = \left(\frac{6\forall}{\pi F}\right)^{1/3}, \quad L = FD = \left(\frac{6\forall}{\pi}\right)^{1/3} F^{2/3}$$

$$S = 4.24\, \forall^{2/3} F^{1/3}$$

$$W_S = 3.94 \times 10^{-3} \times (M \forall F)^{1/2} + \text{glue}$$

Now, for the historical bending strength criteria:

$$M = 1.5 \times 0.018\, q\, \forall^{2/3} L$$

$$= 0.027 \left[\tfrac{1}{2} \rho V^2\right] \forall^{2/3} \left(\frac{6\forall}{\pi}\right)^{1/3} F^{2/3}$$

$$= 40.2 \times 10^{-6} V^2 \forall F^{2/3}$$

where V is the equivalent S.L. design air speed in ft/sec.

The shell weight becomes:

$$W_S = 25.0\, V F^{5/6} \forall \times 10^{-6} + \text{glue}$$

or in terms of the nominal gross buoyancy

$$\text{Shell Wt Fraction} = \frac{W_S}{0.062\ \forall} = 404\ V\ F^{5/6} \times 10^{-6} + \text{glue}$$

Note that the shell weight fraction [neglecting glue] is independent of airship size, is linear with the design velocity and nearly linear with the fineness ratio.

Sample values of the shell weight fraction [less glue] are as follows:

F \ V	100	150	200
3	0.101	0.152	0.202
4.5	0.141	0.212	0.282
6.0	0.180	0.270	0.360

Low fineness ratio and low speed are required to hold the shell weight fraction to small value. Glue weight fraction and minimum gage limitations will be treated later.

Using the current bending strength criteria

$$M = 1.5 \left(0.11 + \frac{3F}{80} \right) \frac{U}{V}\ q\ \forall$$

For $U = 35$ ft/sec S.L. operation

$$M = 0.0624 \left(0.11 + \frac{3F}{80} \right) V\ \forall$$

The shell weight fraction becomes

$$\frac{W_S}{0.062\ \forall} = 16.0\ F^{1/2} \left(0.11 + \frac{3F}{80} \right)^{1/2} V^{1/2} \times 10^{-3} + \text{glue}$$

Note that the weight fraction [less glue] is still independent of airship size, exhibits a more complex dependence on the fineness ratio and a lesser dependence on design velocity.

Sample values of the weight fraction are:

F	$F^{1/2}\left(0.11 + \frac{3F}{80}\right)^{1/2}$	V Ft/Sec 100	150	200	250
3	0.816	0.129	0.158	0.182	0.204
4.5	1.12	0.178	0.218	0.252	0.280
6	1.42	0.225	0.276	0.318	0.356

Note that this bending strength criteria is more severe than the historical values at 100 ft/sec becoming progressively more favorable as the design speed is increased. Slow and short is still the rule for minimum shell weight.

Glue Weight

The sandwich faces are bonded to the honeycomb core with adhesives. In lightweight sandwiches considerable diligence in manufacturing techniques is required to prevent excessive bonding weights. Good practice can hold this weight to 0.10 lb/ft^2 of sandwich.

The total glue weight in the airship shell can be taken as

$$W_G = 0.424\ V^{2/3}\ F^{1/3}$$

Note that this weight is still strictly a function of the surface area and the glue weight fraction will be a function of the airship size and shape but independent of design velocity.

$$\frac{W_G}{0.062\ \mathcal{V}} = 6.84 \left(\frac{F}{\mathcal{V}} \right)^{1/3}$$

Sample values are:

F	$\mathcal{V}$			
	10×10^6	20×10^6	50×10^6	100×10^6
3	0.0456	0.0362	0.0267	0.0212
4.5	0.0523	0.0415	0.0306	0.0242
6	0.0575	0.0456	0.0337	0.0257

MINIMUM GAGE LIMITATIONS

If we take 0.008 as the minimum face thickness, the minimum sandwich proportions will be $t_f = 0.008$, $t_c = 1.38$ In. for minimum weight proportions and the corresponding weight will be:

$$W = 57.6 \quad 0.008 = 0.46\ \#/\square' \text{ plus glue} = 0.56\ \#/\square'$$

The shell weight fraction [less glue]:

$$\frac{W_S}{0.062\ \mathcal{V}} = \frac{4.24\ V^{2/3}\ F^{1/3} \times 0.46}{0.062\ \mathcal{V}} = 31.4 \left(\frac{F}{\mathcal{V}} \right)^{1/3}$$

and the minimum gage limit will occur [using the current bending strength criteria] when:

$$31.4 \left(\frac{F}{\mathcal{V}} \right)^{1/3} = 16.0\ F^{1/2} \left(0.11 + \frac{3F}{80} \right)^{1/2} V^{1/2} \times 10^{-3}$$

and the smallest airship which can be built in this manner without incurring minimum gage weight penalties is:

$$\forall_{min} = \left[\frac{1960}{V^{1/2} \; F^{1/6} \left(0.11 + \frac{3F}{80} \right)^{1/2}} \right]^3$$

Sample values of $\forall_{min}$ are:

F	F * Function	DESIGN VELOCITY FT/SEC			
		100	150	200	250
3	0.569	42×10^6	22.6×10^6	14.9×10^6	10.6×10^6
4.5	0.680	24×10^6	13.3×10^6	8.5×10^6	6.1×10^6
6	0.781	16×10^6	8.8×10^6	5.65×10^6	4.0×10^6

$$*F \text{ function} = F^{1/6} \left(0.11 + \frac{3F}{80} \right)^{1/2}$$

For airships larger than the values shown the required sandwich face thickness will be greater than 0.008 and the sandwich weight will be greater than 0.56 lbs per square foot including adhesives.

SANDWICH FINS

The following is a brief summary of a parametric design of an empennage for the sandwich monocoque rigid airship which was carried out in full detail within the bounds of the following restrictive assumptions:

1. Fin constructed as multicell box beam with all cover panels, shear webs and ribs constructed of sandwich panels.

2. Fin span = 0.75 C_o where C_o is the root chord. - Taper ratio 2.

3. Fin is supported at the root by a carry through section over 40% of the deepest section of the root chord.

4. The fin thickness to chord ratio is under the control of the structural designer and chosen to produce the minimum weight fins. [This optimum thickness tends to be thinner than might be expected.]

5. The maximum fin design load is defined by a gust of 35 ft/sec at the maximum design velocity and C_{L_α} is taken as 2.0/radian.

6. A honeycomb core density of 3.4 #/□' is appropriate, with aluminum alloy face sheets working to high stresses.

7. Spar webs located at a spacing equal to the local section thickness yields near optimum number of cells in the box beam.

8. The total area of 4 fins is a function of the airship size and fineness ratio:

$$4\ A_F = 1.10\ \forall^{2/3} \left(\frac{0.5 + 0.067\ F}{F^{2/3}} \right)$$

9. The unit weight of the fin in the root chord region for the gust condition in lbs/sq ft extended undimished over the entire exposed area and the area of the cruciform carry through will provide a reasonable estimate of the fin weight [including moveable surface] designed to meet maneuvering conditions as well as the gust condition.

10. Buckling properties are based on simply supported edges.

11. Spar webs plus ribs to be equal in weight to one external surface, so that total weight is three times the compression surface weight.

The results of the analysis are as follows:

1. Minimum weight occurs when the cover panels are proportional for maximum bending stiffness [core weight = twice face weight].

2. Minimum weight occurs when the fin thickness to chord ratio is chosen to produce a yield limited critical buckling stress in the cover plates. This requires that

$$a/C = 0.0154 \, (C_N \, q)^{1/2}$$

Where a is the fin thickness at the root section and $C_N q$ is the design ultimate fin loading in lbs per ft^2.

3. The fin weight for the above assumptions and optimum proportions can be expressed as

$$W = \frac{(F)^{1/2}}{136} + 0.30 \ \#/\square' \text{ of planform fin area.}$$

Where F is the design ultimate load for the individual fin, and the 0.30 is the adhesive weight.

4. A study of the size and position of a typical fin installation on an airship hull resulted in an estimate of the cruciform carry through structure at 1/3 the weight of the fin supported.

5. Combining the empennage area determination of assumption (8) with the weight expression of result (3) above results in an overall empennage weight fraction of:

$$\frac{W_E}{0.062\ \forall} = \left[\tfrac{4}{3}\right]\left[\frac{V^{1/2}\ (0.5 + 0.067\ F)^{3/2}}{41\ F}\right]\left[1 + \frac{392}{V^{1/2}\ \forall^{1/3}}\right]$$

in which the first term is the cruciform carry through factor, the second term is the weight of four fins less glue and the third term is the glue inclusion factor.

As before,

V = design velocity - ft/sec
F = hull fineness ratio
$\forall$ = hull gross volume.

This is a well behaved function which decreases with increasing fineness ratio, increases with increasing design velocity, and decreases slightly with increasing hull volume. It exhibits a minimum value of 0.060 at $F = 6$, $V = 150$ and $\forall = 100 \times 10^6$ and a maximum value of 0.12 at $F = 3$, $V = 300$ and $\forall = 10 \times 10^6$.

6. A brief study of the size/velocity limits associated with the minimum gage resulted in the conclusion that the weight estimate is valid [for sandwich fins] for all airships larger than ten million cubic feet.

7. It is noted in passing that a separate derivation using a 3 dimensional [space] truss as the fin structure and a fabric cover resulted in a fin weight exactly one half of the sandwich fin weight shown here. This suggests that the sandwich design shown here is far from the lightest weight design.

TRANSVERSE FRAMES

The sandwich shell in this mode of construction is very stiff compared to a solid aluminum sheet of the same weight. [The bending stiffness ratio is on the order of 3000.] At the same time the shell is very thin compared to the airship diameter and general instability failure would surely occur if no transverse frames were provided to maintain the circular cross section shape. No criteria is available to specify how many such frames but according to Gerard [Reference G-5, p. 129] investigations carried out by Leggett and Hopkins in 1942 showed that introduction of "occasional" frames solves this problem. In the airship hull transverse frames are required for another reason. The lifting gas pressures are broadly distributed over the shell surface and these loads are carried longitudinally by shear and bending stresses over the entire hull section. Large concentrated loads are incurred in the process of harnessing these forces for delivery to the heavy weights to be carried. These concentrated loads must be applied to structural assemblies capable of distributing the load to the hull shell. The transverse frame is ideal for this purpose.

Consider the transverse frame [Figure G-1] in the spoked wheel configuration, consisting of a built up aluminum alloy rim section with a multiplicity of steel wire or cable spokes. The spokes are pretensioned so that no spoke goes slack under the maximum design load.

The frame is loaded with a concentrated load P and supported by a shear flow of the classic VQ/I distribution. [It makes little difference if the load P is actually distributed to several panel points in the lower section of the ring]. The load P is delivered

to the hub of the frame by a heavy cable [or cables] and resisted at that point by increased tensions in the upper spokes and decreased tension the lower spokes.

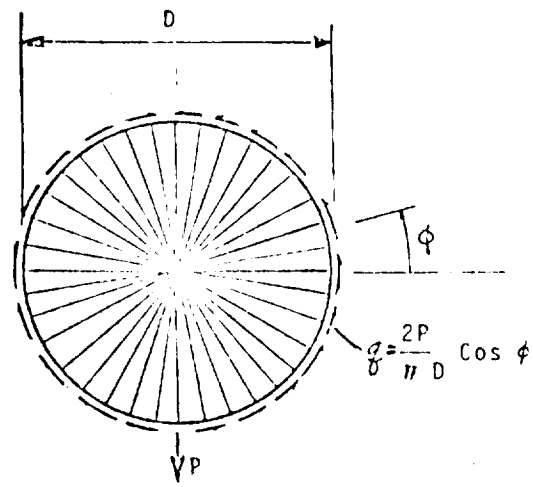

Figure G-1 - Transverse Frame Configuration

Analysis shows that the spoke pretension needs to be equal to 1/2 the maximum loaded tension to insure that no spokes go slack. In the limiting case, the rim load goes to zero at bottom center and increases as a [1 - cos θ] function to a maximum value at top center. The spoke loads show the same distribution as the rim loads, being proportional to the rim load and the change in direction of the spoke to spoke chord.

Allowing for a factor of safety of 1.5 results in the following utlimate design loads:

$$\text{Rim, Axial Compression} = \frac{3P}{\pi}$$

$$\text{Spokes, Tension} = \frac{6P}{n}$$

where n is the number of spokes

loaded spoke - bottom center = P

The weight of the frame required to resist the above loads is

$$W_F = P\ D \left[\frac{3.6}{F_R} + \frac{12.6}{F_S}\right] 1.10$$

where:

D = frame diameter - ft

F_S = allowable ultimate spoke stress

F_R = allowable ultimate rim compressive stress

1.10 = factor for fittings and joints

Taking F_R = 50,000 psi and F_S = 200,000 psi the frame weight becomes:

$$W_F = \frac{0.148\ P\ D}{1000}$$

Observe that the frame weight is linear with both P and D. The total frame weight in the airship hull will be independent of the number of frames and may be chosen by the designer to facilitate the general arrangements, to minimize the weight of secondary structures and provide strong local supports where needed.

The total load P to be delivered out as strong points will be a major fraction of the gross buoyant lift of the hull. A total force of $\Sigma P = 0.75\ [0.062\ \forall]$ will be assumed for weight estimates.

In terms of the airship size and shape the transverse frame weight fraction becomes:

$$\text{With} \quad D = \left(\frac{6\forall}{\pi F} \right)^{1/3}$$

$$\text{and} \quad P = 0.75 \; [0.062 \; \forall]$$

$$\frac{W_F}{0.062 \; \forall} = \frac{0.148 \times 0.75}{1000} \left(\frac{6\forall}{\pi F} \right)^{1/3} = \frac{0.138}{1000} \left(\frac{\forall}{F} \right)^{1/3}$$

A sampling of values of $W_F/01062 \; \forall$

	$\forall$		
F	10×10^6	30×10^6	$100 \quad 10^6$
3.0	0.0206	0.0296	0.0444
4.5	0.0180	0.0259	0.0388
6.0	0.0163	0.0234	0.0350

A POINT ON THE CURVE

In order to test the validity of the algebra and arithmetic of the foregoing an example is appropriate:

Take: Gross Volume $\forall = 100 \times 10^6 \text{ ft}^3$

Fineness Ratio $F = 3.50$

Design Velocity $V = 200$ ft/sec @ 3000 ft

Nominal Gross Buoyant Lift $= 6.2 \times 10^6$ lb

The ellipsoidal shape has the dimensions:

$$D = \left(\frac{6\forall}{\pi F}\right)^{1/3} = 379 \text{ ft}, \quad L = 1325 \text{ ft}$$

$$\text{Surface Area} = 2.75 \times 379 \times 1325 = 1.38 \times 10^6 \text{ ft}^2$$

Fin Area:

$$4\ A_F = 1.10\ \forall^{2/3}\left(\frac{0.5 + 0.067\ E}{F^{2/3}}\right) = 75{,}500 \text{ ft}^2$$

Design Bending Moment:

$$CBM = 0.11 + \frac{3F}{80} = 0.241$$

$$u = 35 \text{ ft/sec} \quad q = \tfrac{1}{2}\ (0.002175)(200)^2 = 43.5\ \#/\text{ft}^2$$

$$M = CBM\ \frac{U}{V}\ q\ \forall = 183 \times 10^6 \text{ ft/lbs [limit]}$$

$$= 275 \times 10^6 \text{ ft/lbs [ultimate]}$$

Sandwich Proportions:

$$\text{Core thickness,} \quad t_c = 3.24 \times 10^{-3}\left(\frac{275 \times 10^6}{379}\right)^{1/2} = 2.76 \text{ In.}$$

$$\text{Face thickness,} \quad t_f = \frac{2.76}{172} = 0.016 \text{ In.}$$

Sandwich Weight:

Faces: $2\ (0.016)\ (0.10)\ (144) = 0.461\ \#/\text{ft}^3$

Core: $2.76 \times \frac{2}{12} = 0.461$

Core + Faces $= 0.922$

Adhesive $= 0.100$

Shell Wt. $W_S' = 0.922 \times 1.38 \times 10^6 = 1.272 \times 10^6$ lbs

Adhesive: $= 0.10 \times 1.38 \times 10^6 = 0.128 \times 10^6$ lbs

Weight Fractions:

Core + Faces $\dfrac{1.272 \times 10^6}{6.2 \times 10^6} = 0.205$

Adhesive $\dfrac{0.138 \times 10^6}{6.2 \times 10^6} = 0.0222$

By Equations:

$$16.0\ F^{1/2} \left(0.11 + \frac{3F}{80} \right)^{1/2} V^{1/2} \times 10^{-3} = 0.207 \quad \text{OK}$$

$$6.84 \left(\frac{F}{V} \right)^{1/3} = 0.0223 \quad \text{OK}$$

Faces Stresses:

$$F_{cr} = 0.52\ E\ \frac{t_c}{R} = \frac{0.52 \times 10^6 \times 2.76}{\frac{1}{2} \quad 379 \quad 12} = 6320 \text{ psi}$$

Allowable load $N_{cr} = 6320 \times 12 \times 2 \times 0.016 = 2430$ #/ft

Ultimate load $N = \dfrac{275 \times 10}{\frac{\pi}{4} \times 379^2} = 2440$ #/ft OK

Empennage:

Design load - 35 ft/sec gust - 200 ft/sec velocity @ 3000 ft

$C_{N\alpha} = 2.0/\text{Rad.}$

$C_N q = 2.0 \times \frac{35}{200} \quad 43.5 = 15.2$ #/□ ft limit, 22.8 ultimate

Fin Area [ea.] = 18,900

Root Chord = 183 ft

Span = 137 ft

Ultimate load = 431,000 lbs

Root Bending Moment = $\frac{4}{9} \times 137 \times 431{,}000 = 26.2 \times 10^6$ ft lbs

Optimum thickness ratio = $0.0154\ (22.8)^{1/2} = 0.0736$

Root Section Thickness = $0.0736 \times 183 = 13.5$ ft

Compression Cover loading [on 40% of the root chord]

$$N = \frac{26.2 \times 10^6}{0.40 \quad 18.3 \quad 13.5} = 26{,}500 \text{ \#/ft} = 2210 \text{ \#/In.}$$

The optimum panel thickness is determined from

$a/h = 42.5$ [for $\sigma_u = 60{,}000$ psi]

Panel thickness $h = \frac{13.5 \times 12}{42.5} = 3.81$ In.

Face thickness $t_f = \frac{2210}{2 \times 60{,}000} = 0.0184$ In.

Face Weight $2 \times 0.0184 \times 14.4 = 0.530$ #/ft^2

Core Weight $3.81 \times 3.4 \div 12 = 1.08$ #/ft^2

[A slight error is indicated in that the equations were set up to yield proportions of maximum bending stiffness which requires that the core weight be twice the face weight.]

Two covers plus a spar and rib weight equal to the weight of one cover results in a total weight in the root region of

$$W = (1.61 + 0.10)\ 3 = 5.13 \quad \#/ft^2$$

Projecting this weight over the area of 4 fins with a 4/3 factor to cover cruciform carry through gives

$$W_E = \frac{4}{3} \times 75{,}500 \times 5.13 = 524{,}000 \text{ lbs}$$

for the weight of the empennage.

The weight estimating equation P. G-13 gives

$$\frac{W_E}{0.062\ \forall} = \frac{4}{3}\left[\frac{V^{1/2}\ (0.5 + 0.067\ F)^{3/2}}{41\ F}\right]\left[1 + \frac{392}{V^{1/2}\ \forall^{1/3}}\right]$$

which for $V = 200$, $F = 3.5$ and $\forall = 100 \times 10^6$

$$= \frac{4}{3}\left[\frac{14.14\ (0.5 + 0.234)^{3/2}}{41 \times 3.5}\right]\left[1 + \frac{392}{14.14 \times 464}\right]$$

$$= \frac{4}{3}\ [0.0620]\ [1.059] = 0.0875$$

For a total empennage weight of:

$$W_E = 0.0875 \times 6.2 \times 10^6 = 542{,}000 \text{ lbs}$$

The weight estimating equation is based on sea level flight. To correct for a design altitude of 3000 ft

$$W_E = 542{,}000 \times \left[\frac{0.002175}{0.002378}\right]^{1/2} = 520{,}000 \text{ lbs}$$

which agrees with design calculation value of 524,000 to slide rule accuracy.

Transverse Frames:

Without further checking, the transverse frames will weigh:

$$W_F = 6.2 \times 10 \times \frac{0.138}{1000}\left(\frac{100 \times 10^6}{3.5}\right)^{1/3} = 252{,}000 \text{ lbs}$$

<u>Summary of Weights</u>

Hull Structural Shell	1,272,000
Transverse Frames	252,000
Empennage	520,000
	2,044,000 lbs
Gross Volume	100×10^6 ft^3
Volume displaced by shell and internal components	1×10^6
Ballonet volume for 5000 ft pressure height	14×10^6

Net gas volume	85×10^6
Buoyant lift @ 0.062	5.26×10^6 lbs

$$\frac{2.044}{5.26} = 0.387$$

Many additional components need to be added to arrive at a total weight empty figure:

Cargo bay and provisions	200,000 *
Control car, crew quarters, etc.	10,000 *
93,000 yd^2 of ballonet fabric @ 9 oz.	52,000
Gas valves, ballonet fullness control system mooring and handling and misc.	250,000 *
Propulsion - 125,000 HP [estimate]	
Engine [turbine] Props, gearing, outriggers	175,000
Fuel for 10 hrs @ cruise [80% of installed HP @ SFC of 0.5]	500,000
Fuel system	50,000
Additional weights	1,237,000
Weight W.O. payload	3,277,000
Nominal payload [1000 mi range @ 136 mph]	991 tons
Producitivity [payload]	135,000 ton mi/hr
Range [with 600 ton payload 75 mph against 15 mph headwind]	9,000 miles
Station keeping endurance 100 ton load - 30 mph wind	400 hours

*Preliminary estimates based on equations of Appendix E

SUMMARY, EVALUATION AND CRITICAL REVIEW

Conclusions and Observations

It has been shown that a large rigid airship constructed as a monocoque sandwich shell exhibits a structural weight empty fraction comparable to smaller airships of conventional construction. Minimum gage considerations tend to limit this approach to very large airships.

The sandwich shell of the 3000 ton example airship exhibits a bending stiffness equivalent to an Oak plank 1.64 inches thick. Even at the minimum gage limit the plank thickness for equal stiffness is 0.82 inch.

It has been shown that of the three major components studied, the airship shell is the dominant weight term. It is interesting to note that the shell weight fraction is independent of airship size if the weight of the adhesive is neglected. With the weight of the adhesive included the shell weight fraction actually decreases slightly with increasing size. Using the gust criteria for the maximum design bending moment results in a shell weight fraction which varies with the square root of the design velocity. The fineness ratio enters into the fraction at the 5/6 power indicating that for minimum weight very low fineness ratios are desirable.

The transverse frames in this parametric study are designed without regard to differential gas pressure since it is assumed that no gas cells or compartmentation of the gas volume is to be provided. It is interesting to note that the transverse frame weight still exhibits a 4/3 power relationship to the airship volume.

The tail surfaces constructed as multi-cell box beams using sandwich panels throughout exhibits an empennage weight fraction which is proportional to the square root of the design velocity. This results from the assumption that maneuvering tail loads will never exceed the loads created by encountering the design gust at the maximum cruise velocity.

The empennage weight fractions shown seem to be larger than might be expected. This results from several factors:

1. The aspect ratio assumed here is higher than in historical airship design practice.

2. The fins are designed to be fully cantilevered with no external bracing, and

3. The sandwich design analyzed here is about twice as heavy as a fabric covered truss work structure of the same strength.

To illustrate the weight dependence on design velocity, compare the weights of the example 3000 ton airship designed for a maximum cruise velocity of 200 ft/sec with the weights of the same airship components for a design velocity of 120 ft/sec.

Component	WEIGHTS 200 ft/sec	120 ft/sec
Hull shell	1,272,000	985,000
Transverse frames	252,000	252,000
Empennage	520,000	403,000
ΣW =	2,044,000	1,640,000
$\frac{\Sigma W}{0.062 \forall}$ =	0.330	0.264

Internal Pressure Considerations

The monocoque sandwich hull has been designed to resist the maximum design bending moments with no help from internal pressure. The existence of internal pressure cannot be ignored however. The lifting gas will expand with temperature increases and altitude if a zero superpressure is maintained. Attempts to operate at 100% fullness in a sealed hull with changes in temperature and altitude will result in intolerable pressure vessel stresses. Of equal importance is the threat of collapse if the internal pressure is allowed to fall much below the ambient external pressure. For these reasons a pressure control system is required. Provisions must be made to allow ambient air into and out of the hull as conditions demand. To avoid mixing of air with the helium, air bags [ballonets] must be provided. The longitudinal location of the internal air volume must be controlled to avoid unstable shifts of the center of buoyancy. From this standpoint a single ballonet located at the center of buoyancy and vented to the atmosphere through a large orifice would be ideal. The vent location should be such that a small positive component of the dynamic pressure is applied to the ballonet in forward flight. As a practical matter the transverse frame structure will require that several ballonets be installed and some control over fore and aft shifting of the ballonet air must be provided.

Critical Review

Conservative Assumptions:

1. The internal pressure has been completely ignored in determination of the compression buckling strength requirements of the hull. Even with no super pressure the internal gas pressure creates tension stresses in the hull and provides a large reserve strength for "sagging" moments. It is very probable, however, that the weight and buoyancy distributions

of such a ship will create a "sagging" moment which is not considered in the analysis. Additional sagging moments will be encountered if the airship is flown "heavy". Only a detailed study of a specific configuration will show whether these effects compensate for each other and result in a critical design moment larger or smaller than assumed.

Introduction of super pressure changes the situation considerably. If we assume a super pressure at some large fraction of the dynamic pressure the hull becomes a pressure stabilized metalclad with no requirement for a sandwich design at flight speeds. Low speed flight and ground loads provide the strength criteria for the non buckling hull in this case. There appears to be much need for trade-off studies in this area.

2. The sandwich shell has been assumed to be uniform over the entire hull. A detail design would undoubtedly reveal large regions where the critical compression loads are lower than the values assumed here. This allows the possibility of reduced sandwich thickness with weight reductions and/or a shift of weight from the core to the faces. The latter would seem to be very desirable in the lower section of the hull to provide a more secure resistance to damage.

3. The weights of the transverse frames have been evaluated on the assumption that the total unbalanced lift is delivered to a single point. Rim and spoke members have been designed for the maximum loads throughout although the loads occur at top center only and diminish considerably around the periphery of the frame. A simplistic radial spoke bracing system has been assumed to facilitate analysis, whereas it is likely

that lighter weight patterns are available. These factors combine to suggest that the frame weight fraction used is very conservative.

4. As mentioned elsewhere in the text, other studies show that the empennage weight fraction is about twice that required for a fabric coverd truss work construction.

Other Considerations:

1. Fineness ratio and shape:

   The parametrics show that low fineness ratios result in the minimum weight design. This results in a very large diameter hull and will require ingenuous construction concepts - a very large facility. The elliptical profile chosen for convenience of analysis results in double curvature throughout the surface with every section different. Tooling costs for forming the skins and bonding the panels would likely be prohibitive. Some improvement in this regard could be had by making this shape symmetrical fore and aft so at least two of everything would be required. A more desirable arrangement would be to build as much of the hull as possible in a straight cylindrical shape thus achieving a multiplicity of identical shell panels and transverse frames. This approach, however, tends to be at cross purposes with the need for a low fineness ratio since a long cylindrical center section is difficult to achieve with a satisfactory aerodynamic shape and low fineness ratio.

2. Non-optimum sandwich proportions:

   Minimum weight for a sandwich circular cylinder in bending occurs when the weight of the faces equals the weight of the

core. Strength requirements dictate that the product of the face thickness times the core thickness be a constant determined by the bending moment and hull diameter. This results in thin face sheets. Some increase in face thickness can be had at a moderate weight penalty. If the face sheet thickness is increased so that

$$t_f/t_{f_{opt}} = \alpha$$

and the core thickness is reduced accordingly so that

$$\frac{t_c}{t_{c_{opt}}} = \frac{1}{\alpha}$$

The weight ratio becomes

$$\frac{W}{W_{opt}} = \frac{1}{2} \left(\alpha + \frac{1}{\alpha}\right)$$

α	W/W_{opt}
1.0	1.0
1.25	1.025
1.50	1.083
2.00	1.25
3.00	1.67

Thus the face thickness can be increased considerably for a minor weight penalty. Acceptance of the weight penalty also reduces the minimum size airship which can be built within the minimum gage limitation. This also provides a mechanism for making the face thickness fall on standard gages with minor weight penalty.

Another approach to increasing the thickness of the outer face sheet is to unbalance the sandwich. Let $t_o/t_i = \beta$.

The critical buckling stress for unbalance face sheets is proportional to

$$F_{ct} = \frac{\sqrt{t_o \, t_i}}{\frac{1}{2}\,(t_o + t_i)}$$

and an optimum balance between face weight and core weight results in an increase in the core thickness in the ratio:

$$\frac{t_c}{t_{c_{opt}}} = \left(\frac{1 + \beta}{2\sqrt{\beta}} \right)^{1/2}$$

and the sandwich weight increases in the same ratio

$$\frac{W}{W_{opt}} = \left(\frac{1 + \beta}{2\sqrt{\beta}} \right)^{1/2}$$

β	$W/W_{opt} = \left(\frac{1 + \beta}{2\sqrt{\beta}} \right)^{1/2}$
1.0	1.0
1.25	1.005
1.50	1.011
2.00	1.031
3.00	1.072

Large unbalance between the outer and inner face sheet thickness can be used with a minor weight penalty.

The face thicknesses become

$$\frac{t_i}{t_{opt}} = \frac{\sqrt{2}}{\beta^{1/4}(1 + \beta)^{1/2}}$$

$$\frac{t_o}{t_{opt}} = \beta \frac{t_i}{t_{opt}}$$

For the design example of the 3000 ton airship

$$t_{c_{opt}} = 2.76$$

$$t_{opt} = 0.016$$

$$\text{Weight} = 0.922\ \#/ft^2 + 0.10\ \#/ft^2\ [\text{glue}] = 1.022$$

If the faces are unbalanced at $\beta = 2.0$

$$t_i = \frac{0.016 \times \sqrt{2}}{(2)^{1/4}\ (3)^{1/2}} = 0.0110$$

$$t_o = 2 \times 0.011 = 0.022$$

$$t_c = 2.76 \left(\frac{1 + 2}{2\sqrt{2}} \right)^{1/2} = 2.84$$

The resulting unbalanced sandwich weight:

Core: $\frac{2.84}{12} \times 2 = 0.474$

Outer face	0.22×14.4	=	0.316
Inner face	0.011×14.4	=	0.158
Glue			0.100
			1.048

This compares to 1.022 for the optimum sandwich. Since the shell typically amounts to 25% of the nominal gross lift or less it would seem to be desirable in most cases to sustain a slight weight penalty to permit use of thicker face sheets on the outside surface. It appears relatively large increases can be made for a very small penalty in useful load. In the above example the useful load penalty is on the order of 1% for an outer face thickness increase of 37%.

References

G-1 Burgess, C.P.; The Ultimate Airship, Design Memo No. 274, August 1937

G-2 Pavlecka, V.H., and Roda, J.; The State of the Art of Metalclad Airships, Proceedings of the Interagency Workshop on Lighter-Than-Air Vehicles, FTL Report R75-2, Jan. 1975

G-3 Goodyear Aerospace Corporation, Feasibility Study of Modern Airships, NASA-CR-137692, Volume III, Historical Overview, July 1975

G-4 HEXCEL TSB123, October 1967, Design Handbook for Honeycomb Sandwich Structures

G-5 Gerard, Minimum Weight Analysis of Compression Structures, New York University Press, 1956

G-6 Burgess, C. P., Airship Design, Ronald Press Co., 1927

APPENDIX H

DESIGN OPTIONS

CONVERSION FACTORS FOR APPENDIX H

1 lb	=	0.4536 Kg
1 lb/HP	=	0.4536 Kg/HP
1 Kg/HP/HR	=	0.4536 Kg/HP/HR
1 ft^3	=	0.02832 m^3
1 knot	=	0.51389 m/sec
1 ft/sec	=	0.3048 m/sec
1 ton mi/hr	$\cong$	1460 Kg-Km/hr
1 lb/ft^3	=	16.02 Kg/m^3

This Appendix presents the results of the brief investigations of several advanced technology design options of potential interest to modern airship applications. The design options discussed include:

1) Alternate Powerplants
2) Buoyancy Management
3) Artificial Superheat
4) Boundary Layer Control
5) Stern Propulsion
6) Alternate Lifting Gases

The results of a brief sensitivity analysis for a 2×10^6 pound gross weight conventional rigid airship are also included.

Alternative Powerplants

One part of the overall parametric analysis effort included an analysis of alternate propulsion systems. Basically, three factors were regarded to be of major importance with regard to these alternate sources and these factors are:

1) Bare engine weight per horsepower (weight density)
2) Specific fuel Consumption (SFC)
3) Availability of a particular type of propulsion system over the power rating(s) required

Items (1) and (2) above are rather obvious considerations of importance and with given data in both categories for a variety of propulsive systems, a given mission profile in terms of range and velocity, and a given vehicle configuration straight forward trade-offs can be made to determine the more effective system. Prior to discussing item (3) above the following simplified trade-off analysis of the baseline and selected alternative propulsion

systems is provided for a 2×10^6 pound gross weight conventional airship configuration. For a cruise velocity of 70 kts into a fifteen kt head wind, approximately 14,000 horsepower are required. Recognizing that the "optimum" or best engine cycle is a function of range and hence must be considered for each specific mission application, the following example illustrates the relative performance for a long range mission/application. For purposes of this analysis a hypotetical range of 5000 nautical miles was assumed. Table H-I presents the uninstalled engine plus fuel weight required for this range for the system considered.

The basic propulsion system weight density [engine weight per unit horsepower] and performance characteristics [SFC] used in the analysis are presented in Figures H-1 and H-2, respectively, for the following engine cycles:

The turboprop engine [Brayton cycle] represents the current state-of-the-art as does the air-cooled reciprocating engine [Otto cycle]. Air cooled aircraft Diesel engines are the product of past development which have not been used in recent years. The Rankine cycle data are based on the aircraft steam engine currently being developed by Lear in the low horsepower class. The Stirling cycle engine is represented here by work performed by General Motors. The nuclear propulsion systems weight density also depicted here is based on NASA Lewis Research Center's concept of a helium-cooled reactor with a heat exchanger in a turbine engine and the associated weights including provisions for adequate shielding and crash safety. Such a turboprop engine could also be employed as a conventionally fueled chemical engine for takeoff and landings.

Estimated fuel consumption characteristics are presented in Figure H-2. To be compatible with the engine weight definition based on the continuous operating cruise horsepower the specific fuel consumption [SFC] should also be based on this horsepower.

Table H-I - Comparison of Baseline (Turboprop) with Alternate Propulsion Systems

System	Weights (lbs) Fuel	Uninstalled Engine for 1400 HP	Fuel Plus Uninstalled Engine (lbs)
1. Stirling, (Four 3500 horsepower engines; SFC = 0.48)[1]	373,333	75,600	448,933
2. Nuclear-Turboprop (one 14,000 hp engine)	-	252,000	252,000
3. Steam			
a. Four 3500 horsepower engines[2] SFC = 0.42	326,666	41,500	368,166
b. Four 3500 horsepower engines[3] SFC = 0.42	326,666	17,500	344,166
4. Air-Cooled Reciprocating			
a. Four 3500 horsepower engines at max continuous hp; SFC = 0.76)	591,111	14,000	605,111
b. Four 7,000 horsepower engines at best SFC(0.44); Power setting = 0.50	342,000	28,000	370,000
c. Twenty eight 1,000 horsepower engines at best SFC(0.44); Power setting = 0.50	342,000	33,600	375,600
5. Turboprop (Four 3500 horsepower engines; SFC = 0.48)	373,333	2,800	376,133
6. Air Cooled Diesel (Four 3500 horsepower engines; SFC = 0.37)[4]	287,777	29,400	317,177

1) Based on improved weight density paralleling other engines of Figure H-I

2) Based on same weight density as indicated for 165 hp Lear engine.

3) Based on improved weight density paralleling other engines of Figure H-I

4) Based on extrapolation of data from Figure H-I and Figure H-2

Reciprocating Otto cycle [gasoline] engine do not exhibit their best [least] SFC at maximum horsepower but at a fraction thereof. Such a variance has not been found to be associated with the other engine cycles. The aircooled Diesel's SFC is observed to have the most favorable value outside the obvious superiority of the nuclear-turboprop propulsion system.

Several factors are apparent from the admittedly approximate results of Table H-I. It is believed the conclusions drawn subsequently, however, are basically the same as those that would be obtained from a much more extensive analysis. Relative to the results presented, the following comments seem appropriate:

1. The Stirling cycle based upon an assumed favorable extrapolation to larger size engines does not appear to be worthy of further consideration unless a substantial improvement in SFC is realized.

2. As has been shown frequently in prior analyses, the nuclear engine is an interesting consideration. However, specific inquiries by Goodyear relative to this subject in past years has indicated development costs to be extremely prohibitive. Unless such a system becomes available on more or less of a spin-off basis it will probably never be seriously considered for LTA vehicles.

3. The steam engine has an indicated competitive capability based upon a favorable extrapolation of available weight density. It is not believed to be the alternative propulsion system that should be evaluated in detail during Phase II. This is basically due to development status and the limited availability from a power output standpoint.

4. It appears that an air-cooled reciprocating engine, operating at an approximate power setting of 0.50, would be competitive from the standpoint of the measure of comparison of Table H-I

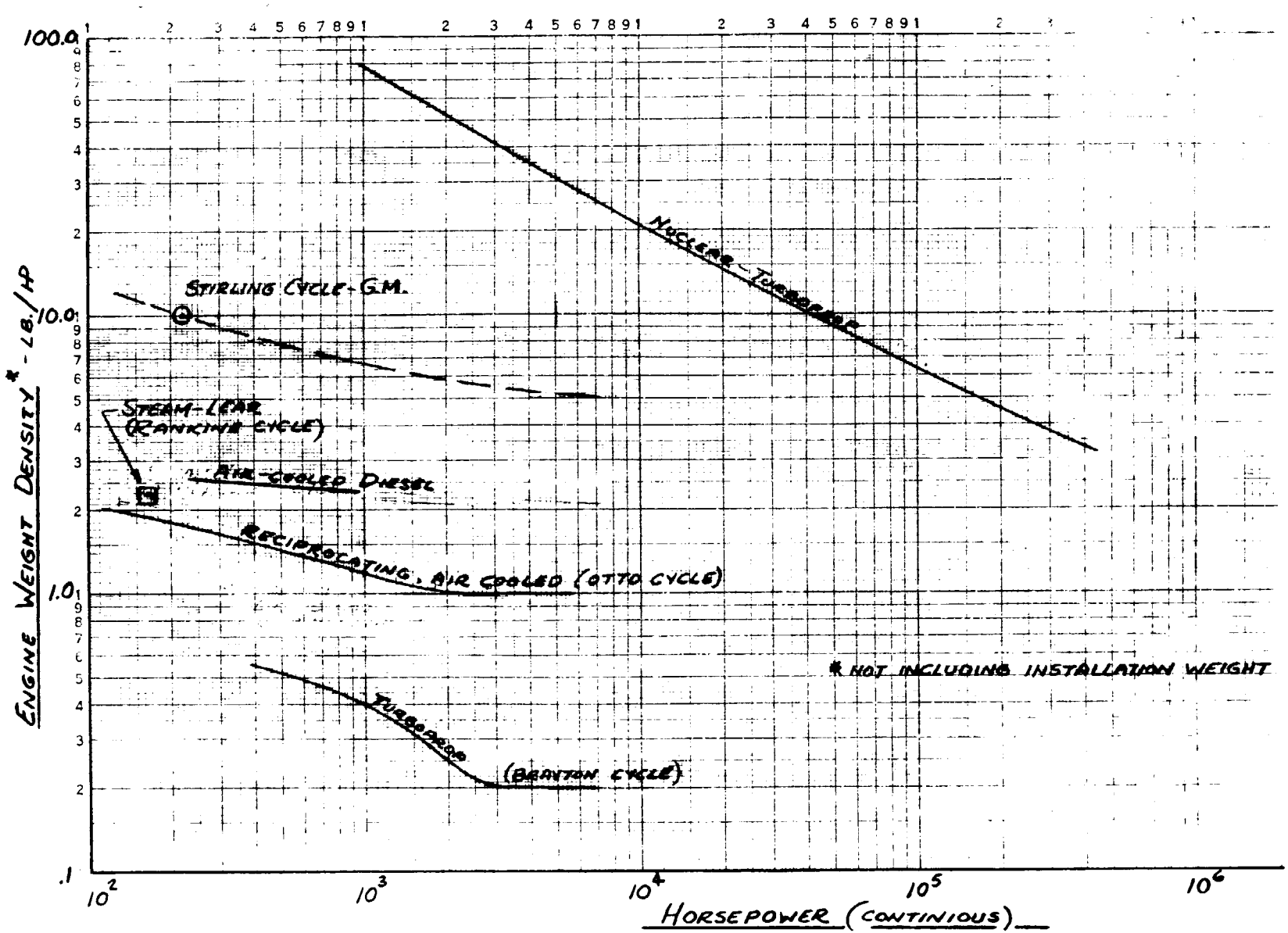

FIGURE H-1 - WEIGHT DENSITY OF VARIOUS PROPULSION ENGINE CYCLES

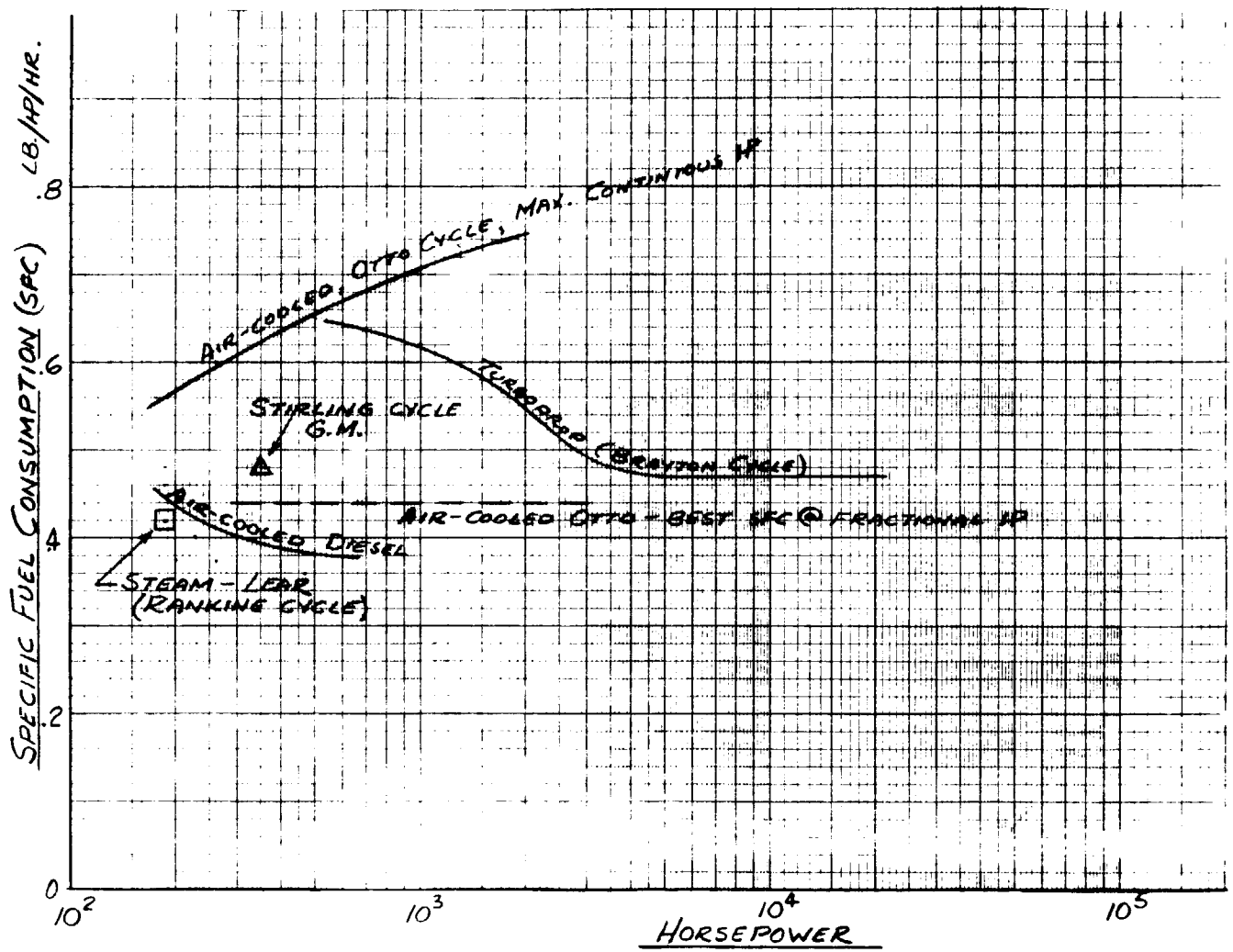

FIGURE H-2 - SPECIFIC FUEL CONSUMPTION OF VARIOUS PROPULSION ENGINE CYCLES

with the baseline turboprop. However, the availability factor in the over 1,000 horsepower class would probably lead to perhaps as many as 28 individual engines being required.

5. The turboprop is the baseline for the study and is available over the range of sizes of interest. In general as range decreases, the turboprop becomes more desirable because of its low weight density. The range of 5,000 nautical miles, for the example being currently discussed was purposely considered because alternatives tend to compare more favorably at the longer ranges for the reason just cited.

   Probably the most uncertain consideration surrounding the use of the turboprop is the consideration of accommodating fuel burn off: e.g., buoyancy management.

6. The air cooled diesel appears, on the basis of a favorable extrapolation of data presented in Figure H-I, to be the alternative propulsive system that should be considered in detailed during Phase II. Factors leading to this statement are:

   a. The favorable comparison between the turboprop and the diesel in Table H-I.

   b. The fact that the diesel engine is well suited to buoyancy via water recovery.

   c. A successful history of application in past airships [i.e. the Hindenburg and Graf Zeppelin II].

   d. A favorable comparison with respect to fuel cost.

Buoyancy Management*

In order to achieve a manageable vehicle at low or zero speed it was necessary in rigid airships to prevent the gross weight from becoming less than the static lift. This was an especially important design consideration for the long range and the high endurance vehicles. Realizing that a large MAV's may have comparatively large fuel loads initially and undergo a corresponding large change in gross weight during flight, this aspect of buoyancy management becomes very important to the preliminary design efforts of Phase II of this study also. In order to adjust the loss of fuel weight some ballast must be added or the volume of lifting gas decreased. Different ways to do this have been utilized dependent upon the type of engines used and various interrelated mission considerations. Several demonstrated and/or proposed approaches (some of which are practical) are listed below and discussed subsequently:

1. Water recovery from fuel combustion products (used often in past rigid airships (Akron, Macon),
2. Use of a neutrally buoyant gaseous fuel (used in Graf Zeppelin),
3. Use of a lifting gaseous fuel to counteract liquid fuel weight,
4. Valving lifting gas (past German ships using hydrogen).
5. Compressing and storing lifting gas,
6. Taking on ballast from local bodies of water in transit (used in past non-rigids),
7. Artificial superheat.

---

*The discussion here does not include the non-rigid requirement of a ballonet system which would remain in future pressurized airships essentially unchanged from the automatic, manual override system used in the ZPG-3W.

Water recovery, to have a reasonable maintainability, must be used with lead free fuels. Only engines which can operate with the back pressure imposed by a moderate weight recovery heat exchanger can be used. This restricts the choice of currently available power plants with the diesel and stirling systems best suited to the water recovery techniques.

The water recovery system principle is based on the fact that the combustion of a hydrocarbon fuel will produce water and carbon dioxide. The water is in the form of a vapor but if the combustion products are passed through a heat exchanger the water can be condensed out and retained on board the vehicle as ballast to replace the weight of the fuel burned. Although the carbon dioxide is lost, every two hydrogen atoms combine with an oxygen atom from the air. The result is that the gross weight of the ship can be maintained during flight.

The use of a neutrally buoyant gas as a fuel means that the loss of gas during flight has no net effect on the airship buoyancy. A mixture of hydrocarbon gases such as methane and propane and/or butane can be composed to have density equal to that of air. The negative aspect of this method is the inflammable gas on board the vehicle. A gas blend, however, was successfully used on the Graf Zeppelin over its nine year operational life in complete safety. One method to enhance the safety associated with the use of a gaseous fuel is to place it in cells within the inert helium lifting gas. This would likely reduce the probability of a combustible mixture of gas and air occurring considerably.

Another method is to combine the use of gaseous fuel and liquid fuel by using a lifting gas. Two lifting gas fuels are readily available. They are hydrogen and methane. In this method enough of the lifting gas is carried to counteract the weight of the liquid fuel. Both the liquid and gaseous fuels are used in the engines and consumed at rates to maintain the lift-weight balance.

Those methods which employ the use of a gaseous fuel are most conveniently compared in terms of the volume of gas required per pound of fuel carried. This is shown below. One variant of item (3) of the prior listing is to burn the lifting gas not in the engines but in a water recovery unit. Depending on the mission, this approach could have an ancillary value such as Auxiliary Power generation, Environmental Control, etc. This reduces the volume of gas required but increases the effective specific fuel consumption (SFC) from the cost, not weight or range, point of view. That is, the gaseous fuel consumed must be paid for but since no vehicle weight change occurs due to its consumption, the range determinant SFC is unchanged.

Buoyancy Control Method		Vol. of Gas $(Ft)^3$ per Pound of Fuel	Change in SFC
Neutrally buoyant gaseous Fuel	Hydrocarbon Blend*	13.1	0
Lifting Gaseous Fuel with Liquid Fuel	H_2	14.0	
	CH_4	29.2	
Lifting Gaseous Fuel with Water Recovery	H_2	8.6	+0.045*
	CH_4	7.7	+0.326*
Valving Helium	-	15.2	0
Compression and Storage of Helium	0	13.1	0

*Cost only, not range

The compression and storage of helium looks good until the weight of the tanks to hold the gas is considered. Valving helium is very expensive and too wasteful of a limited resource.

The use of water from lakes and sea as ballast is a method that has been used but is obviously restricted to certain missions and terrain.

Artificial super heat as a means of providing a workable solution to buoyancy control consideration has been the subject of significant past study. The subject of artificial super heat is addressed in the following section.

In summary it is Goodyears opinion that the following should be considered during the preliminary design effort of Phase II:

A. Turboprop engine considering buoyancy control by:

   1. Use of neutraully buoyant gas (blend of hydrocarbon fuels) contained within helium cells.

   2. Use of hydrogen gas/hydrogen liquid fuel contained within helium cells.

B. Diesel engine and conventional water recovery technique.

The above recommendations are basically all state-of-the-art in that no new technology would be required. It is true in the case of the diesel engine that an engine manufacturer would have to be contracted to provide a unit suitable for airborne use. However, similar engines have been made in the past. Specifications would require updating, initial units would be somewhat expensive, etc. but in reality the acquisition of suitable diesel engines should not be a significant problem.

The turboprop suggestions are based on the rationale that the hydrocarbon blend of fuels to attain a gas of a density equal to that of air has been demonstrated and is safer than a hydrogen gas/hydrogen liquid fuel.

The rationale supporting further consideration of hydrogen gas/hydrogen liquid is related to the fact that it is not a petroleum derivitive, is readily available, and if safety considerations can be adequately addressed, could have favorable national energy and environmental aspects.

Artificial Superheat

The modulation of aerostatic lift by artificial superheat may have considerable merit in the design of an LTA vehicle. Such a system could permit an airship to be appreciably heavy on the ground while being handled and could further permit a neutrally buoyant condition to be maintained (in many cases) throughout the flight. The provision of heat exchangers to effect an increase or modulate the temperature of the lifting gas above ambient conditions would result in performance and economic impacts which must be compared with the alternative systems described above for each specific mission. The following discussion will describe the potential of artificial superheat for aerostatic lift modulation as constrained by envelope temperature, volumetric expansion, and propulsive waste heat recovery.

For this example, the lifting gas is helium and volumetric expansion is allowed to take place at constant pressure. Figure H-3 shows the relationship of helium temperature, volumetric expansion ratio, and the aerostatic lift ratio. It can be observed that for a superheat of 174 deg F, an increase of 30% in the aerostatic lift can be expected with an accompanying increase in helium volume of 36%.

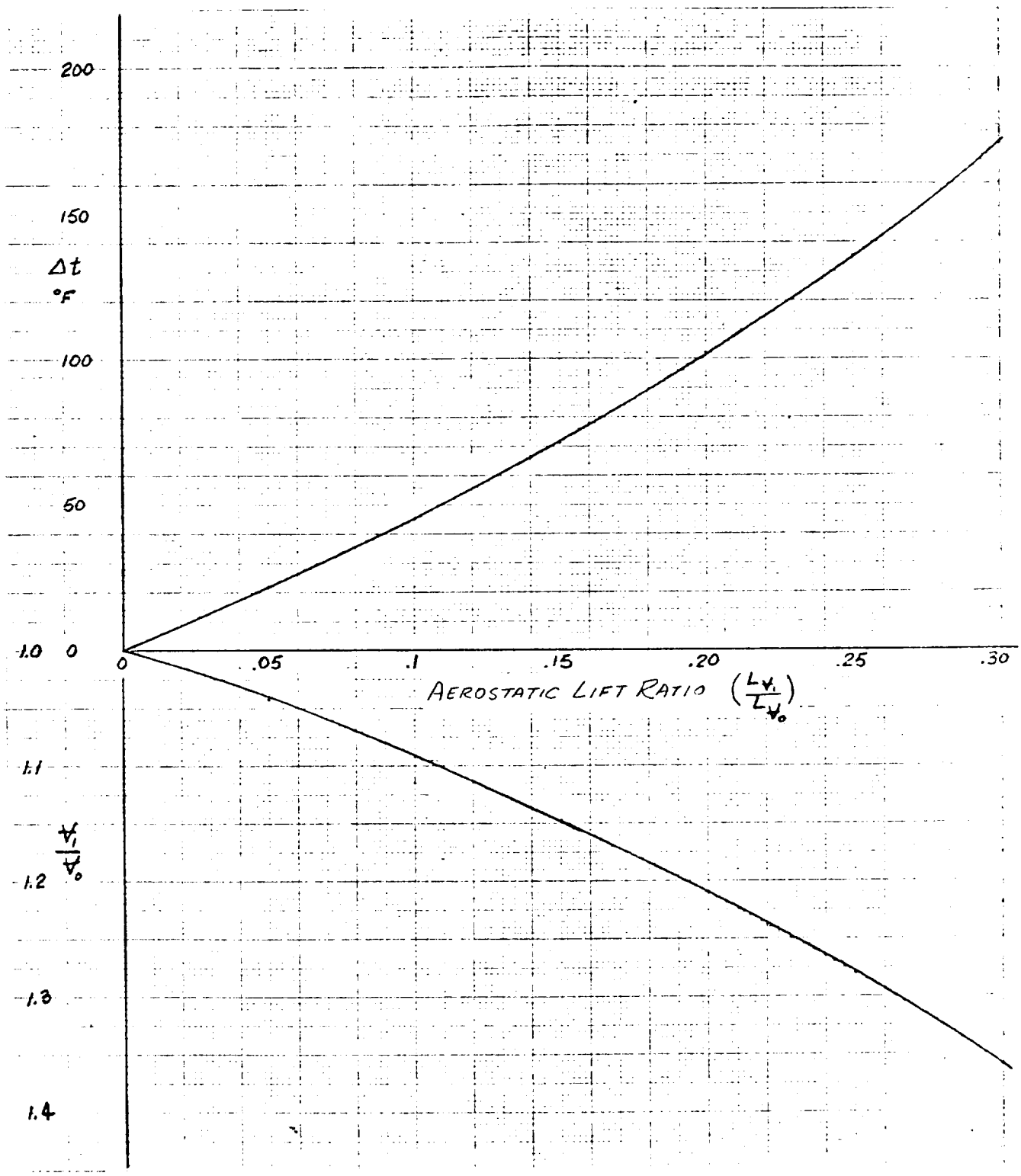

FIGURE H-3 - RELATION OF SUPERHEAT, VOLUME RATIO, AND AEROSTATIC LIFT RATIO

An assessment of envelope material temperature associated with a helium temperature of this magnitude was conducted. The thermal analysis included the appraisal of heat losses through internal convection, conduction through the envelope material, and external convection. This analysis was performed assuming a conventional non-rigid airship with a polymer coated fabric which experiences forced convection external heat losses while in flight. When the flight velocity is zero the envelope temperatures so determined would be applicable to the conventional rigid airship construction where the gas cells are within the outside structure. Figure H-4 indicates the envelope temperatures, which are within the state-of-the-art of materials and seams for joining.

A further consideration in this concept is the possibility of recovering a portion of the waste heat of the propulsion engines as a source of heat to sustain/modulate the superheat. The heat losses through internal and external convection and through envelope conduction were estimated for conventional airships of volumes up to 6 million cubic feet and for various degrees of incremental aerostatic lift ratio, Figure H-5. Also shown in this figure is the heat available from the propulsion engines when these airships are designed to fly a various velocities up to 70 knots. The assumptions used in the heat available analysis are:

a. Specific fuel consumption is 0.5 lb/HP/hr
b. Propulsion efficiency is 0.70
c. 67% of the thermal energy of the fuel is available
d. Heat exchanger recovery factor is 60%
e. Heat value of the fuel is 20,000 BTU/lb.

Figure H-5 indicates that the concept has merit. Sufficient propulsion engine waste heat is available for continually maintaining helium superheat. For considerably larger sizes and somewhat higher velocities, sufficient heat is available to provide modulation of the superheat such that static lift and gross weight can be equalized.

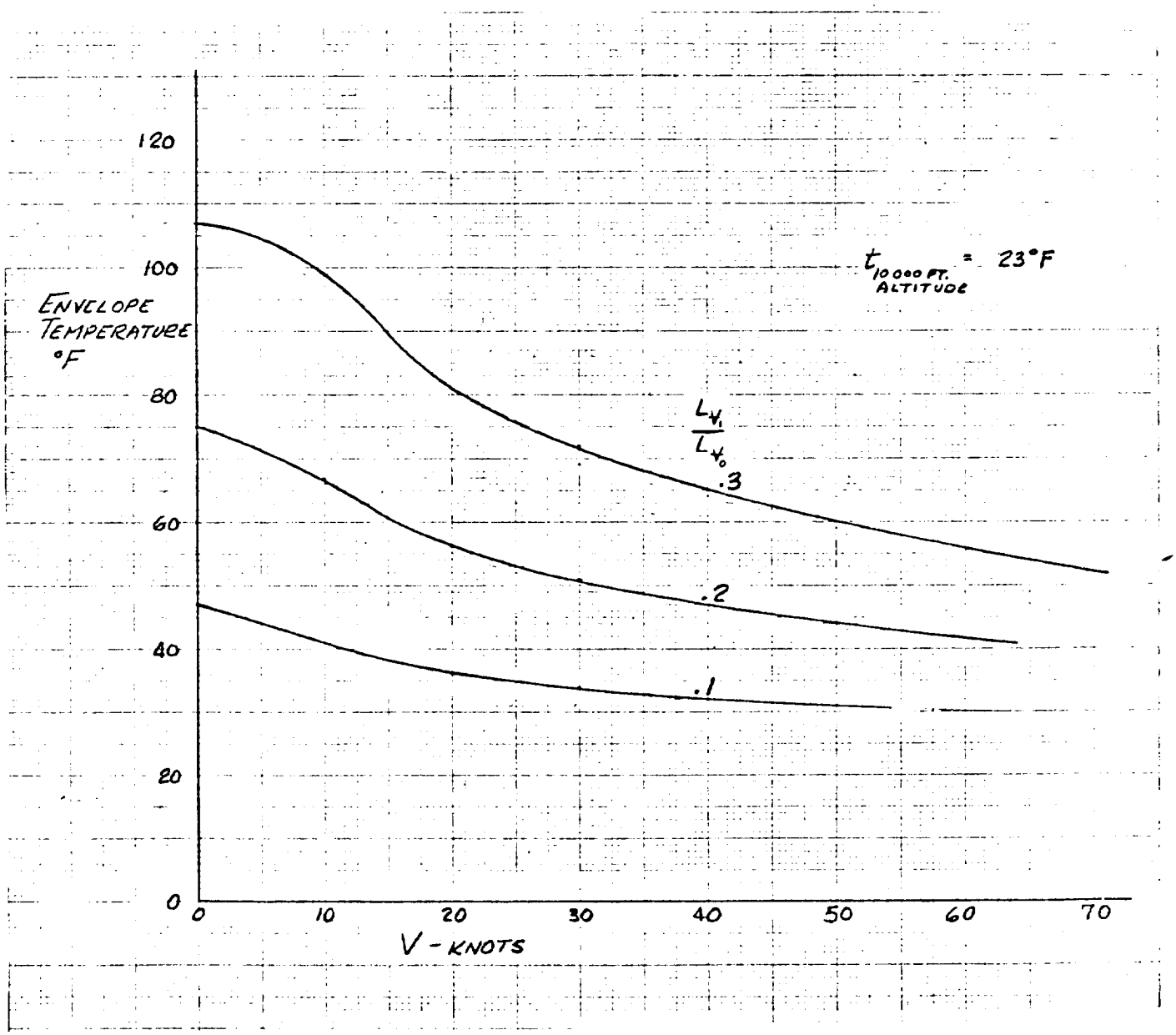

FIGURE H-4 - ENVELOPE TEMPERATURE

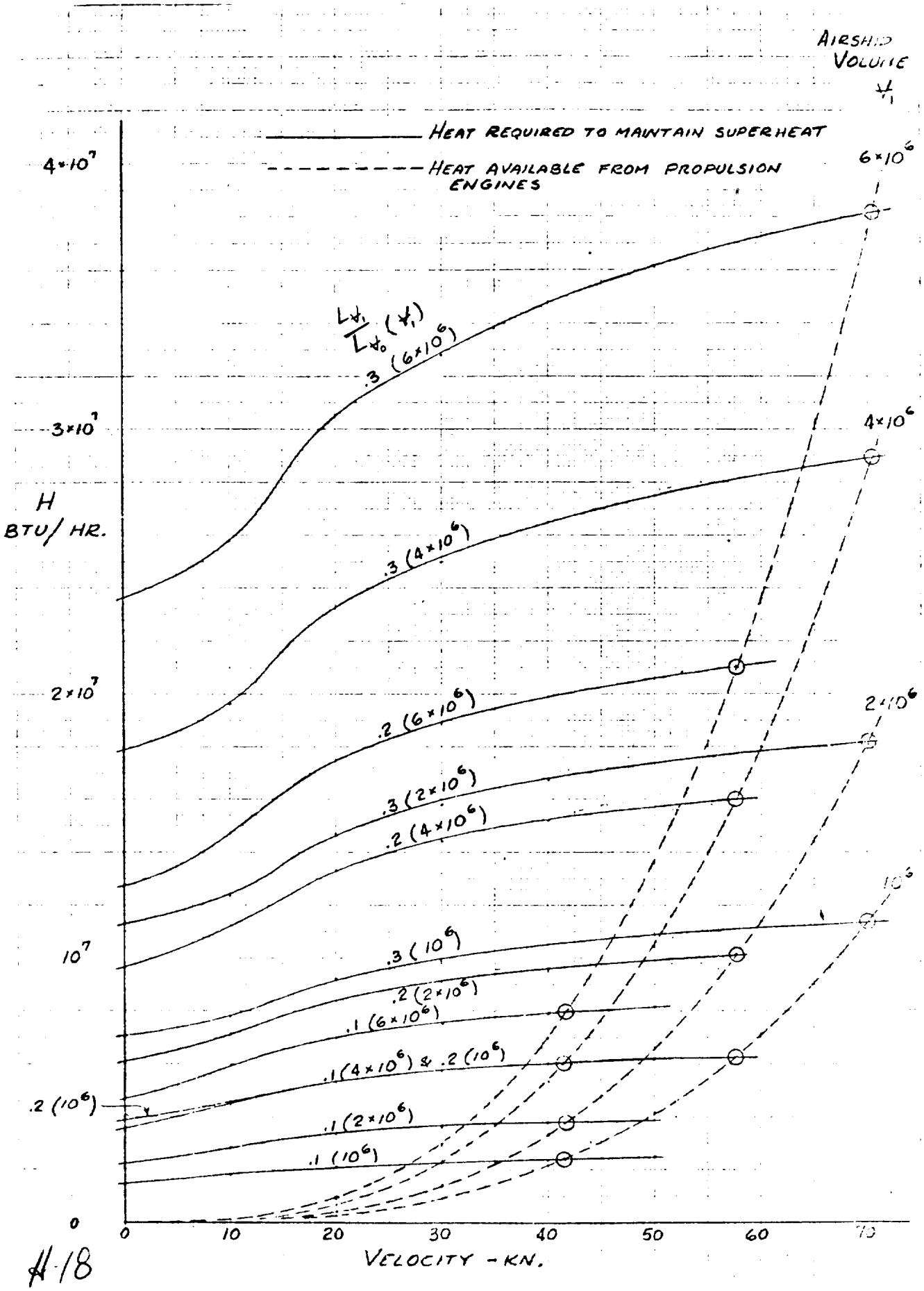

H-18

FIGURE H-5 - HEAT RATE REQUIRED TO MAINTAIN SUPERHEAT AND HEAT RATE AVAILABLE FROM PROPULSION ENGINES

The following is a brief description of how the application of artificial superheat will be considered in the preliminary design effort of Phase II of a large rigid MAV:

(1) For missions requiring a fuel load on the order of 20% of the vehicle gross weight (which includes many missions of interest), artificial superheat will be considered with the use of an external heat source as well as the alternative approach of operating the main propulsion system.

(2) A reasonable design temperature rise on the order of 100°F can be considered. Preliminary analysis indicate a minimal impact on the helium gas cell weight due to this temperature.

(3) Heat recovered from the exhaust will be sufficient to modulate the superheat condition such that the aerostatic lift can be made equal to the gross weight throughout the flight.

In Phase II, artificial superheat will be investigated in more detail as a design option for the recommended vehicle/mission combinations.

Use of artificial superheat for missions/vehicles with fuel loads greater than 20% of the gross weight is feasible but may require initial gas temperatures in excess of 100°F above ambient. For these cases the following factors must be addressed:

(a) Increased temperature of helium gas cells will result in heavier cell structure.

(b) Initial heat will have to be supplied by external sources while on the ground and aerodynamic lift plus the heat recovered from the exhaust may have to be used in the initial portions of the flight.

Boundary Layer Control

The concept of boundary layer control [IBLC] as applied to airship design is presently envisioned as a mechanism whereby flow separation is prevented from the aft surface of the airship hull. A turbulent boundary layer prevails at the high Reynolds number typical of airship hulls with no attempt being made to achieve laminar flow as in some BLC concepts. This BLC concept was the subject of analytical and experimental study under an Office of Naval Research, Contract NOnr 1412(00) LI which was concluded with a comparative analysis of the BLC airship with a conventional non-rigid airship (ZPG-2) at an equal volume of 1,000,000 ft^3. (Ref. H-1 as noted in the Historical Overview summarizes the results of that study). A physical comparison of the airships is noted in Figure H-6. The propulsive power requirements are compared in Figure H-7 for two different missions.

The BLC airship displays a propulsive power advantage for both the towing mission and the flight speed mission. With some 15% propulsive power reduction associated with the BLC airship the same order of percentage is associated with: a) the fuel load for a given flight range, b) the range for the same fuel load, and c) the weight of the propulsive system. The payload will be enhanced from both the fuel load reduction and the propulsive weight reduction for an airship designed for a given range mission. Thus:

$$(\Delta W_{fuel})_{BLC} = -0.15\ (W_{fuel})_{conv.}$$

$$R_{BLC} = \frac{(R)_{conv.}}{0.85}$$

constant fuel load

$$(\Delta W_{payload})_{BLC} = 0.15\ (W_{fuel})_{conv} + 0.15\ (W_{propulsion})_{conv}$$

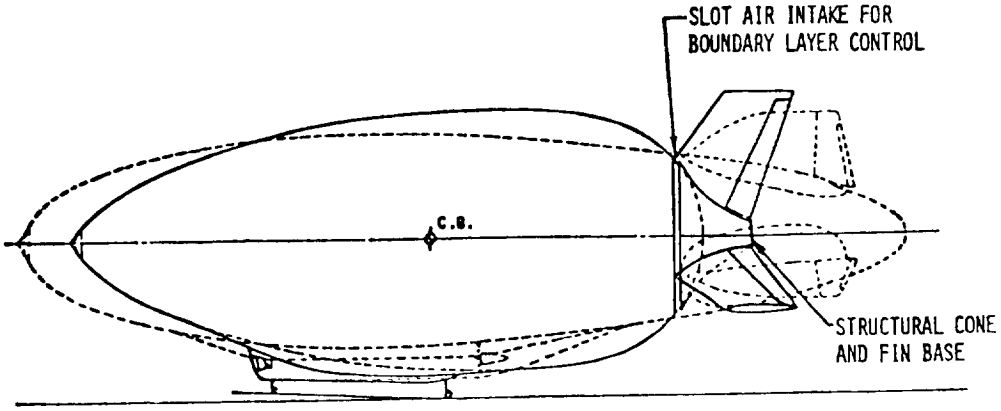

FIGURE H-6
Comparison of BLC Airship with Conventional
For Equal Volume

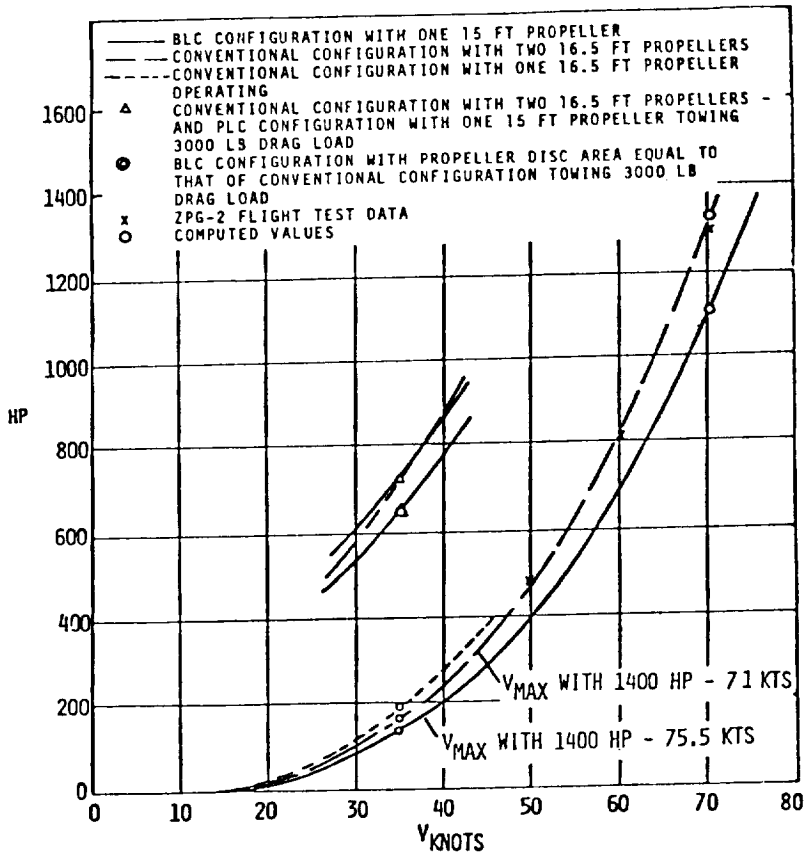

FIGURE H-7
Horsepower Requirements vs Flight Velocity
For BLC & Conventional Airships $\forall = 10^6$

There are four major assumptions in this cursory appraisal of the BLC consideration:

a. The weight empty of the two airships excluding the propulsion system are alike.

b. The slenderness ratio of the BLC airship at 3.0 is best for reduced drag.

c. The airships are neutrally buoyant, i.e., the angle of attack is zero.

d. The "reference" airship is a non-rigid airship whose slenderness is 4.5.

Thus, the BLC appraisal is rather finite as to the airship geometry and deviation from this set of comparison for an estimate of BLC effectivity would require careful examination.

It does not appear at this time that adequate information or justification exists for considering BLC from a preliminary design standpoint in Phase II. The technology plan to be developed in Phase II, however, will address the question of what added investigation in the BLC area is in order. As noted in the Historical Overview these efforts would probably be integrated with further stern propulsion efforts discussed in the following section.

Stern Propulsion

The appriasal of the stern propulsion consideration has as its base the wind tunnel work on a conventional airship hull of 4.8 slenderness ratio with a specially designed stern propeller for efficient operation in the wake of the hull, Ref. H-1. The results of the study discussed herein should be considered as an achievable propulsive proficiency based on experiment with a possibility of improvement.

Figure 11 of Ref. H-1 defines the power expended to overcome the model drag at 139 ft/sec wind tunnel velocity at the maximum propeller efficiency to be 3.87 HP. At this same wind tunnel velocity assuming the conventional outrigger propulsion system with a propeller efficiency of 0.90, the power requirement becomes: 4.38 HP. Thus the use of this stern propeller has reduced the power requirements to the ratio:

$$\frac{HP_{stern}}{HP_{conv}} = 0.88$$

There is a potential for further reduction of this ratio by redesign of the propeller to lessen the pressure drag on the hull's stern arising from the operation of the propeller.

Relative to the use of stern propulsion it must be cautioned however, that if the airship hull is at an angle of attack the wake's characteristics will change from that associated with zero angle of attack. Information from aforenoted reference indicates the stern thrust requirements would double with a 10 degree angle of attack with a consequent change in propulsive efficiency. The propulsive efficiency of the conventional outrigger system, however, is not as sensitive with angle of attack changes.

In a recent Advanced Reserach Projects Agency sponsored program, a Goodyear advertising airship was modified to accommodate a gimbaled stern propulsion system. The feasibility of gimbaled stern propulsion to provide low speed propulsion and control was adequately demonstrated.

As mentioned above, the Phase II technology development plan will include an assessment of both stern propulsion and BLC.

Secondary Study Parameters and Alternate Lifting Gases

The performance evaluation of alternate buoyant fluids as well as the effects of winds and cruise altitude can best be illustrated relative to a baseline vehicle configuration. The baseline vehicle selected for the performance assessment is a neutrally buoyant conventional rigid airship with the following design characteristics:

GW = 2×10^6 pounds @ helium lifting gas

Design Altitude = 5000'

Volume = 39.86×10^6 ft^3

V_C = 82 knots (into 15 kt headwind) for maximum productivity @ 3000 n.m. range.

The sample GASP output in Table H-II is a complete definition of the vehicle design and performance characteristics. The impact of various design options and secondary study parameters will be illustrated in terms of one of the following figures of merit:

(1) Useful Lift [1 - EW/GW] ratio relative to the baseline vehicle value

(2) Productivity at zero range, UL $\cdot$ V_C = 53,300 TM/HR

The brief sensitivity analysis discussed in the final section will also be presented in terms of these figures of merit.

TABLE H-II - SAMPLE GASP OUTPUT FOR BASELINE SENSITIVITY STUDY VEHICLE

VHTYPE	TOTYPE	VARTYP	TPRINT	ENGTYP	H2ORCV	NBLDS	NFINH	VOLGVN
1	0	1	1	1	0	4	0	0

WGROSS	BETA	DRHO	HDES	VC	VW	ETAHUL	ETAPRP
.200000E 07	1.00000	.620000E-01	5000.00	138.000	25.3000	.940000	.900000

ENGKWT	PCTRES	THROTL	WNPSK	ANDFNV	ALPHSD	STBMRG	FINARM
1.00000	.000000	.800000	1.00000	.000000	.000000	.000000	.000000

NR	VTIP	VMAXCL	AF	VTOSF	VG	VDESI	VOLREQ
.800000	800.000	.000000	120.000	.200000	35.0000	.000000	.000000

RDES
200.000

VLOVRD	CPRIS	PBETA
7.60000	.643800	.000000

VOLREQ	ROOTL	AWET	AXAM	NORMAM	BODAMT	AHORZE	VOL23	AFINS
.398248E 08	1656.95	889607.	3113.08	93498.1	92165.3	10845.4	116617.	29915.3

CDSTOT	CDSHUL	CDSFIN	CDSCAR	CDSOTR	CDSMSC	CDZV23
1874.50	1408.13	235.157	20.0000	140.813	70.4063	.160740E-01

REYBOD	CFRICT	DRGLDK	CBM	MA	MM	M40
.152396E 10	.145545E-02	1.08754	.392800	.988861E 08	.120942E 08	.378468E 08

WPROP	WGRBOX	WBRENG	WPREGG	NENG	WENG	WNACEL
933.460	859.592	891.461	3597.10	6.00000	21582.6	912.591

DPROP	DLC	DLTC	TPERHP	TPRENG	HPPESL	QTO	RPM
31.5041	10.9343	33.6223	2.77664	8531.77	3565.85	48270.5	485.016

WPC	HPINST	FUELRT	ALIFT	DRAGSZ	ALPHAC	CDRGSZ	BSFC
18436.2	21395.1	8650.48	.000000	51190.6	.000000	.160740E-01	.469212

RW1							
191764.	98507.8	10644.5	219316.	48986.9	7885.58	19103.5	67136.7
10473.9	3562.72	4540.02	12146.5	.000000	114385.	20520.2	16589.0

WNPSTR	WSTOGR	WEMPTY	WUSFUL	WSETA	EWTOGW
845561.	.422781	867144.	.113286E 07	.000000	.433572

ULTMPH	TMPLBF	ULTOGW	ULTOEW	ANSIDE	ULTMGW	ULTMEW
53294.3	6.16084	.566428	1.30642	176655.	53.2943	122.919

RANGE = 6160.84 WUSFUL/2 = 566428. CTE = .348967E 10

RANGE	WFUEL	FURTR	WPLD	PLDTMH	PTMPLF	PLDTGW	PLDTEW
.000000	.000000	8650.48	.113286E 07	53294.3	6.16084	.566428	1.30642
1087.67	100000.	8650.48	.103286E 07	48589.9	5.61701	.516428	1.19110
3263.00	300000.	8650.48	832856.	39181.0	4.52935	.416428	.960459
4350.66	400000.	8650.48	732856.	34476.6	3.98551	.366428	.845138
5438.32	500000.	8650.48	632856.	29772.2	3.44168	.316428	.729817
6525.99	599999.	8650.48	532856.	25067.8	2.89785	.266428	.614496
7613.66	699999.	8650.48	432857.	20363.4	2.35402	.216428	.499175
8701.32	799999.	8650.48	332857.	15659.0	1.81018	.166428	.383854
9788.98	899999.	8650.48	232857.	10954.6	1.26635	.116428	.268533

RA	PLDTEW	PLD/GW
200.000	52429.2	.557233
500.000	51131.7	.543442
1500.00	46806.4	.497473
3000.00	40318.5	.428518
5000.00	31668.0	.336578

ORIGINAL PAGE IS
OF POOR QUALITY

Alternate Buoyant Fluids

Several investigators (Ref. H-2, H-3, and H-4) have discussed the utilization of alternate buoyant fluids from a performance basis. Reference H-2, states, "The choice of a disposable or nondisposable buoyant fluid must be made on the basis of vehicle operation at cruise." In reality, however, the choice of the buoyant fluid will be dictated by the operational requirements for the specific mission to be performed, the economic impact, and the safety requirements associated with each alternative. One very desirable operational advantage that can be realized by the use of a disposable fluid such as hot air or steam is improved altitude capability as discussed in Reference H-2. An interesting illustration is offered by comparing the cost per pound of lift resulting from burning a hydrocarbon fuel and the cost per pound of lift resulting from helium. A cost ratio of 1770 (He/Hot Air) is presented. A very promising result indeed. However, several additional factors must be considered for a true comparison of either hot air or steam as lifting fluids. These include:

(1) For the same absolute magnitude (in pounds) of life capability, the lower unit lift gases will require larger vehicle volumes. Alternately as shown in Figure H-8, for a given volume and the empty weight characteristic of this volume, a lower limit exists on the unit gas lift at which the vehicle can only lift its empty weight: No payload, no fuel, no crew, etc.

(2) Type of vehicle construction (rigid, non rigid, pressurized) and the weight and complexity associated with the heat source.

(3) The total quantity of heat to be delivered over a given mission profile and not merely the cost of the <u>INITIAL</u> lift. This mission dependency of course requires evaluation of heat losses through the airship skin as have been discussed in the section on artificial superheat.

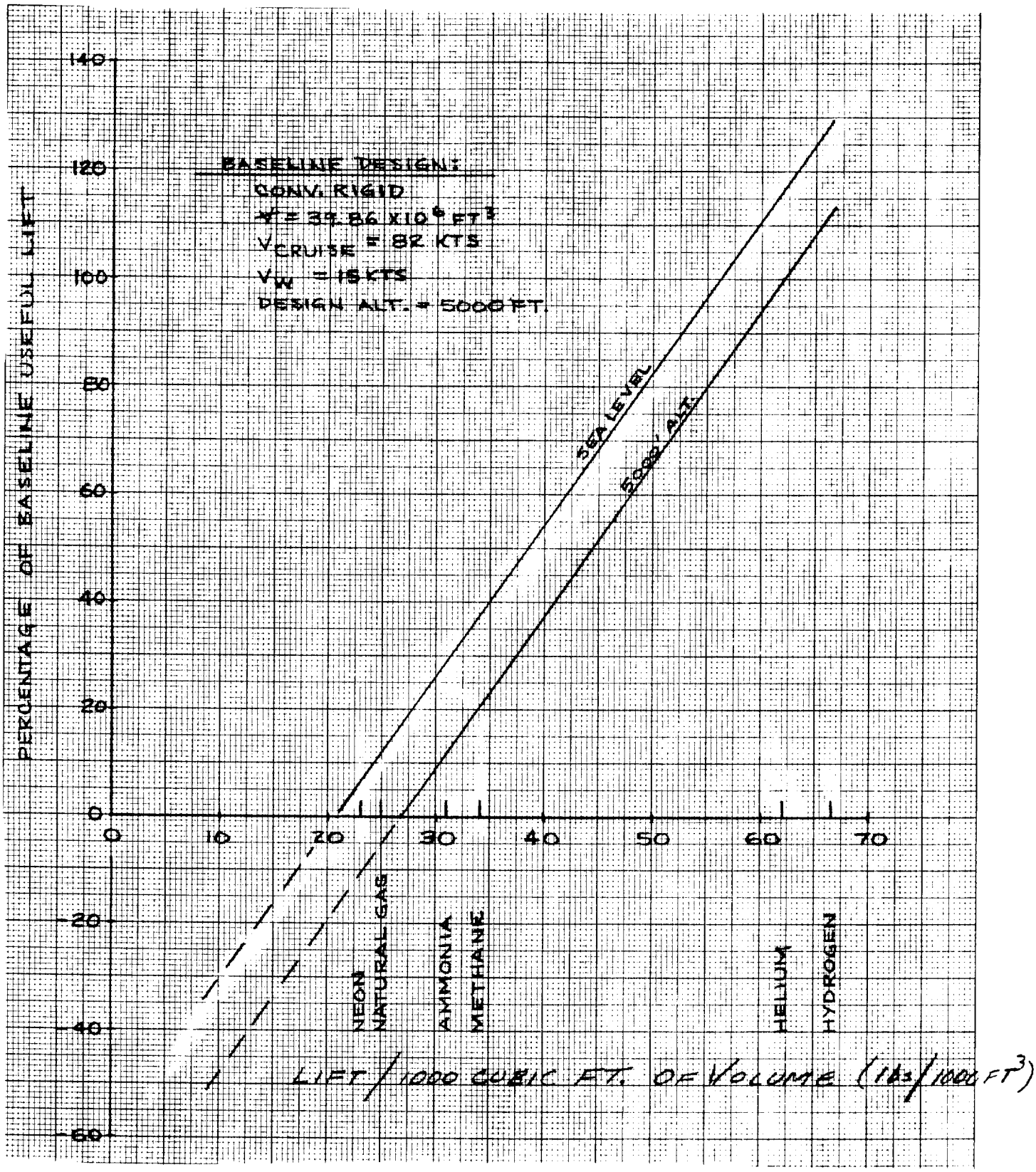

FIGURE H-8 - PERCENTAGE OF BASELINE USEFUL LIFT VERSUS LIFT/ 1000 CUBIC FT OF VOLUME

(4) The cost of the "heated lift" over the total vehicle life relative to the cost of helium or any alternative fluid.

(5) The empty weight increase associated with insulation and heat source (if other than waste engine heat).

(6) The impact on total material life of gas cells or envelope material resulting from the multiple heating cycles.

(7) Finally and possibly most importantly, the impact on the ground and flight operations of the system for the specific mission under consideration. This factor is possibly the most important consideration for further investigation from mission economic standpoint.

The performance of several potential light gases can be evaluated based on their relative lift capabilities as shown below after Reference H-2.

Gas		Lift in Lbs. per 1000 Ft^3
Air	T* = 0°F	0
	= 100°F	13.3
	= 200°F	22.7
	= 300°F	26.3
Helium		62
Hydrogen		68
Ammonia		31
Natural Gas		25
Methane		34

T = T gas - T ambient air

The useful lift ratio relative to the helium baseline vehicle for these fluids is shown in Figure H-9.

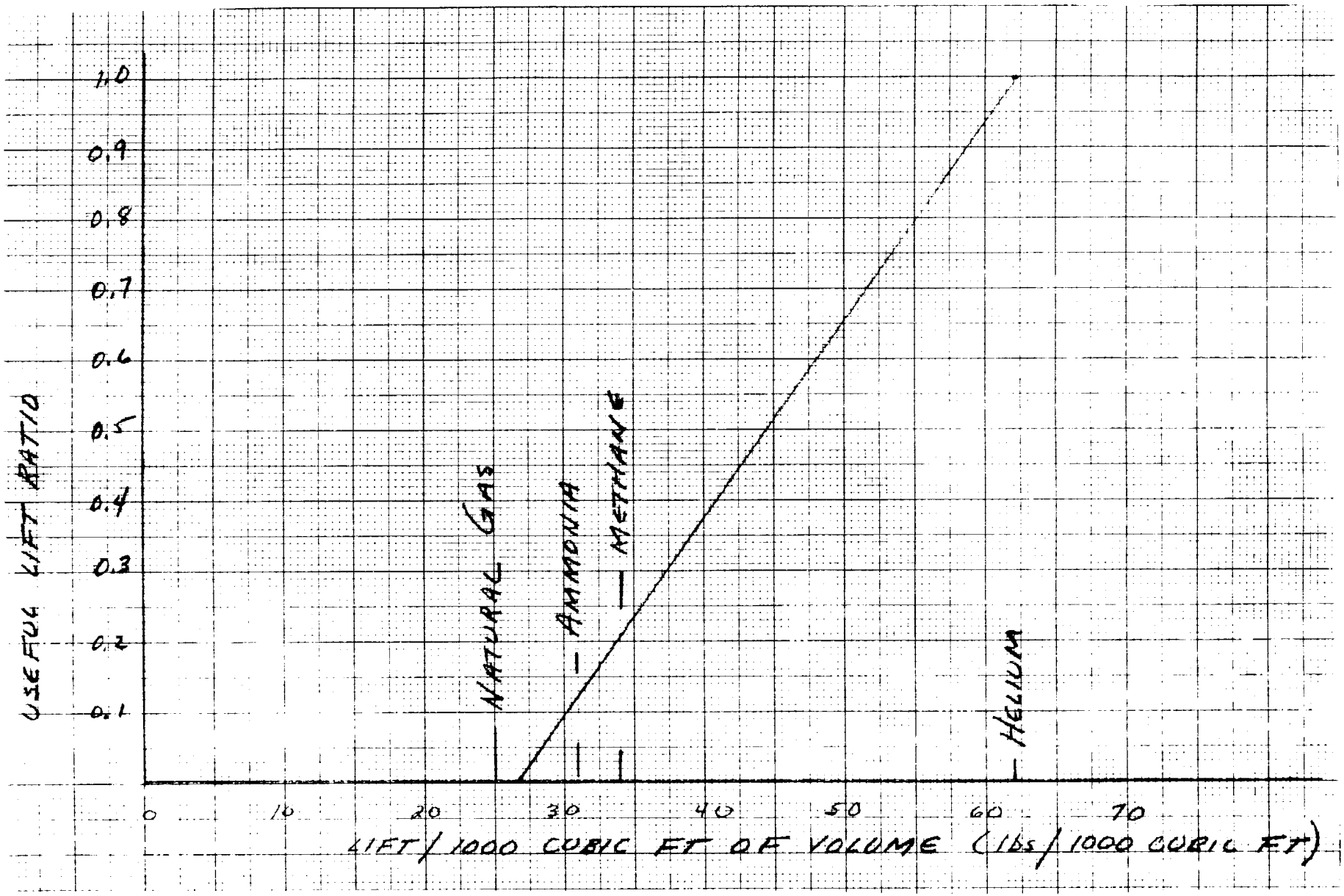

FIGURE H-9 - USEFUL LIFT RATIO VERSUS LIFT/1000 CUBIC FT OF VOLUME

In conclusion, from a collective consideration of the above and the many years of experience with potential alternative fluids that for most typical airship missions; helium is the most desirable lifting gas. There are specialized and/or unique missions in which alternate lifting gases may represent viable alternatives. However, Goodyear recommends consideration of only helium as a lifting gas for the baseline Phase II vehicle/mission combinations.

Sensitivity Analysis

A very abbreviated Sensitivity Analysis was conducted near the conslusion of the study for several vehicle concepts. A typical set of results for the Baseline Neutrally Buoyant Rigid Airship of Table H-II is presented in Table H-III. A complete sensitivity analysis will be conducted at the start of the Phase II study for each mission/vehicle combination.

TABLE H-III: SENSITIVITY STUDY RESULTS

2×10^6 Pound Gross Weight Rigid Airship Baseline

Parameter	Baseline Value	% Change in UL·VC +20%	% Change in UL·VC -20%
V_W	15 Knots	-4	+4
V_C	82 Knots	+1.03*	-6.7
Cruise Altitude	5000 ft	-8	+8.1
Fineness Ratio	7.4	-1	-0.06
Hull Volumetric Efficiency, $_H$	0.94 (= 5%)	+8.7	-8.7
Engine Weight (Total Wt/Installed HP)	1.01 lbs/HP Installed	-0.02	+0.018
Non Propulsive Structure Weight	845561 Pounds	-15	+15

*82 knot cruise speed is not optimum for Zero Range Productivity but is optimum at 3000 mile range.

References

1. McLemore, H. C.; Wind Tunnel Tests of a 1/20-Scale Airship Model with Stern Propellers; NASA TND-1026, Jan. 1962.

2. Nichols, J. B.; The Basic Characteristics of Hybrid Aircraft, Proceedings of the Interagency Workshop on Lighter Than Air Vehicles, FTL Report R75-2, Jan. 1975.

3. Havill, C. D. and Harper, M.; A Semi Buoyant Vehicle for General Transportation Missions, Proceedings of the Interagency Workshop on Lighter Than Air Vehicles, Jan. 1975.

4. Havill, C. D.; A Lifting Body Drigible for Air Transport Missions, NASA MA-72-3 Dec. 1972.

Bibliography

1. Goodyear Aerospace Corporation, A Theoretical Aerodynamic Analysis of a Boundary-Layer Controlled Airship Hull, GER-6251, Akron, Ohio (14 September, 1954).

2. Cerreta, P. A., Wind Tunnel Investigation of the Drag of a Proposed Boundary Layer Controlled Airship, Navy Dept., David Taylor Model Basin Aerodynamics Laboratory, Aero Report 914 (March, 1957).

3. Horshe, M. L., Pake, F. A., and Wasson H. R., Air Investigation of a Boundary Layer Controlled Airship, GER 8399, Goodyear Aerospace Corporation, Akron, Ohio (15 October, 1957).

APPENDIX I

CONFIGURATION SCREENING EXERCISE

CONVERSION FACTORS FOR APPENDIX I

1 lb	=	0.4536 Kg
1 ft	=	0.3048 m
1 ft^2	=	0.0929 m^2
1 ft^3	=	0.02832 m^3
1 inch	=	0.0254 m
1 ft/sec	=	0.3048 m/sec
1 ton mi/hr	≅	1460 Kg-Km/hr

A fairly broad spectrum of hybrid configuration was investigated during the study. The selection rationale which lead to the selection of the baseline modified delta planform hybrid was discussed in the body of the report, Ref. 1.

In arriving at the selected vehicle configuration various semi rigid structural design approaches were investigated for the lifting body vehicles. This appendix discusses some of the semi rigid vehicles considered and presents some further information on the investigation of winged airship configurations.

Semi Rigid Vehicle Concepts

Any general discussion of airship design concepts usually includes rigids, non-rigids and semi-rigids. In the early days of airship development, some semi-rigids were built. Later on, and for a long period ot time, nearly all airships were of the rigid type. More recently [during the last 40 years], the airships which have been built have been predominantly non-rigids.

Who no semi-rigids? There must be a reason. A recent look at the specified minimum operating pressure for a recent non-rigid revealed that the specified pressure was established to prevent wrinkling of the envelope due to bending moments expected when flying in gusty air. Alternately one might decide that the minimum operating pressure was established to prevent cave-in of the nose of the envelope since the required pressure would be nearly the same. One might conclude from this that a non-rigid airship of conventional design could not benefit appreciably from a long keel structure designed to relieve the envelope of flight bending moments.

On the other hand, a typical non-rigid airship [ZPG-3W for example] does have some features of the semi-rigid in that the bending strength of the car structure and the fanned out geometry of the suspension system serve to distribute the large concentrated loads of the car mass over a significant portion

of the envelope, thus reducing the structural requirements of the envelope in much the same manner as would be conceived in a semi-rigid design.

Even if it is true that the semi-rigid approach is inferior to both the rigid and non-rigid designs for airships of conventional configuration, that does not mean that semi-rigid approaches can forever be excluded from consideration. In particular, when unconventional arrangements to enhance dynamic lift characteristics are being considered, the merits of the semi-rigid approaches must be re-evaluated.

Conceptual non-rigid airships consisting of pressurized cylindrical and multilobed shapes show excellent structural characteristics insofar as longitudinal bending and shear are concerned. Transfer of large loads [lift or weight] laterally however does present a problem. This is the problem which can be solved by the semi-rigid approach. Rigid structures can be used either entirely externally to the envelopes or partially internal to transfer large loads laterally or longitudinally in such a way as to make maximum use of the merits of the non-rigid components. Figure I-1 shows some promising concepts.

In the dual hulled concept two hulls of more or less standard blimp construction would be used side by side as shown. Each envelope would contain catenary curtains and suspension cables arranged as in the GZ-20 airship, in which the lift of the envelope is delivered to two internal points. Between the two envelopes would be a structural framework of substantial depth to provide a "keel" to support and distribute concentrated loads. The lift of each envelope would be transferred to the keel by penetrating the envelope with two struts from the top of the keel structure to the suspension points and by two cables attached to the bottom of the keel structure and the suspension points. Thus four penetrations with suitable reinforcements and gas tight sleeves would be required in each

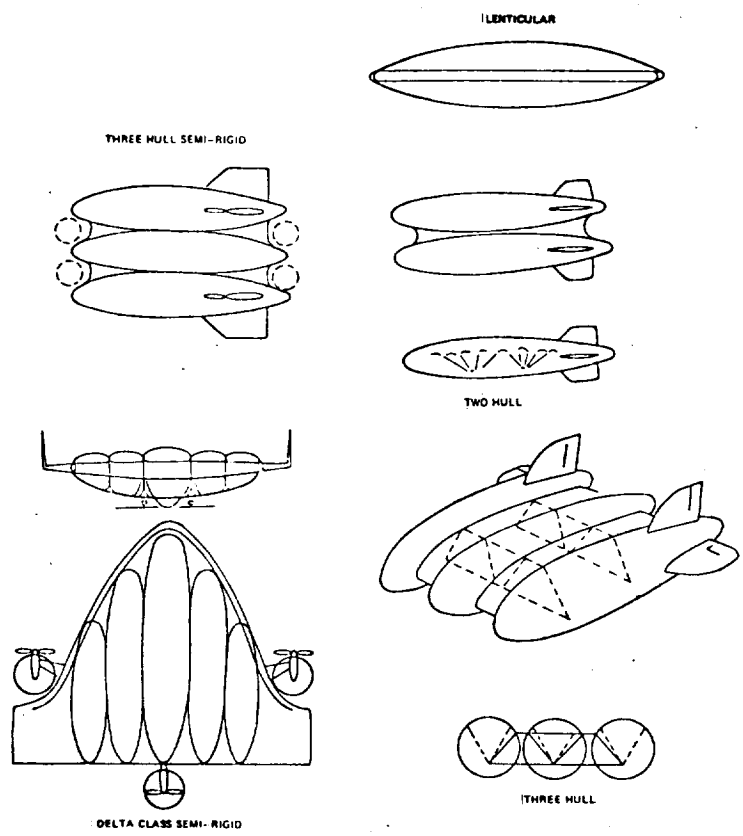

FIGURE I-1 - SEMI-RIGID VEHICLE CONCEPTS

envelope. Otherwise the envelopes would be of standard construction and configuration. All mechanical equipment, accommodations and payload would be housed in the keel structure. The keel structure would be enclosed in a fairing which would also be laced to the envelopes.

The concept can be extended to airships with three or more non-rigid hulls at the expense of more internal structs and braces. Figure 1 illustrates several of the multilobed concepts considered.

Another area where the semi-rigid approach might be useful is in the lenticular planform where the rim would be hard structure

with the buoyant gas and ballonets configured as huge unsupported domes [spherical segments] with their outer edges restrinted by the peripheral ring structure.

All stabilizing and control surfaces would be supported by the peripheral ring structure. Engines, mechanical gear, etc. would also be supported.

Although the lenticular planform geometry appeared structurally promising, the large horizontal tail areas expected to achieve satisfactory stability characteristics [Reference I-2 and I-3] or put another way the uncertainty in the acceptability of this shape from the stability and control standpoint was one factor which led to the selection of the baseline modified delta planform shape.

Winged Airships

The other class of "hybrid" concepts consisted of winged airships. Initial expectations were that some promising configurations might result in combining the highly structurally efficient basic airship shape with more aerodynamically efficient wing structures. The family of winged airship configurations which were briefly examined are shown in Figure I-2.

The results of this effort viewed in light of the conventional airship heaviness trade study generally do not indicate that in terms of productivity, winged airships are competitive for the gross weights of under perhaps 500,000 pounds. However since other considerations [low speed control, deflected slip steam VTOL, engine mounting for non-rigid vehicles, etc] might dictate further consideration of winged airship vehicles, the results of the screening exercise are presented, herein. Two independent evaluations of the configuration matrix, Figure I-2, were conducted. Basically the results were the same. Conventional airships or airships with minor modifications rank very high in terms of the qualitative factors considered. Low body

FIGURE I-2 - WINGED AIRSHIP CONFIGURATION SCHEMATICS FOR EVALUATION/SCREENING EXERCISE

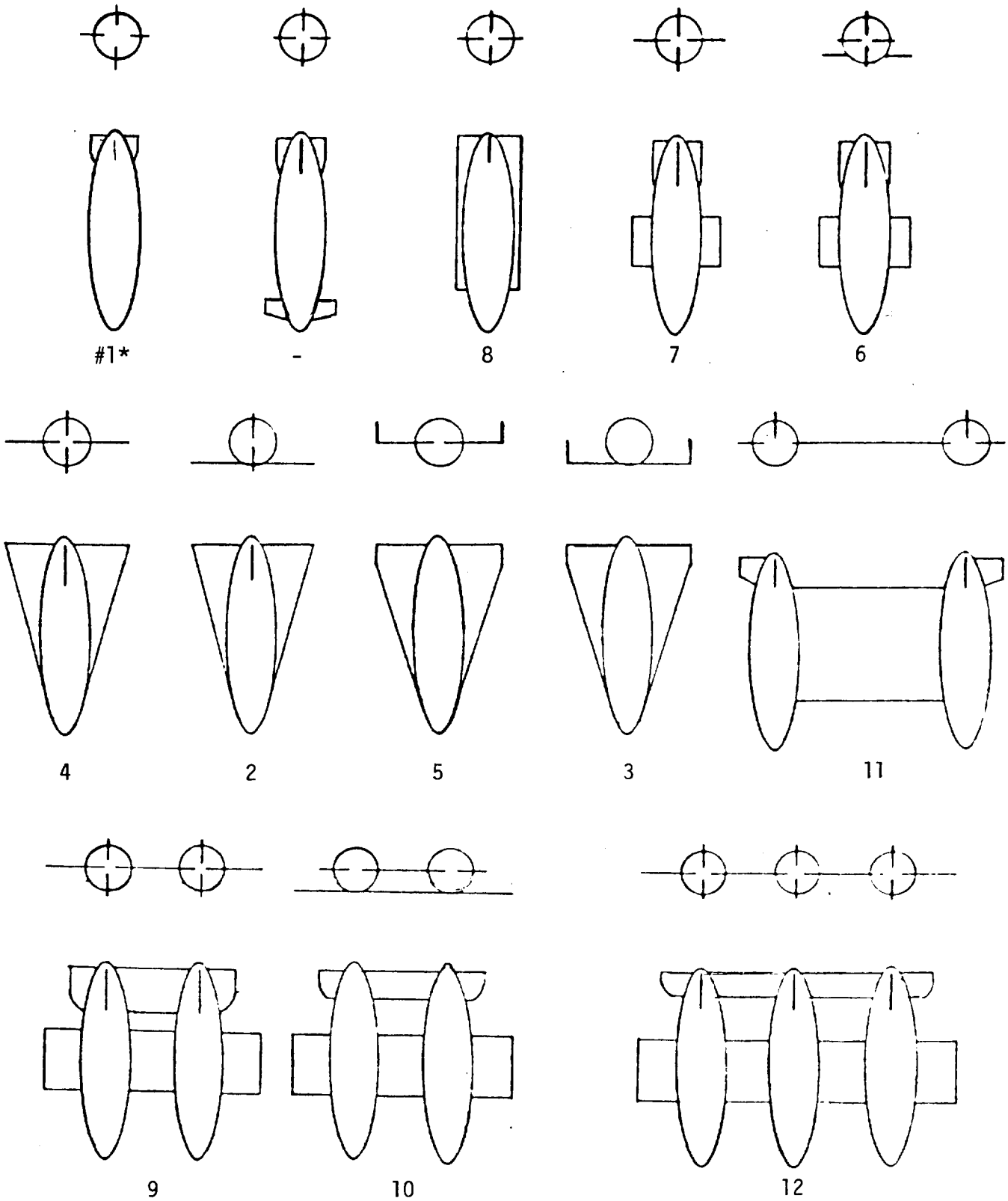

* CONFIGURATION NUMBER CORRESPONDS TO TABLED RESULTS FROM SCREENING/EVALUATION.

and mid-body straight wing configurations appeared most desirable based on aerodynamic structural and estimated cost to manufacture. The multihulled concepts were universally ranked very low. A rather detailed structural weight analysis was conducted assuming conventional wing technology to establish an "upper limit" on several representative configuration concepts. A preliminary analysis of a wing structure based on a fabric covered truss structure construction concept indicated the "upper limit" weight values might be reduced by 40 to 60%. With these weight values, the "best" configuration, the low body straight wing concept still produced a slight improvement in productivity but were still worse than the heavy flying [β = .5] basic airship hull for the 400,000 pound gross weight considered.

The results of the qualitative evaluation matrix are presented in Table I-I. Table I-II presents general comments on the configurations. The aerodynamic methods employed are briefly described followed by a brief report on the methods employed in establishing the "upper limit" on the wing and hull weight penalties.

The specific configuration characteristics, maximum wing plus hull weight estimates are presented in Table I-III.

Parametric Wing Size and Drag Estimates

Estimates of wing size and thrust required to satisfy a given set of cruise conditions are essential to comparative screening assessments. Since surface size can be varied at constant lift, but with changing drag, the estimates needed are necessarily parametric. To provide the latter, the lift characteristics of each configuration selected for preliminary screening were estimated over a range of surface geometries and arrangements. The angles of attack required to maintain level flight at selected cruise conditions were then determine and the corresponding drag estimated. Typical results are shown in Figures I-3 thru I-6. The general procedure and principal assumptions are described

TABLE I-I - QUALITATIVE EVALUATION MATRIX RESULTS

Winged A/S Configurations	20-Accumulation of water, ice, snow	19-Major problem area or area of R&D required to prove viability of this config	18-Major virtue(s) of this configuration	17-Potential ground handling problems	16-Sensitivity to ground winds	15-Accessibility of cargo access	14-Potential handling/stability and control problems	13-Potential landing problems	12-Acceptability of landing gear hardpoints	11-Potential engine out problems for VTOL concepts	10-Acceptability of engine hardpoints VTOL-C/STOL)	9-Applicability to VTOL or VTOL config limitations	8-Estimated production cost relative to conventional rigid airship (Akron)*	7-Estimated engineering cost relative to conventional rigid airship (Akron)*	5-Config adaptability to stern propulsion (for improved low speed control)	4-Config adaptability vectored thrust	3-Config adaptability to B.L.C. approaches	2-Config adaptability to unique propulsion systems concepts	1-Config adaptability or applicability to (A) press/fabric, (B) press/metal, (C) conventional rigid, (D) semi-rigid	POINTS
1. 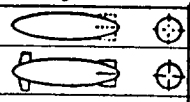	B	B	N	B	N	N	B	B	See 10	B	N	B	N	N	G	G	G	A	ABCD	33
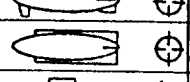	B	B	N	B	N	N	B	B		B	N	B	N	N	G	G	G	A	ABCD	32
9. 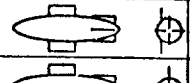	B	B	N	B	N	N	B	B		B	N	B	N	N	G	G	G	A	ABCD	30
6. 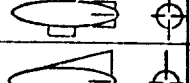	B	B	N	B	N	N	B	B		B	N	B	N	W	G	G	G	A	CD	32
14, 15 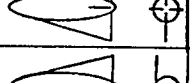	B	B	N	B	N	N	B	B		B	N	B	N	W	G	G	G	A	C	32
4, 13 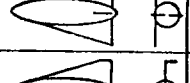	N	N	B	N	W	N	N	N		N	B	N	W	W	G	A	G	A	C	25
2. 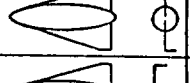	N	N	B	N	W	N	N	N		N	B	N	W	W	G	A	G	A	CD	25
5.	N	N	B	N	W	N	N	N		N	B	N	W	W	G	A	G	A	CD	25
3.	N	N	B	N	W	N	N	N		N	B	N	W	W	G	A	G	A	C	25
11.	W	W	W	W	W	B	W	W		W	B	W	W	W	G	P	A	A	CD	17
8.	W	W	W	W	W	B	W	W		W	B	W	W	W	G	P	P	A	C	17
10. 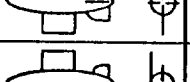	W	W	W	W	W	B	W	W		W	B	W	W	W	G	P	P	A	CD	17
12.	W	W	W	W	W	B	W	W		W	B	W	W	W	G	P	P	A	C	17

Note:

Columns 1-5 were evaluated

G - Good
A - Average
P - Poor.

Columns 7-20 were evaluated

B - Better, 3 pts
N - No Difference, 2 pts
W - Worse, 1 pt.

Total points are representative of columns 7-20.

TABLE I-II

GENERAL COMMENTS ON WINGED AIRSHIP CONFIGURATIONS

Low Wing Delta and Clipped Delta: Harder to carry wing loads into pressurized hull than into rigid hull. Low wing good for mounting propulsion and landing gear.

Mid Wing Delta and Clipped Delta: Harder to carry wing loads into hull than for low wings. Cargo and landing gear remain in lower hull causing long load paths. Wing location not suitable for mounting landing gear.

Low and Mid Straight Wings: Same comments as for delta wings. Straight wing probably better aerodynamically, structurally, and cost of manufacture.

Strakes: Matrix Evaluation shows strakes rank poorly. Basically no change from conventional. Aerodynamic improvement marginal relative to conventional airship. Weight increases probably substantial.

Two Hull Low Wing - Similar to Low Straight Wing but loads will be higher due to asymmetric conditions. Stern propulsion requires two systems. Two cargo areas with balanc- problems. Twin hulls and large span cause landing and ground handling problems.

Two Hull Mid Wing - Similar to Two Hull Low Wing except not as suitable for mounting landing gear.

Three Hull Mid Wing - Similar to Two Hull Mid Wing but much worse:

briefly in the following paragraphs.

All estimates were made within a framework of simplifying assumptions; some of necessity since, as a first iteration, needed configuration inputs were not known a priori, and others because of configuration complexities and attendant analytical difficulties beyond the scope of exploratory appraisals. Nevertheless, an effort was made to introduce the assumptions with a reasonable degree of consistency "across-the-board" so as to reflect fair configuration-to-configuration comparisons.

Lift

The lift estimates neglected the incremental changes due to trim and were determined from -

$$C_L = C_{L_B} + C_{L_{T+I}} + C_{L_{W+I}}$$

where:

C_{L_B} = bare hull lift coefficient

$C_{L_{T+I}}$ = fin lift coefficient including tail/body interference

$C_{L_{W+I}}$ = wing [or strake] lift coefficient including wing/body interference

The bare hull lift contribution was obtained from Reference I-4 which reports the results of wind tunnel tests conducted using a 1/40-scale model of the Akron, which is geometrically similar to the hull shapes assumed here. The same reference also provided the fin lift inputs used for all configurations. Considering the magnitude of the fin-body contributions, relative to the large wings of interest, this generalization introduces negligible "error" in the wing lift and total weight requirements.

The lift coefficients of the wing were assumed to vary linearly over the low to moderate angle-of-attack range of present inerest, viz.

$$C_{L_{W+I}} = (C_{L_\alpha} \cdot \alpha)_{W+I}$$

In estimating the lift contributions of the very low aspect ratio strakes it was considered necessary to account for viscous effects. Consequently, the strake lift coefficients were expressed as

$$C_{L_{W+I}} = (C_{L_\alpha} \alpha)_{W+I} + C (\sin^2 \alpha)$$

in which a crossflow drag coefficient, C, of 3.1/rad^2 was used. This value was obtained from Reference I-5 and is related to an assumed aspect ratio of 0.25.

Wing along lift was obtained from linear theory and, where appropriate, wing-body interference lift was estimated using slender-body theory lift ratios, adjusted empirically for individual configuration peculiarities.

Zero-Lift Drag

The zero-lift drag estimates, as for the lift predictions, also neglected trim effects and were approximated using the general expression

$$C_DS)_{Total} = (C_DS)_{Hull} + (C_DS)_{Fins} + (C_DS)_{Engines} + (C_DS)_{Misc} + (C_DS)_{Car}$$

Values for the fins, engines, car and miscellaneous drag contributions are based on a general correlation of airship flight test data with a similar drag summation in which it was assumed that the bare hull increment is predicted by Reference I-6.

The zero-lift wing drag components were estimated using the Datcom method, Reference I-7 for wing alone and assumed values for wing thickness ratio resulting in

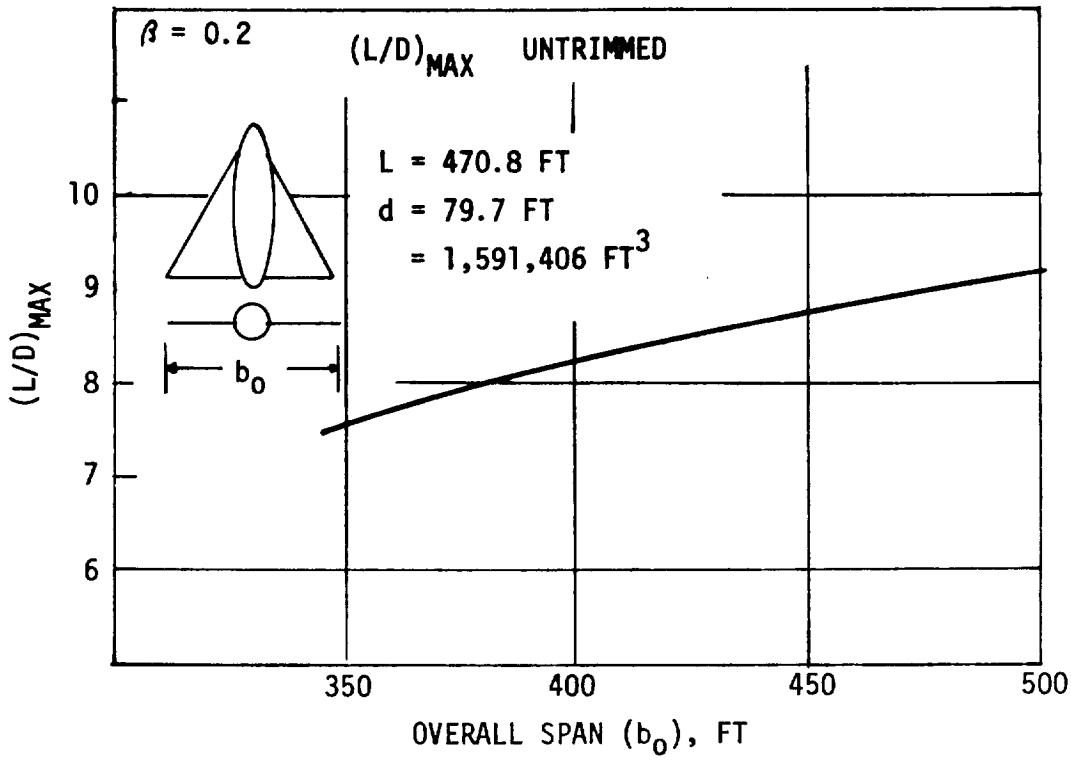

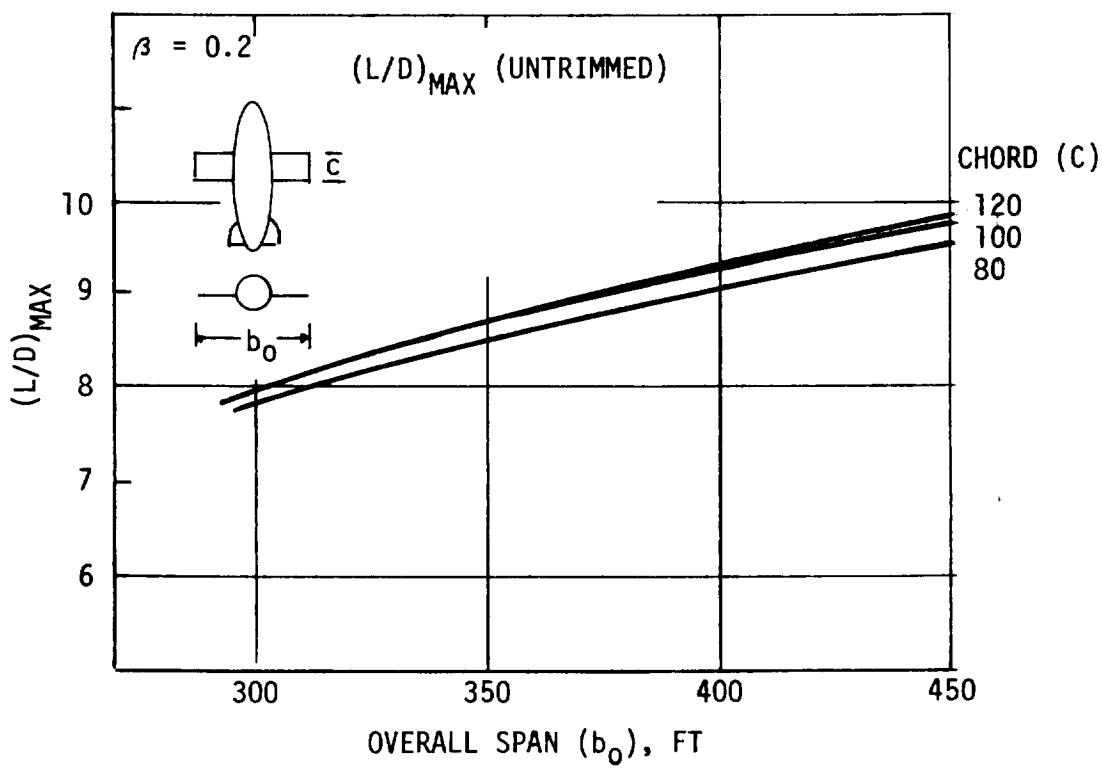

FIGURE I-3 - WINGED AIRSHIP AERODYNAMIC ESTIMATES

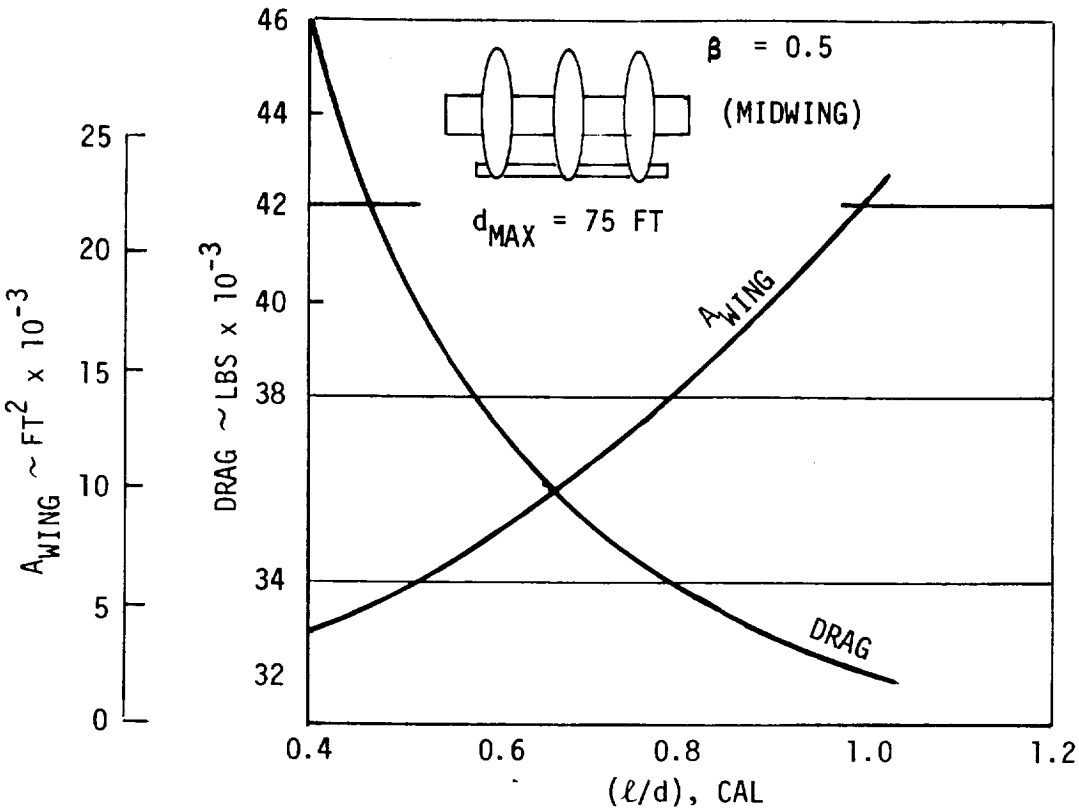

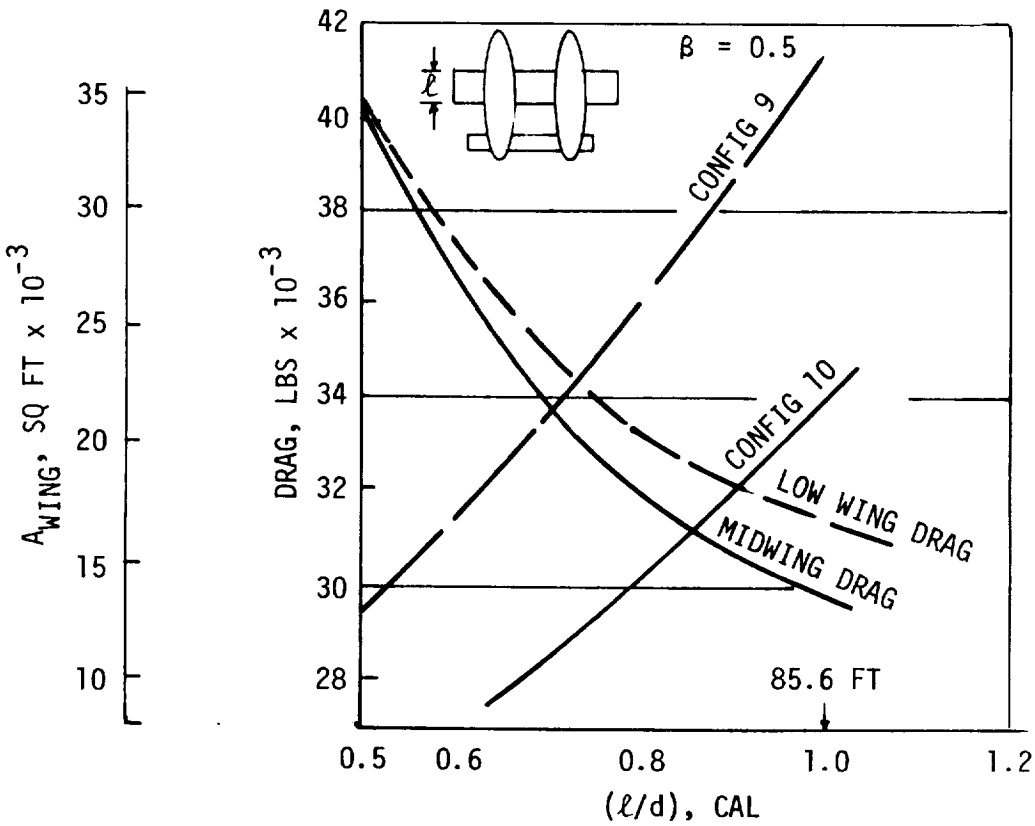

FIGURE I-4 - WINGED AIRSHIP AERODYNAMIC ESTIMATES

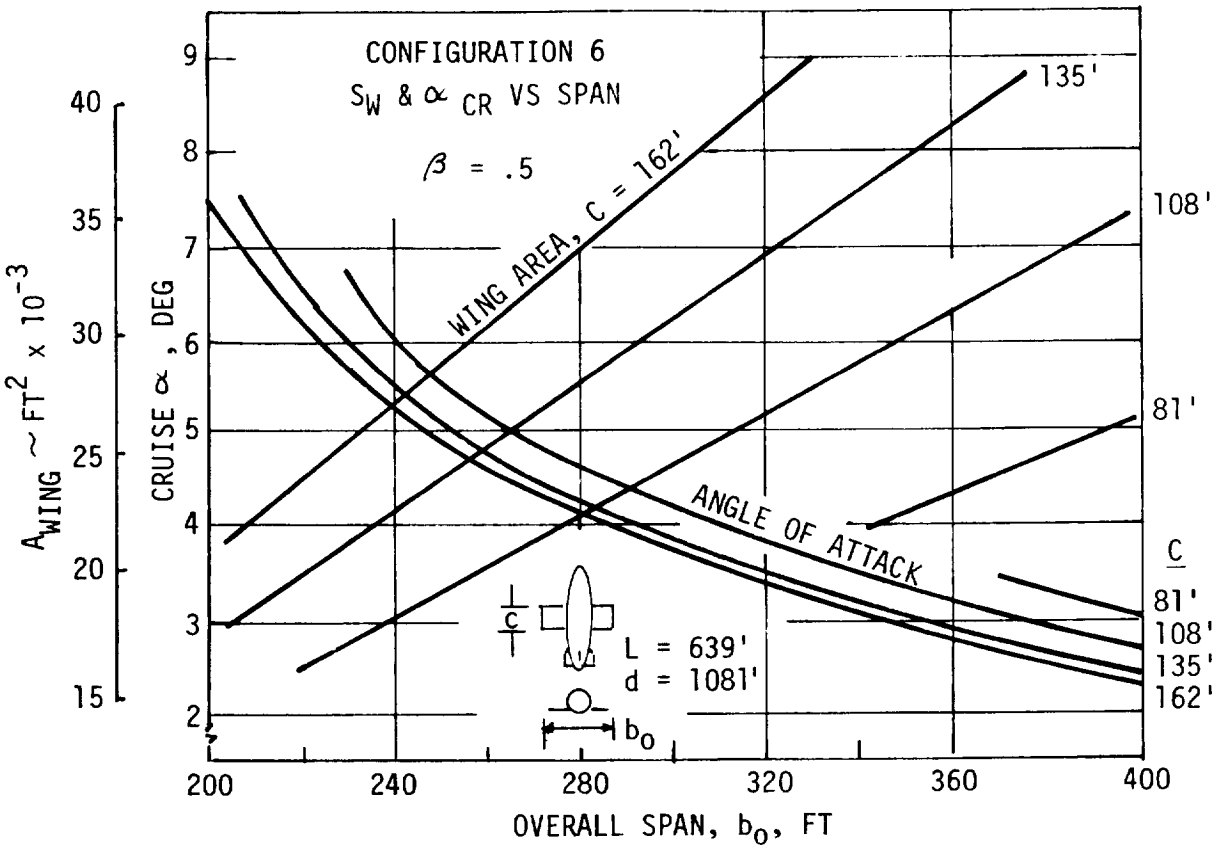

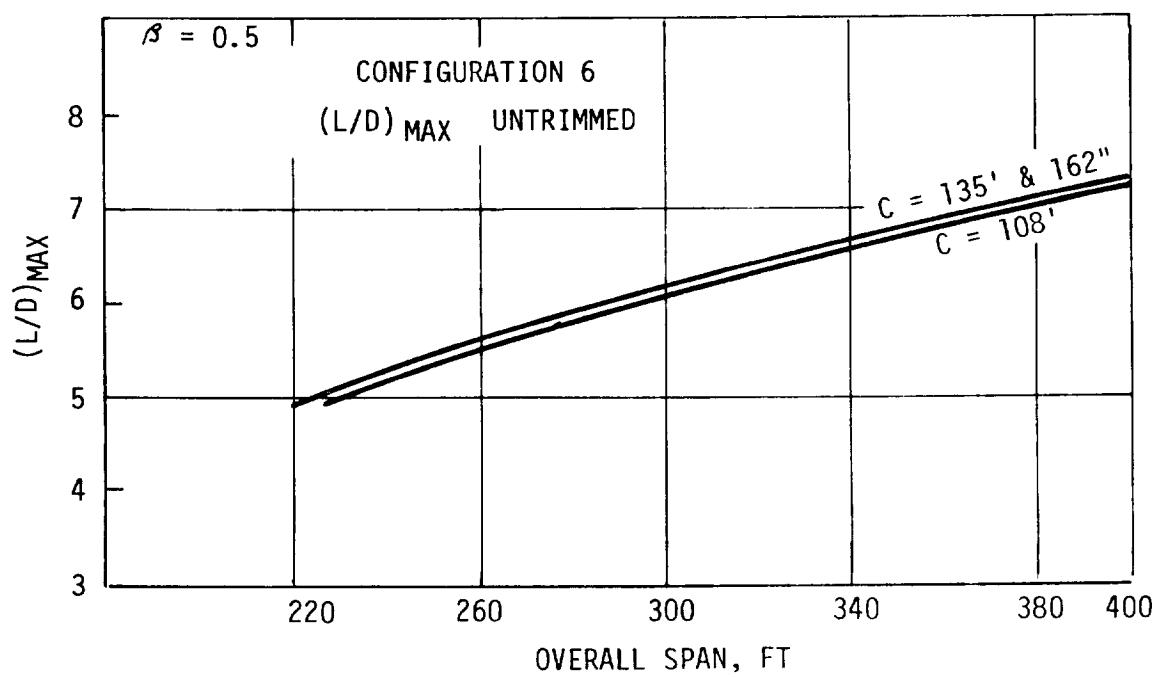

FIGURE I-5 - WINGED AIRSHIP AERODYNAMIC ESTIMATES

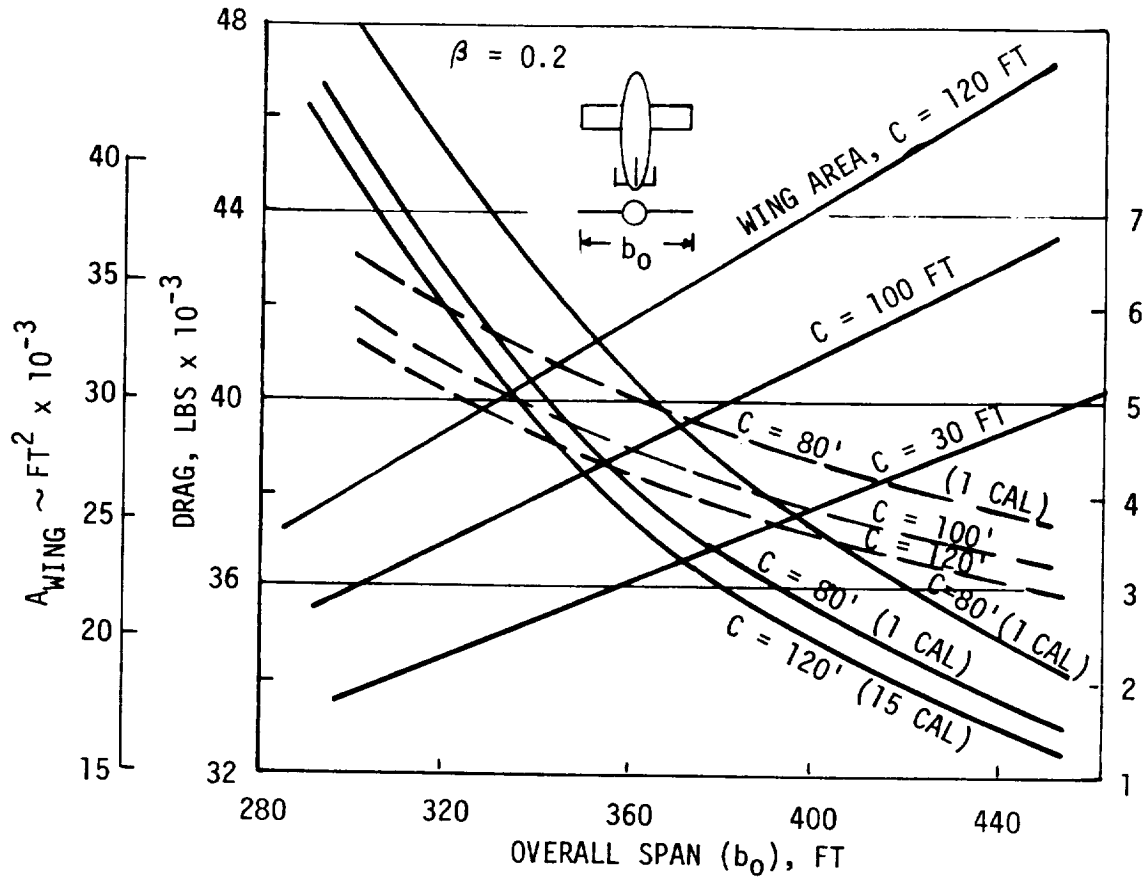

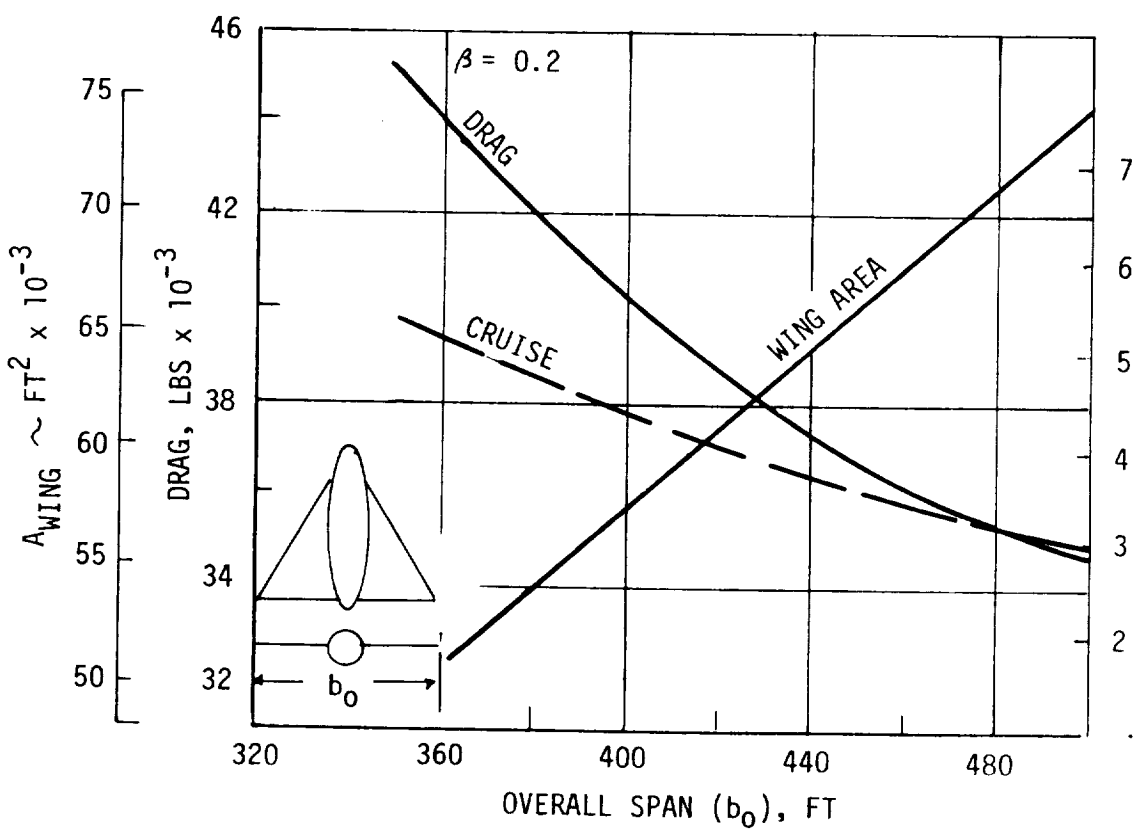

FIGURE I-6 - WINGED AIRSHIP AERODYNAMIC ESTIMATES

$$(C_D S)_w = 2.45\ C_f\ S_w;\ \text{for the delta planforms}$$

$$(C_D S)_s = 2.83\ C_f\ S_w;\ \text{for the rectangular planforms}$$

where:

C_f is based on the wing mean aerodynamic chord

S_w is the exposed planform area

In evaluating the drag of the multi-body configurations, no allowances were made for interference resulting from drag proximity.

Drag Due to Lift

The drag due to lift was assumed equal to $C_L \tan\alpha$.

ESTIMATION OF WING AND ADDED HULL WEIGHT

The novelty and size of the configurations considered precluded the use of any empirical weight-estimating relations. It was therefore decided to adopt the procedures presented in Reference I-7. In general, the data in Reference I-8 for "conventional" 24S-T [2024] aluminum construction were used. These weights should represent an upper bound on the actual weight, since the large sizes and low wing loadings undoubtedly require a different type of construction in order to realize full efficiency.

The procedures in Chapter 7 of the reference, modified to separate the weight into portions for the wing and carrythrough structure, were used for the rectangular planforms. The procedures in Chapter 13, similarly modified, were used for the delta planforms. In either case, equivalent root areas are found that will carry the root shear and bending moment resulting from a symmetric pull-up at an ultimate load factor n_f.

The volume [and thus weight] is found by integrating these areas over the wing. Where necessary, appropriate spanwise distributions of parameters are assumed, with empirical correction factors included to account for deviations from the assumed distributions. Summaries for the rectangular and delta planforms are given below.

Rectangular Planforms

The "conventional" structure is broken up into four parts - shear webs, bending flanges [skin], rib shear webs, and rib flanges. The root equivalent areas for these components are computed as follows:

Shear web -

$$A_{SR} = N_{SPAR} C_S k_S^2 \ (h/C)^2 \ C^2 + J_n \ \frac{n_f W_g}{2F_{SO}}$$

Flanges -

$$A_{FR} = C_c L_o \ (B/C) \ C + \frac{J_n k_b n_f W_g \ (b - w_{ct})}{4 k_e h F_a}$$

Rib shear -

$$A'_{RS} = \frac{\bar{t}_{ro}}{L} \ (h/C)(B/C) \ C^2 + \frac{n_f W_g}{2SF_{SO}} \ (B/C) \ C^2$$

Rib flanges -

$$A'_{RF} = \frac{n_f W_g}{4SF_{ar}} \ (B/C)^2 \ C^2 \ (h/C)^{-1}$$

The notation used here generally follows that in Reference I-8.

b	total wing span, in.
B/C	ratio of structural box width to cord
C	chord, in.
C_S	constant for optimum allowable shear stress

C_c constant for optimum allowable compressive stress

F_a equivalent "axial" allowable stress, psi

F_{ar} allowable stress for rib flange material, psi

F_{SO} fictitious allowable shear stress, psi

h wing maximum thickness, in.

h/C wing thickness-to-chord ratio

J_n load relief factor due to wing weight, $\frac{W_g - W_w}{W_g}$

k_b bending-moment span distribution factor

k_e ratio of structural box effective depth to wing depth h

k_s ratio of average depth of shear members to wing depth h

L spacing between ribs, in.

L_o effective rib spacing, $L/\sqrt{1.5}$, in.

n_f ultimate load factor

N_{SPAR} number of spars in structural box

S total wing area, in.^{2}

$\bar{t}_{ro}$ rib minimum thickness, in.

w_{ct} span of carry through structure, in.

W_g vehicle gross weight, lbs

W_w wing weight, lbs

The total "optimum" cross-sectional area at the root is the sum of the four components:

$$A_R = A_{SR} + A_{FR} + A'_{RS} + A'_{RF}$$

To obtain the total volume of structural material, the expressions for the various components need to be integrated over the span. At this point a departure is made from the procedure in Reference I-8, in that the wing and carrythrough structure are

treated separately. For the wing, it is assumed that the airfoil thickness ratio h/C, the structural width ratio B/C, and the rib spacings L and L_o remain constant, as do the parameters relating to material properties, such as C_D and F_{SO}. Thus, for some of the area terms, all that is needed are the integrals

$$2\int_0^{(b-w_{ct})/2} C\,dx = S_{exp}$$

$$2\int_0^{(b-w_{ct})/2} C^2\,dx = \overline{C}S_{exp}$$

where S_{exp} is the exposed wing area, and $\overline{C}$ is the exposed wing mean aerodynamic chord. For some of the shear and bending area terms, there are factors involving $n_f W_g$ that represent either shear or bending moment at the root. It is now assumed that the spanwise shear distribution is triangular and the spanwise moment distribution parabolic, with correction factors k_{is} and k_{ib} applied to account for deviations from these distributions. This permits integrating these terms to give

$$V_s = k_{is}A'_{SR}\,(b - w_{ct})/2$$

$$V_b = k_{ib}A'_{FR}\,(b - w_{ct})/3$$

where A'_{SR} and A'_{FR} are the load-dependent terms [those involving $n_f W_g$] in A_{SR} and A_{FR}, respectively. Combining these integrals with the others gives the "optimum" volume of the wing structural box as

$$V_W = \left[N_{SPAR} C_S k_s^2 \ (h/C)^2 \ \bar{C} + C_c L_o \ (B/C) + \frac{\bar{t}_{ro}}{L} \ (h/C) \ (B/C) \ \bar{C} \right] S_{exp}$$
$$+ \tfrac{1}{2} \ J_n n_f W_g \left[\frac{k_{is}}{2F_{SO}} + \frac{k_b k_{ib}}{3k_e F_a} \frac{(b - w_{ct})}{2h} \right] (b - w_{ct})$$
$$+ \tfrac{1}{2} \ n_f W_g \left[\frac{B}{CF_{SO}} + (B/C)^2 \ (h/C)^{-1} \ \frac{1}{2F_{ar}} \right] \frac{\bar{C} S_{exp}}{S}$$

For the carrythrough structure, it is assumed that the root area A_R is carried across the hull without variation. To account for "non-optimum" effects - joints, rivets, the use of standard skin gages, etc., factors k_{xw} and k_{xct} are defined for the wing and carrythrough structure. Finally, an area density J_{LT} is used to account for leading- and trailing-edge material, and the total weight is written as

$$W_T = W_W + W_{ct} = \rho k_{xw} V_W + J_{LT} S_{exp} + \rho k_{xct} A_R w_{ct}$$

The incremental hull weight by W_{ct}; ρ is the weight density of aluminum [in lbs/in^3 and the weights in lbs]. Since V_W contains the factor J_n, which in turn contains W_W, some iteration is required, or the expression for J_n must be substituted into the above equation so that W_W can be found explicitly. Note also that there are certain terms that are independent of the load applied. These terms become a substantial portion of the total weight for large, lightly loaded wings such as the ones treated herein. It is clear that any construction method that will improve the efficiency of these wings must in effect reduce the relative contributions of such terms.

Delta Planforms

Although a delta planform can be viewed as a highly swept trapezoidal planform of zero taper ratio and low aspect ratio, the

assumption that loads are carried by a structural box beam occupying, say, 40 percent to 50 percent of the chord is obviously invalid. A more representative "conventional" construction might be that described in Chapter 13 of Reference I-8 where most of the loads are carried in the skin, and the skin in turn is supported by spanwise through members or individual posts or separators. The upper skin thickness is then sized by a different buckling criterion, and terms for separator weight replaces those for rib weight. As with the rectangular planforms, the volume of the carrythrough structure is estimated by multiplying the wing-root equivalent area by an average carry-through span. The equivalent root area is given by

$$A_R = \left[2C_s k_s^2 \ (h/C)^2 + (B/C) \ (h/C) \ k_e k_{sp} \sqrt{\frac{F_c}{k_{cr}\bar{E}}}\right] C^2$$

$$+ n_f W_g J_n \left[\frac{J_s}{2F_{SO}} + \frac{k_b \ (b - w_{ct})}{4k_e h F_a}\right]$$

$$= A_1 C^2 + n_f W_g J_n \ (A_2 + A_3)$$

The new parameters introduced here are

$\bar{E}$	effective modulus of elasticity, psi
F_c	compressive critical stress, psi
J_s	factor to account for wing thickness-taper contribution to shear-carrying capacity
k_{cr}	buckling constant
k_{sp}	ratio of average separator thickness to wing skin thickness

The wing weight and carrythrough structure weight are now given by

$$W_w = \rho k_{xw} \left[A_1 \overline{C} S_{exp} + n_f W_g J_n \left(\frac{k_{is}}{2} A_2 + \frac{k_{ib}}{3} A_3 \right) (b - w_{ct}) \right]$$

$$+ J_{LT} S_{exp}$$

$$W_{ct} = \rho k_{xct} A_R w_{ct}$$

Since the delta planforms involve even larger areas and lower wing loadings, the geometric effect on weight becomes even more important. The key parameter governing this effect is k_{sp}.

Parameter Selection

The parameters to be selected are of two types - those representative of the geometry, and those representative of the material used. As mentioned earlier, material constants for 24S-T (2024) aluminum were used, since these data were the most common in Reference I-8. The geometric parameters were selected by intuition or by inferring reasonable values from pertinent comments in the reference. The choices for three particularly important ones - the non-optimum weight factors k_{xw} and k_{xct}, and the ultimate load factor n_f - are discussed below.

As indicated in Chapter 11 of Reference I-8, the sources of non-optimum weight include weight additions for hard points, landing gear, cutouts, fuel tanks, joints, doublers, etc. After estimating "reasonable" values for these sources, k_{xw} for the rectangular planforms was set at 2.133. Certain of these effects are not applicable to the carrythrough structure, so k_{xct} = 1.633 was used there. For the delta planforms, k_{xw} and k_{xct} were both set at 1.600.

A number of criteria were considered for determining the ultimate load factor. One possibility is the positive limit maneuvering load factor of 2.5 that is specified in FAR Part 25.337. For a hybrid vehicle, this must be diminished by the fraction β of

total lift carried aerostatically, and then multiplied by 1.5 to get the ultimate value:

$$n_f = 1.5\ (2.5 - \beta)$$

Another possibility is the load factor resulting from a 35-fps gust at the design speed V_d. This was determined by estimating the lift-curve slope for the configuration and calculating an overall change in angle of attack resulting from the gust. A possible limiting consideration here is the resulting lift coefficient. It was assumed that the maximum limit load factor would be determined by the minimum of [2.5 - β] or that resulting from a lift coefficient of unity. The load factors resulting from the 35-fps gust were generally much smaller. This criterion was not used, therefore, because it was considered unconservative for weight estimation. It should be noted that asymmetric flight conditions might well be more critical for the multiple-hull configurations. However, it did not appear to be worthwhile to consider any other criteria at this point in the study.

When the loads were computed, it was assumed that the aerodynamic lift was produced only by the exposed portions of the wings, in spite of the fact that wing-hull interference will result in additional lift equivalent to that obtained over the enclosed portions. The sole exception was the straked configuration #8, where the external strakes carried only a proportion of the total lift given by the ratio of exposed area to total area.

Values of parameters used for all the configurations are given in Tables I-III and I-IV.

Special Design Considerations

All of the weight-estimation techniques in Reference I-8 assume

TABLE I-III

SUMMARY OF PARAMETERS USED IN WING WEIGHT ESTIMATION - RECTANGULAR WINGS

CONFIGURATION	N_{SPAR}	k_s	h/C	C_c	L, in.	B/C	n_f	$k_b k_{ib}$	k_{is}	k_e	w_{ct} ft.	β	J_{LT} psi
6 A	4	.96	.10	.002	40	.5	3.0	.85	1.0	.74	60	.5	.00544
B			.10				3.0						.00594
C			.12				3.3						.00623
7 A	4	.96	.10	.002	40	.5	3.0			.74	108		.00385
B			.10				3.0						.00476
C			.12				3.5						.00528
8 A	9	.90	.021	.0005	80	.78	3.0			.6	108		.00324
B													.00308
9 A	4	.96	.12	.002	40	.5		1.0		.74	2(50)		.00523
B													.00556
10 A			.12								2(85.6)		.00369
B													.00425
11 A			.10								2(85.6)		.00477
B													.00477
C													.00515
12 A			.12								3(75)		.00402
B													.00346
13 A							1.76	.85			126.4	.8	.00612
B							2.20						.00674
C							2.85						.00703
D													.00701
E													.00699
F													.00719
14 A							3.36				79.7	.2	.00766
B							3.45						.00730
C													.00731
D													.00732
E													.00733

$\rho = 0.10$ lbs/in^3

$C_S = 0.0025$

$\bar{t}_{ro} = 0.02$

$F_{SO} = 20{,}500$ psi

$F_a = 58{,}700$ psi

$F_{ar} = 60{,}000$ psi

$k_{xw} = 2.133$

$k_{x_{ct}} = 1.633$

TABLE I-IV

SUMMARY OF PARAMETERS USED IN WING WEIGHT ESTIMATION - DELTA WINGS

CONFIGURATION	k_s	h/C	B/C	n_f	$k_{ib}k_b$	k_{is}	k_e	k_{sp}	J_S	J_{LT} psi	w_{ct} ft.	$\bar{C}$ ft.	β
2 A	0.6	0.06	0.7	3.0	1.0	1.0	0.7	0.02	0.7	0.005	47.0	245	0.5
B	↓	↓	↓	↓	↓	↓	↓	↓	↓	↓	↓	260	↓
3 A	↓	↓	↓	↓	↓	↓	↓	↓	↓	↓	↓	258	↓
B	↓	↓	↓	↓	↓	↓	↓	↓	↓	↓	↓	270	↓
4 A	↓	↓	↓	↓	↓	↓	↓	↓	↓	↓	80.0	307	↓
B	↓	↓	↓	↓	↓	↓	↓	↓	↓	↓	↓	305	↓
5 A	↓	↓	↓	↓	↓	↓	↓	↓	↓	↓	↓	309	↓
B	↓	↓	↓	↓	↓	↓	↓	↓	↓	↓	↓	309	↓
15 A	↓	↓	↓	3.45	↓	↓	↓	↓	↓	↓	60.0	225	0.2
B	↓	↓	↓	↓	↓	↓	↓	↓	↓	↓	↓	↓	↓
C	↓	↓	↓	↓	↓	↓	↓	↓	↓	↓	↓	↓	↓
D	↓	↓	↓	↓	↓	↓	↓	↓	↓	↓	↓	↓	↓

$\rho = 0.10 \text{ lbs/in}^3$

$F_a = 48{,}000$ psi

$C_S = 0.00025$

$\sqrt{\dfrac{F_{cr}}{k_{cr}\bar{E}}} = 0.0375$

$F_{SO} = 17{,}150$ psi

$k_{xw} = k_{xct} = 1.6$

the traditional arrangement of a symmetric wing and a single fuselage. Further adaptation was necessary to treat the multiple-hull configuration.

For configurations 9 and 10, the lifting surface was considered in three components: the outboard wing, the carrythrough structure, and the center section. The usual bilateral symmetry was assumed. Ultimate shear and bending-moment diagrams, such as the ones shown in Figure I-7 for configuration 9, were derived under an assumption of uniform spanwise loading. The outboard component was treated as a conventional wing, with root shear and bending moment given by the values determined from the diagrams. The carrythrough structure was sized by computing a required equivalent area based on the mean shear and bending moment. For the center section, the shear distribution was assumed to be constant at the maximum computed value, and the weight equations were rederived on the basis of constant and triangular shear and moment distributions, respectively, rather than the triangular and parabolic ones assumed in Reference I-8.

For configuration 11, bilateral symmetry was again assumed, and the center wing weight was estimated by rederiving the equations to reflect the shear and moment distributions given in Figure I-8. A similar procedure was followed for the carrythrough structure.

For configuration 12, there are four components: the outboard wing, the outboard hull carrythrough structure, the inboard wing, and the center hull carrythrough structure. The modifications of the volumes of the shear and bending material follow the same procedure as outlined for configuration 9, with the center carrythrough structure sized as for configuration 6. The shear and moment diagrams used are shown in Figure I-9.

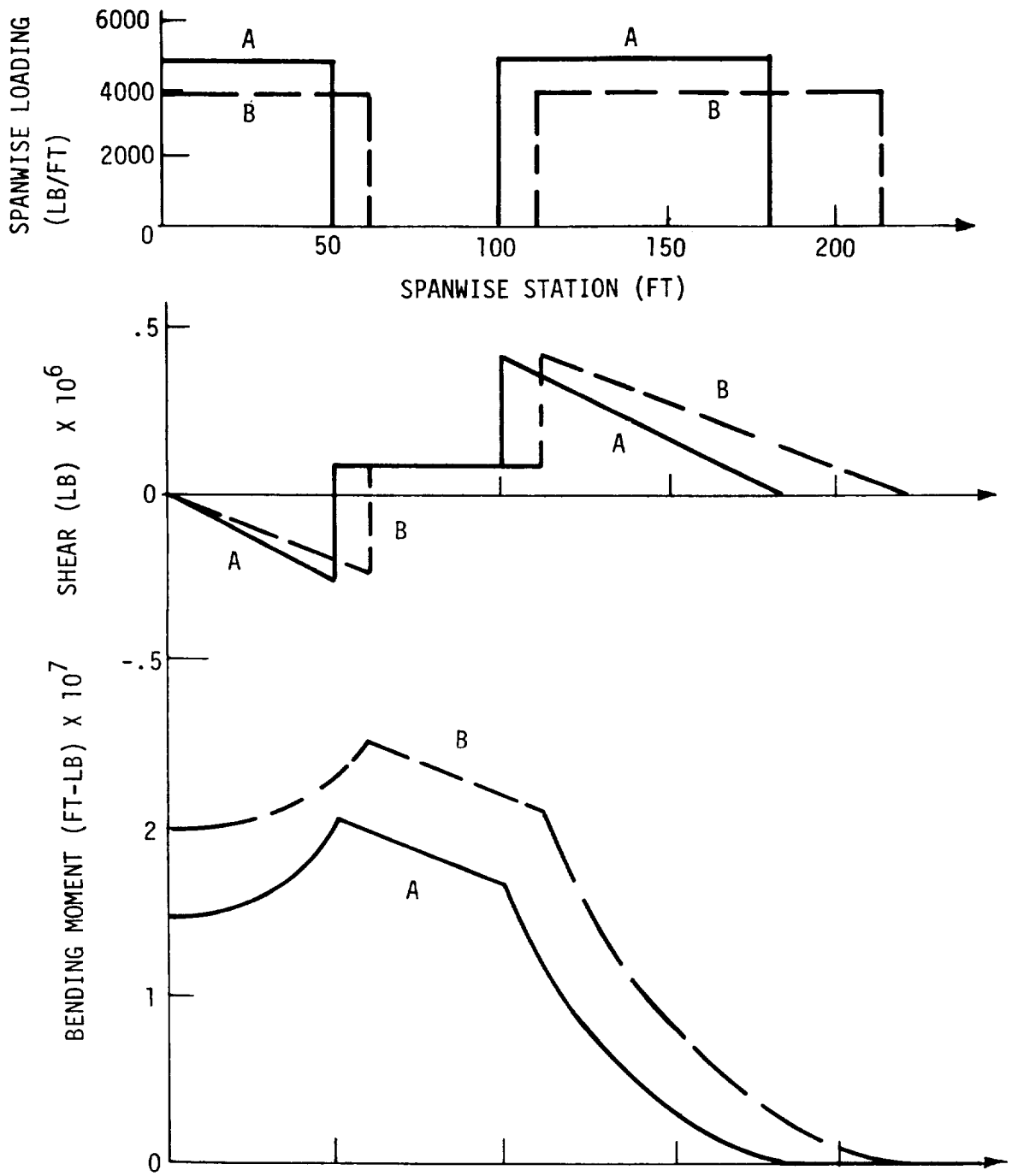

Figure I-7. Ultimate Shear and Bending Moment Diagrams Configuration 9 A/B

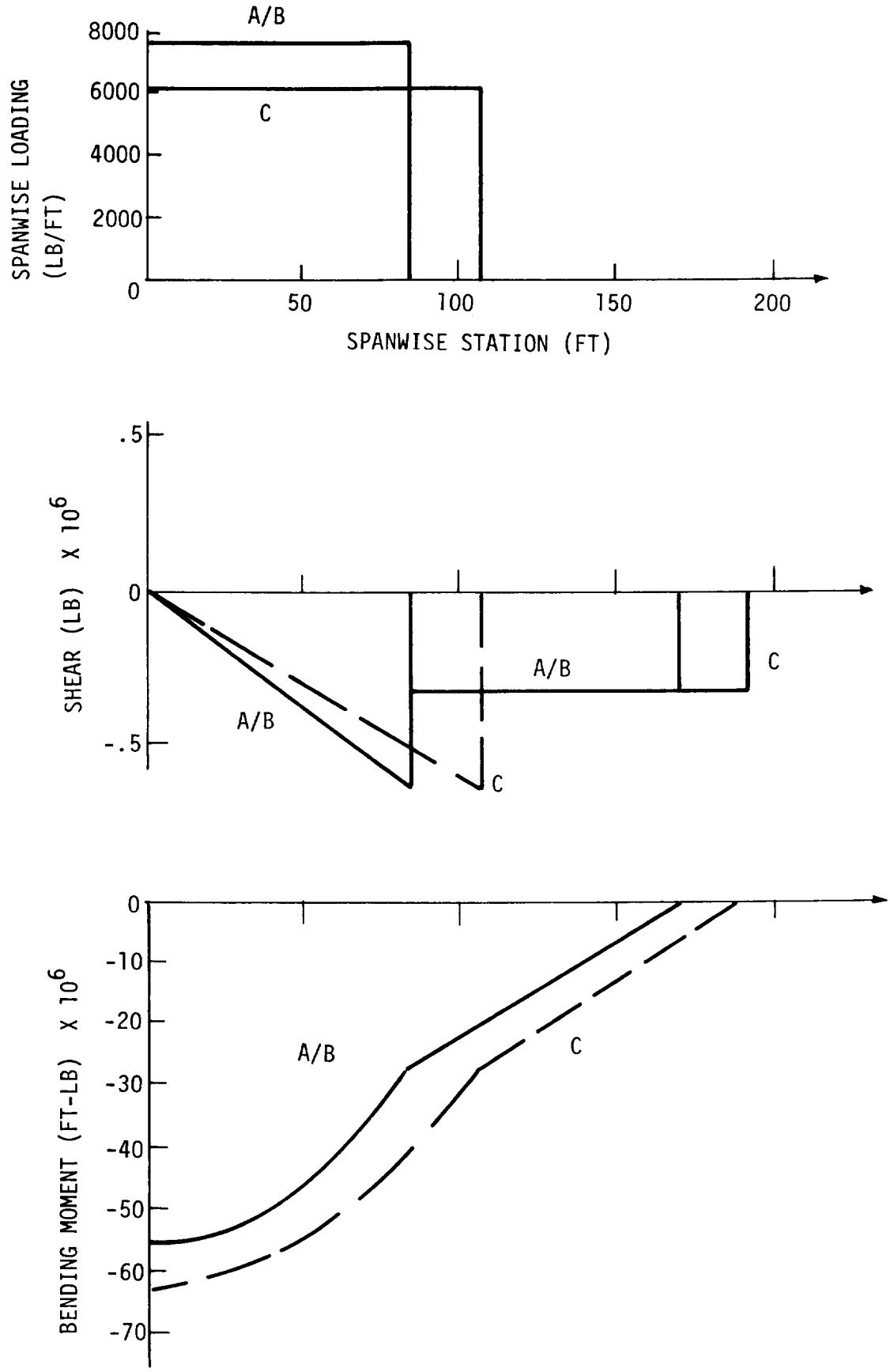

Figure I-8. Ultimate Shear and Bending Moment Diagrams Configuration 11 A/B/C

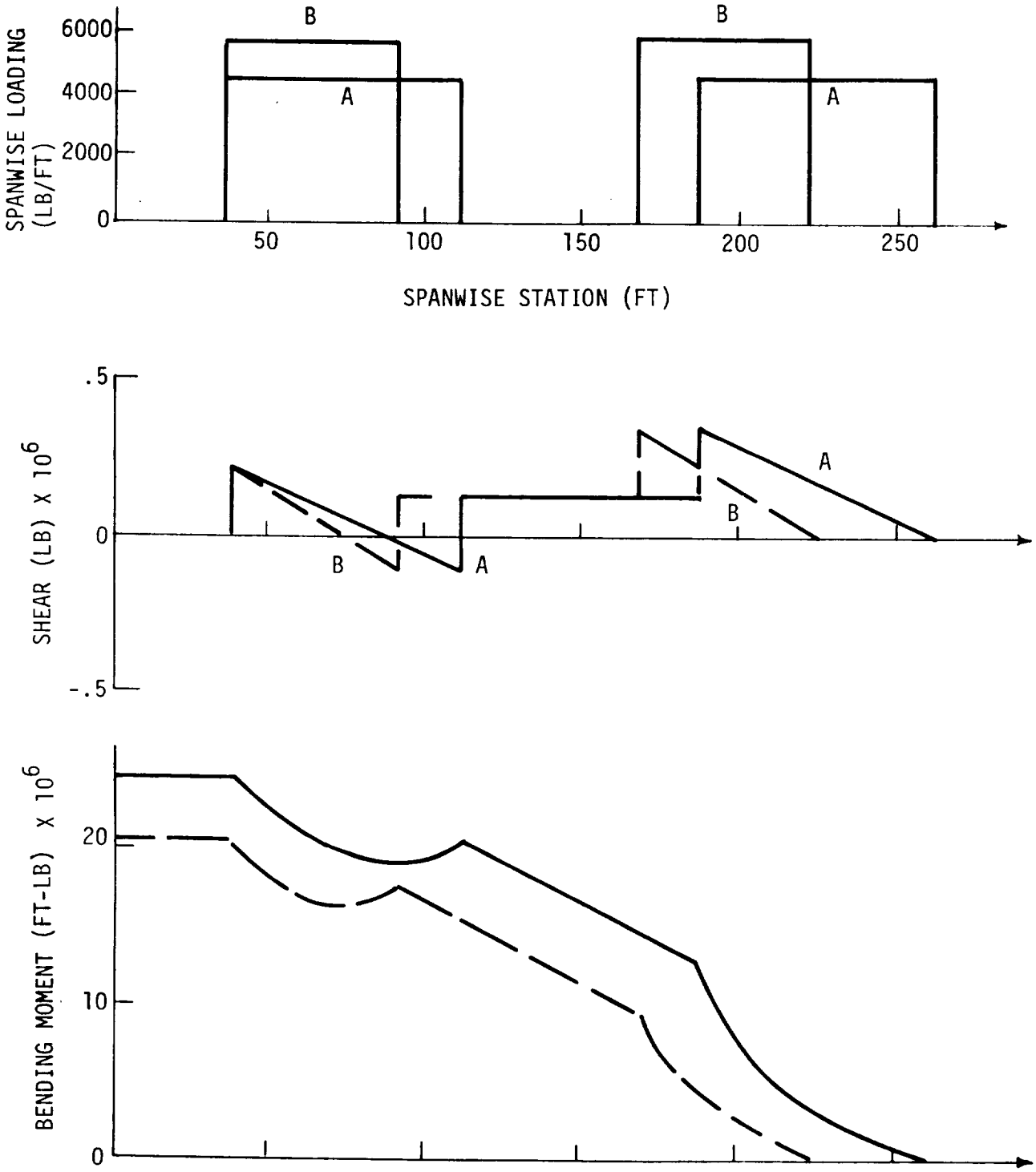

Figure I-9. Ultimate Shear and Bending Moment Diagrams Configuration 12 A/B

Concluding Remarks

From the foregoing discussion, it can be seen that there were many arbitrary decisions that had to be made concerning structural layout, sizing criteria, and so forth. Many other choices might seem equally plausible. Although the actual weights derived may be very speculative, they still should provide a reasonably accurate indication of the relative merits of the configurations. In general, there is no single parameter whose uncertainty is so great as to cause marked uncertainty in the weights, other than the parameter k_{sp} that appears in the equations for the delta planforms. The value finally chosen - 0.02 - implies very light internal support structure, and it is simply not known if this is a realistic value. However, it is certain that if the delta planforms are at all viable, they must be built with area densities much lower than those for the trapezoidal or rectangular planforms.

The hull penalty has been estimated by equating it to the estimate for the wing carrythrough structure. In actual practice, there would undoubtedly be additional material in the hull to provide load paths into the hull for the wing loads. For Akron-type hull construction, for example, some frames would need to be strengthened to carry shear at the wing root, leaving only the bending moment to be carried by the carrythrough structure. The use of both shear and bending equivalent areas to calculate the volume of the carrythrough structure is intended to account for this. It is not necessarily implied that all of the added weight will go into the carrythrough in an actual design.

The wing weight estimates based on the methods of Reference I-8 were intended to provide an "upper limit" the wing weights for the winged airship configurations and furthermore to indicate the <u>relative</u> weight relationships between the various concepts. The combined wing + hull structure weight penalty are presented in Table I-V. Based on these results the mid-body straight

ORIGINAL PAGE IS
OF POOR QUALITY

TABLE I-V - WINGED AIRSHIP CONFIGURATION CHARACTERISTICS AND EVALUATION RESULTS

Config. Number and Description		Total Wing & Hull Weight Penalty 10^3 Lbs	UL.VC 10^3 Ton Mi/Hr	Total Span & (Chord) Ft	Exposed Wing Area Ft^2
β = 1.0					
1	Conv. Rigid	0	11.7		
β = 0.5					
2A	Low Wing Delta	135.2	9.89	240	55
2B	Low Wing Delta	190.1	7.55	320	73
3A	Low Wing	155.3	8.97	240	62
3B	Clipped Delta	215.8	6.34	320	82
4A	Mid Wing Delta	267.4	3.92	320	94.7
4B	Mid Wing Delta	318.0	1.68	400	73
5A	Mid Wing Clip	285.9	3.09	320	61
5B	Ped Deltas	342.9	0.56	400	81.5
6A	Low Body +	108.5	11.13	240 (108)	18
6B	Straight Wing	141.7	9.85	320 (108)	26.8
6C	L. B. + S. W.	176.5	8.34	400 (81)	26.5
7A	Mid Body Str Wing	112.4	11.01	240 (108)	14
7B	Mid Body Str Wing	157.8	9.18	320 (108)	23
7C	Mid Body Str Wing	192.4	7.64	400 (81)	24
8A	Straked A/S	134.6	9.46	190	39
8B	Straked A/S	166.4	8.17	210	50.6
9A	Two Hull-Low Wing	88.4	11.51	1/d = .75	22
9B	Two Hull-Low Wing	132.2	9.37	1/d =1.0	17
10A	Two Hull-Mid Wing	83.	11.8	1/d = .75	32.8
10B	Two Hull-Mid Wing	128.7	10.37	1/d =1.0	13.5
11A	Large-Center Wing	228.2	4.94	c/d = 2 b/d = 2	29.3
11B	Large-Center Wing	168.4	7.7	c/d = 1.5 b/d = 2	22
11C	Large-Center Wing	183.8	7.09	c/d = 1.5 b/d = 2.5	27.5
12A	3-Hull Mid-Wing	134.1	8.83	1/d = 1.0	22.4
12B	3-Hull Mid-Wing	88.3	10.87	1/d = .75	12.6
7A	Mid Body Str. Wing*	43.7 (89.9)**	13.7		
7B	Mid Body Str. Wing*	80.6 (126.2)	11.8		
7C	Mid Body Str. Wing*	96.6 (153.9)	10.9		
β = 0.2					
14A	Str Wing Mid-Body	121.0	13.21	300 (80)	16.6
14B	Str Wing Mid-Body	149.2	12.12	350 (80)	21.5
14C	Str Wing Mid-Body	201.6	9.82	350 (120)	32.2
14D	Str Wing Mid-Body	175.5	11.06	400 (80)	25.5
14E	Str Wing Mid-Body	200.7	9.98	450 (80)	29.5
15A	Delta Wing Mid-Body	177.9	10.69	350	49
15B	Delta Wing Mid-Body	201.0	9.77	400	57.5
15C	Delta Wing Mid-Body	223.8	8.85	450	66
15D	Delta Wing Mid-Body	246.	7.88	500	74

*Most promising configurations selected for evaluation using fabric covered truss structure construction.

**Wing component only, hull carry through structure assumed unchanged. Value in parenthesis is "upper limit" wing alone weight value.

wing configuration [#7] was evaluated using a fabric covered truss structure construction concept. Results also shown in Table -III indicated that the "upper limit" weight estimates might be reduced by 40% to 60%. Using these weight estimates provided a slight improvement in the UL-V_C figure of merit relative to the conventional neutrally buoyant airship. However, in light of the results of the parametric analysis of conventional ellipsoidal airships it appears that the best winged airship configuration remains inferior to aerodynamic lift augmented airships at 400,000 pounds gross weight.

REFERENCES

1) Goodyear Aerospace Corp, "Feasibility Study of Modern Airships", Vol. II - Parametric Analysis, NASA-CR-137692, July 1975.

2) Mayer, N.J.; Advanced Airship Concepts for Antenna Platform, Proceedings of the Seventh Scientific Balloon Symposium, AFCRL-TR-73-0071, 1973.

3) The Skyship Project, Aircraft Engineering, December 1974.

4) Freeman, H.B.; "Force Measurements on a 1/40-Scale Model of the U.S. Airship "AKRON", NACA TR 432, 1932.

5) Gersten, K.; "Nonlinear Airfoil Theory for Rectangular Wings in Incompressible Flow", NACA RE 3-2-59W, February 1959.

6) Hoerner, Dr.; - Ing S. F.; "Fluid Dynamic Drag", published by the author, 1965.

7) U.S. Air Force Stability and Control DATCOM, October 1960, revised 1974.

8) Shanley, F.R.; Weight-Strength Analysis of Aircraft Structures, Dover Publication, Inc., New York, New York, 1952.

NTIS does not permit return of items for credit or refund. A replacement will be provided if an error is made in filling your order, if the item was received in damaged condition, or if the item is defective.

Reproduced by NTIS
National Technical Information Service
U.S. Department of Commerce
Springfield, VA 22161

This report was printed specifically for you order from our collection of more than 1.5 million technical reports.

For economy and efficiency, NTIS does not maintain stock of its vast collection of technical reports. Rather, most documents are printed for each order. Your copy is the best possible reproduction available from our master archive. If you have any questions concerning this document or any order you placed with NTIS, please call our Customer Services Department at (703)487-4660.

Always think of NTIS when you want:
• Access to the technical, scientific, and engineering results generated by the ongoing multibillion dollar R&D program of the U.S. Government.
• R&D results from Japan, West Germany, Great Britain, and some 20 other countries, most of it reported in English.

NTIS also operates two centers that can provide you with valuable information:
• The Federal Computer Products Center - offers software and datafiles produced by Federal agencies.
• The Center for the Utilization of Federal Technology - gives you access to the best of Federal technologies and laboratory resources.

For more information about NTIS, send for our FREE *NTIS Products and Services Catalog* which describes how you can access this U.S. and foreign Government technology. Call (703)487-4650 or send this sheet to NTIS, U.S. Department of Commerce, Springfield, VA 22161. Ask for catalog, PR-827.

Name _____
Address _____
_____
_____
Telephone _____

NTIS - *Your Source to U.S. and Foreign Government Research and Technology.*